POWER QUALITY ENHANCEMENT USING AI BASED INDUCTIVELY COUPLED DSTATCOM FOR INDUCTIVELY COUPLED LOADS

Thesis Submitted for the Award of the Degree of

DOCTOR OF PHILOSOPHY

In

Electrical Engineering

By

K.Praveen kumar yadav

Registration Number: 41800837

Supervised By

Dr. Suresh Kumar Sudabattula (21628)

Power System, Associate Professor,

SEEE, Lovely Professional University,

Punjab

Co-Supervised by

Dr. Mrutyunjaya Mangaraj

Assistant Professor

Department of Electrical & Electronics Engineering, SRM University, Amaravathi, Andhra Pradesh

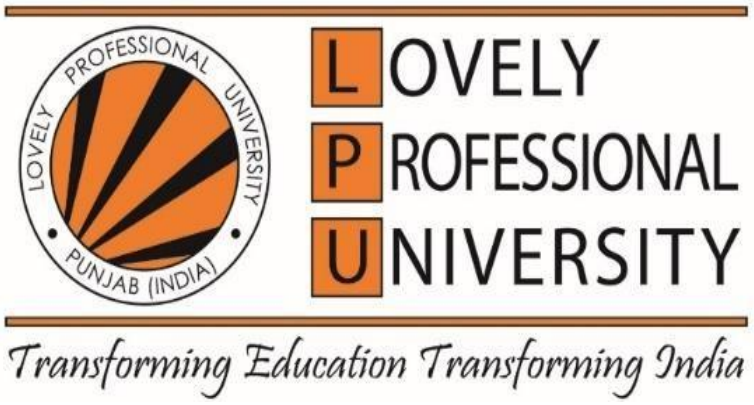

LOVELY PROFESSIONAL UNIVERSITY, PUNJAB

2024

DECLARATION

I, hereby declared that the presented work in the thesis entitled "**POWER QUALITY ENHANCEMENT USING AI BASED INDUCTIVELY COUPLED DSTATCOM FOR INDUCTIVELY COUPLED LOADS**" in fulfillment of degree of **Doctor of Philosophy (Ph. D.)** is outcome of research work carried out by me under the supervision of Dr. Suresh Kumar Sudabattula, working as Associate Professor, in the School of Electronics and Electrical Engineering of Lovely Professional University, Punjab, India and under the Co-supervision of Dr. Mrutyunjaya Mangaraj, working as an Assistant Professor, in the Department of Electrical and Electronics Engineering of SRM University, Amaravathi, India. In keeping with general practice of reporting scientific observations, due acknowledgements have been made whenever work described here has been based on findings of other investigator. This work has not been submitted in part or full to any other University or Institute for the award of any degree.

Name of the scholar: K.Praveen kumar Yadav

Registration No.: 41800837

Department/school: Department of Electrical Engineering

Lovely Professional University,

Punjab, India

CERTIFICATE

This is to certify that the work reported in the Ph.D. thesis entitled "**POWER QUALITY ENHANCEMENT USING AI BASED INDUCTIVELY COUPLED DSTATCOM FOR INDUCTIVELY COUPLED LOADS**" submitted in fulfillment of the requirement for the reward of degree of **Doctor of Philosophy (Ph.D.)** in the Department of Electrical Engineering, is a research work carried out by K.Praveen Kumar Yadav 41800837, is bonafide record of his original work carried out under my supervision and that no part of thesis has been submitted for any other degree, diploma or equivalent course.

Name of supervisor: Dr. Suresh Kumar Sudabattula

Designation: Associate Professor

Department/school: School of Electronics and Electrical Engineering

University: Lovely Professional University

Name of Co-Supervisor: Dr. Mrutyunjaya Mangaraj

Designation: Assistant Professor

Department: Department of Electrical & Electronics Engineering

University: SRMU

PREFACE/ACKNOWLEDEMENT

This thesis would not have been possible without the support of glorious people who motivated me during my doctoral study. I am thankful from my bottom of my heart toward the numerous persons who assisted me while conducting this study.

First of all,I would like to thank my Supervisor, Dr. Suresh Kumar Sudabattula, for his worthy guidance, support, and suggestions, in every step of this research project during my Ph.D. journey. Dr. Suresh Kumar Sudabattula has an optimistic personality with helpful nature, he has always made himself ready to clarify my doubts and it was a great opportunity to work under his supervision. He always shed light whenever I was feeling stuck in my path of research ambitions.

I wish to express my gratitude and indebtedness to my revered Co- Supervisor Dr. Mrutyunjaya Mangaraj, for his constant support, kind encouragement, immensely valuable ideas, and suggestions and for having an unwavering attention. I have been amazingly fortunate to have a Co-supervisor who gave me the freedom to explore the research findings on my own

It is my privilege to thank my family members for their continuous encouragement throughout my research time. I am extremely thankful to the Management, Principal, HOD and all Faculty members of Lendi Institute of Engineering & Technology, Vizianagaram, India for supporting and providing the necessary inputs.

I would like to express my gratitude toward the entire Lovely Professional University family for providing suitable infrastructure and environment for completing my research work in a time-bound manner. Also, I like to thank the Division of Research & Development and School of Electronics and Electrical Engineering for their help and encouragement in my entire Ph.D. journey.

Especial thanks to my wife Mrs Swati Mattam and daughter Kundala Jahnavi yadav to support my dreams. I thank my beloved parents for their continuous love and relentless support throughout my work. Finally; I like to thank almighty God who helped me to achieve such a big milestone.

Date: 05/08/24 K.Praveen Kumar Yadav

ABSTRACT

This research study explains about Power quality (PQ) enhancement using AI based inductively coupled DSTATCOM for inductively coupled loads. The main purpose is to develop an improved adaptive control algorithm for the distributed flexible AC transmission systems (DFACTS) device to improve PQ under various loading conditions in the electric power distribution system (EPDS). The current related PQ issues and its remedial measures are carried out throughout the thesis. The DSTATCOMs are developed since 2009. It is also regarded as direct coupled distributed static compensator (DSTATCOM). These control techniques are implemented for DC-DSTATCOM to provide better solutions for PQ issues. But, this research illustrates the process of IC-DSTATCOM strategy to carry better solutions over the DC-DSTATCOM. In this study, the proposed method aims an opportunity for the EPDS to provide the solutions in term of better PQ performance.

In the first chapter, it is mainly explained about the different PQ issues which affect the efficiency of the EPDS. It is also focused on the techniques those are existed in the current EPDS, and necessary the requirements to update the EPDS, and also to overcome the PQ issues.

In the second chapter, IC-DSTATCOM is employed to enhance the PQ in the EPDS and protect the system by decreasing the harmonic level to the best possible range. For efficient function of DC-DSTATCOM and IC-DSTATCOM, *icosϕ* control technique is implemented. In order to investigate the usefulness of the PQ with economic and reliable operation, the different balanced and unbalanced loadings are considered. The primary objective is the harmonic reduction. The secondary objectives of this system are to improve the voltage regulation, minimize the DC link voltage and improve (P.F) power factor. Numerical results of *icosØ* control technique based IC-DSTATCOM is presented better as it is compared with DC-DSTATCOM.

The third chapter focused on cascaded inductively coupled DSTATCOM (CIC-DSTATCOM) to improve the PQ. In this chapter, the *icosϕ* control structure was utilized to breed the switching pulses to both cascaded inductively coupled DSTATCOM (CDC-DSTATCOM) and CIC-DSTATCOM. This inverter is mainly composed of a number of identical H-bridge power cells connected in cascade. Here, the comparison is conducted

in between the CIC-DSTATCOM and CDC-DSTATCOM in terms of harmonic distortion, voltage regulation, reduced DC link voltage, voltage balancing and improved P.F. Numerical results show that the CIC-DSTATCOM method is successful than CDC-DSTATCOM in solving the PQ issues.

Some back steps like un-tuned filter and clustered weight are bringing unfavorable solution for the conventional technique even though putting lot of efforts to solve the PQ issues. But, in the third chapter, the un-tuned and clustered weights are updated using DBSCAN technique which is based on machine learning algorithm for DC-DSTATCOM and IC-DSTATCOM. This learning algorithm is a special type of artificial intelligence which is utilized to minimize the total harmonic distortion and improve the P.F. According to numerical results, it is examined that the healthier solutions are found than the *icosϕ* control algorithm by keeping the %THD minimum based on IEC-41000-1-3& IEEE-519-2018 values. This technique has achieved the better multiple objectives voltage regulation, reduction in DC link potential, voltage balancing. From the comparative study of DBSCAN supported DC-DSTATCOM and IC-DSTATCOM is compared with the conventional *icosϕ* control Algorithm.

For further analysis, the different comparisons are made among (i) *icosϕ* and Density based spatial clusturing algorithm with noise (DBSCAN) control algorithm, (ii) Naive Back Propagation (NBP) based *icosϕ* and *DBSCAN* algorithm, (iii) Conjugate gradient back propagation (CGBP) based *icosϕ* and *DBSCAN* algorithm, (iv) Kernel Hebbian Least Mean Square (KHLMS) and DBSCAN algorithm, (v) Levenberg Marquard back Propagation (LMBP) based *icosϕ* and *DBSCAN* algorithm, (vi) Sparse least mean square (SLMS) and *DBSCAN* algorithm, (vii) Hebbian least mean square (HLMS) and *DBSCAN* control algorithm, (viii) Syncronous Reference frame (SRF) and *DBSCAN* based IC-DSTATCOM.

TABLE OF CONTENTS

CHAPTER 2: LITERATURE REVIEW

CHAPTER 3: VSI BASED DSTATCOM USING *ICOSϕ* CONTROL TECHNIQUE

CHAPTER 4: CASCADED VSI BASED DSTATCOM USING *ICOSϕ* CONTROL ALGORITHM

CHAPTER 7: CONCLUSION & FUTURE SCOPE

	LIST OF FIGURES	
Fig. No.	**Description**	**PageNo.**
1.1	Types of 3 phase sources	2
1.2	Types of 3 phase loads	2
1.3	Power quality problems	3
1.3	EPDS with DFACT devices	4
1.5	Classifications of Power quality compensators	4
1.6	Classifications of DSTATCOM	5
1.7	Direct coupled DSTATCOM	7
1.8	Inductively coupled DSTATCOM	8
3.1	EPDS with DC- DSTATCOM	25
3.2	EPDS with IC- DSTATCOM	25
3.3	Two-level self-supported capacitor supported VSC based DSTATCOM	26
3.4	Switching signals generation for IC-DSTATCOM	29
3.5	Inside control signal of the control technique	30
3.6(a)	Waveform of three phase input potential, supply current, output current, compensator current and DC-link potential with DC- DSTATCOM	32
3.6(b)	Source side powerfactor with DC- DSTATCOM	32
3.6(c)	Load side powerfactor with DC- DSTATCOM	33
3.6(d)	Source current THD with DC- DSTATCOM	33
3.6(e)	Load current THD with DC- DSTATCOM	34
3.7(a)	Waveform of three phase input potential, supply current, output current, compensator current, DC-link potential with IC-DSTATCOM	34
3.7(b)	Source side powerfactor with IC-DSTATCOM	35
3.7(c)	Load side powerfactor with IC-DSTATCOM	35
3.7(d)	Source current THD with IC-DSTATCOM	36
3.7(e)	Load current THD with IC-DSTATCOM	37

	LIST OF Tables	
Table. No.	**Description**	**Page No.**
1.1	Comparisons between DC and IC – DSTATCOM	6
1.2	Comparative analysis between different control strategies	11
3.1	Performance parameter of DC-DSTATCOM and IC-DSTATCOM	37
3.2	Simulation formation parameters	38
3.3	Basic name plate rating parameters of the IFCT	39
3.4	Measured active and reactive power of IFCT	39
3.5	Comparative study on kVA rating, DF, HCR, DIN, FF, RF, HF and C-Message weight of DC-DSTATCOM and IC-DSTATCOM	42
4.1	Performance parameter of CDC-DSTATCOM and CIC-DSTATCOM	59
4.2	Simulation formation parameters	60
4.3	Basic rating parameters of the IFCT	61
4.4	Measured active and reactive power of IFCT	61
4.5	Comparative study on kVA rating, DF, HCR, DIN, FF, RF, HF and C-Message weight of CDC-DSTATCOM and CIC-DSTATCOM	64
5.1	Performance parameter of DC-DSTATCOM and IC-DSTATCOM	83
5.2	Simulation formation parameters	84
5.3	Basic name plate rating parameters of the IFCT	85
5.4	Measured active and reactive power of IFCT	85
5.5	Comparative study on kVA rating, DF, HCR, DIN, FF, RF, HF and C-Message weight of DC-DSTATCOM and IC-DSTATCOM	88
6.1	Comparative analysis between *ICOSϕ* control algorithm and *DBSCAN* control algorithm	92
6.2	Comparative analysis between *ICOSϕ* control algorithm and	93

LIST OF ABBREVATIONS

S.No	Notation	Abbreviation
1	EPDS	Electrical power distribution system
2	PQ	Power quality
3	DSTATCOM	Distribution static compensator
4	VSI	Voltage source inverter
5	CPD	Custom power devices
6	PCC	Point of common coupling
7	DC-DSTATCOM	Direct coupled DSTATCOM
8	IC-DSTATCOM	Inductively coupled DSTATCOM
9	IFCT	Inductively filtering converter transformer
10	PF	Power factor
11	PW	Primary winding
12	SW	Secondary winding
13	FW	Filtering winding
14	THD	Total harmonic distortion
15	DF	De-rating factor
16	HCR	Harmonic compensation ratio
17	DIN	Distortion index
18	FF	Form factor
19	RF	Ripple factor

20	HF	Harmonic factor
21	CDC-DSTATCOM	Cascaded Direct coupled DSTATCOM
22	CIC-DSTATCOM	Cascaded Inductively coupled DSTATCOM
23	VSI	Voltage source inverter
24	CT	Current transformer
25	ML	Machine learning
26	DBSCAN	Density based spatial clustering and noise
27	KCL	Kirchhoff's current law
28	IGBT	Insulated-gate bipolar transistors
29	CB	Circuit Breaker
30	AI	Artificial intelligence

CHAPTER-1

CHAPTER-1

INTRODUCTION

1.1 Chapter introduction

1.1.1 Research back ground

The 3-phase sources are considered of various types such as i) Balanced, ii) Un-Balanced, iii) Distorted and iv) Non Distorted which is shown in fig 1.1

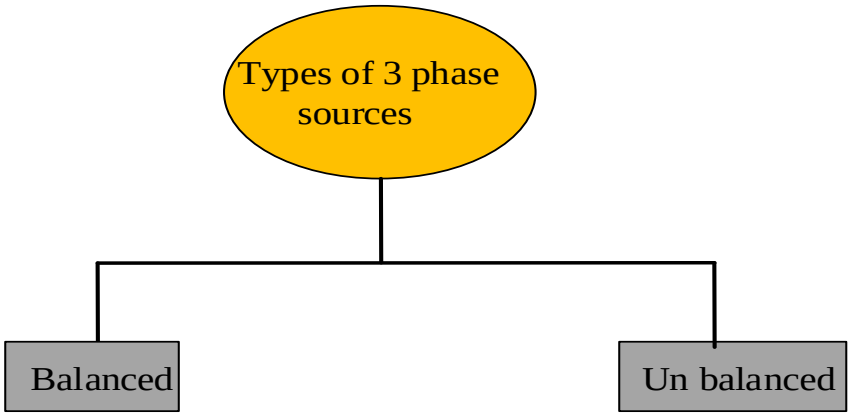

Fig. 1.1 Types of 3-phase sources

In the similar way the different types of 3-phase loads are used in the Electrical power distribution system [EPDS] which is shown in fig 1.2.

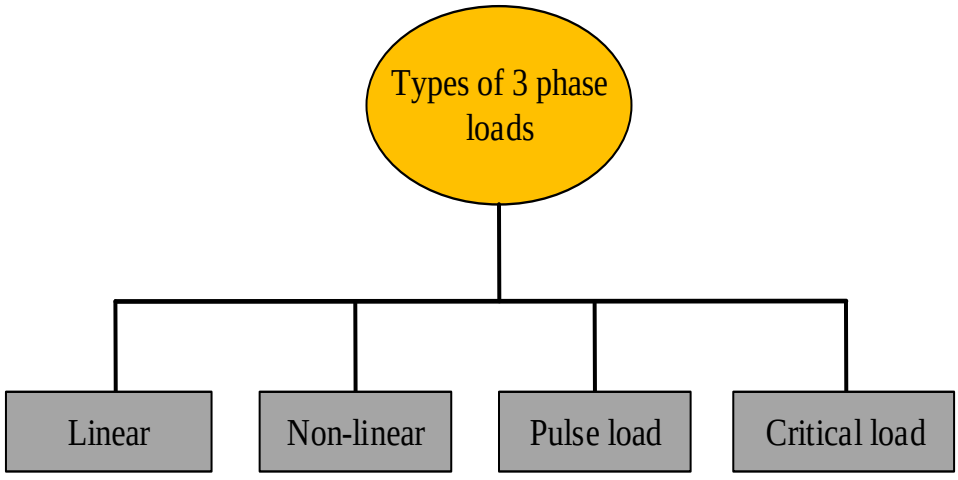

Fig. 1.2 Types of 3-phase loads

1.1.2 Power quality Problems

The prime motivation of EPDS is attracted to the consumers and service provider to offer secure, consistent, quality & efficient source of energy. Therefore, the EPDS must be well-thought-out, well-designed & safely operated. When in operation, EPDS often experiences a higher number of failures and disturbances. Increase in energy demands, less long-standing plan, open access to consumers, minimum security, nonlinear loads, unplanned load switching are the reasons faced frequently.

These following reasons may further cause the different power quality problems such as voltage un-balancing, transient source current harmonics, low PF, interference, and improper voltage regulation which were shown in fig 1.3.

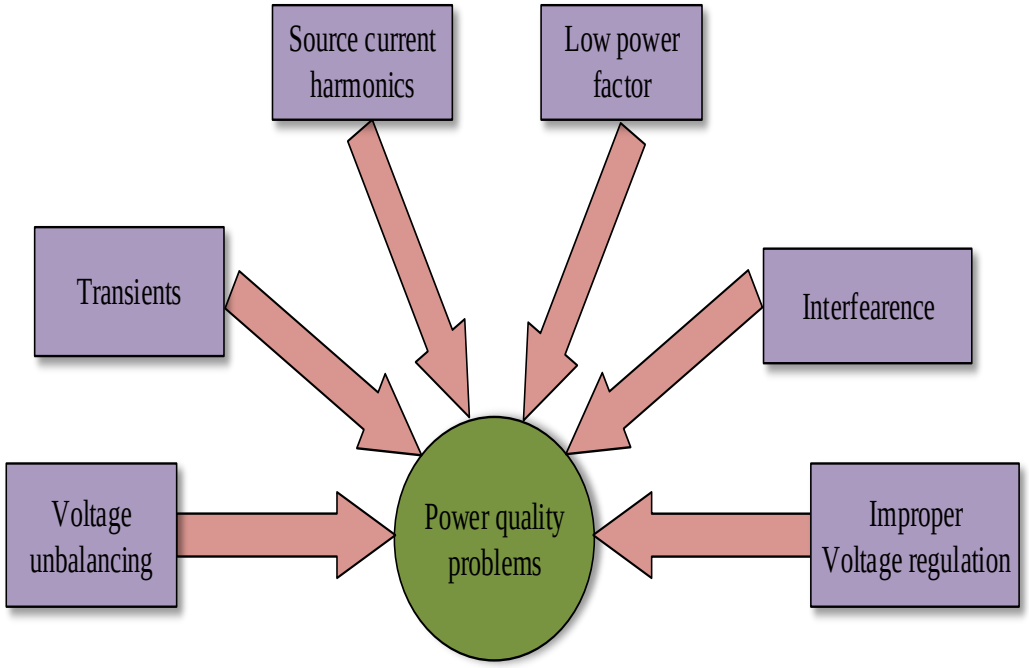

Fig. 1.3 PQ problems

As a result, experts in the field of power system operation require innovative methods for enhancing PQ performance. With this motivation for improving the PQ performance in the EPDS, the DSTATCOM is the important choice for current related PQ issues. Even though, DSTATCOM is playing a major role in the EPDS, still on the other side of the coin, diversification of the DSTATCOM is a growing role for the modern EPDS. Hence, the challenging task is to provide flexibility and sustainability for all above scenarios. Pertinent selection of voltage source inverter (VSI), extension of VSI, design of control algorithm, IFCT design, impedance matching are the major research areas for the improvement of the PQ. From last three decades, most of the

researchers and several R&D organizations focused on different CPDs to neutralize the PQ issues. All the CPDs perform flexible, reliable and quick reaction to inject reactive power at PCC of system. The connection of DFACT devices with EPDS is shown in fig 1.4. Where the classification of the different types of PQ compensator is shown in fig 1.5.

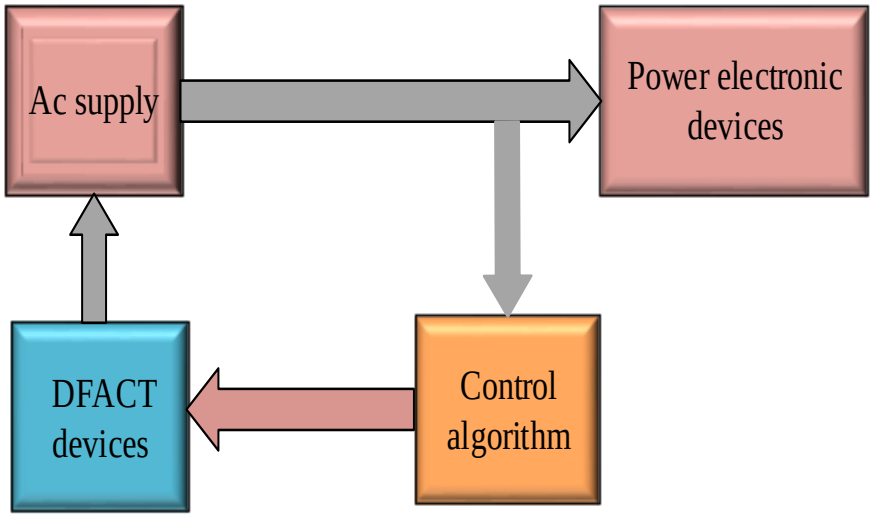

Fig. 1.4 EPDS with DFACT devices

1.1.3 PQ compensators

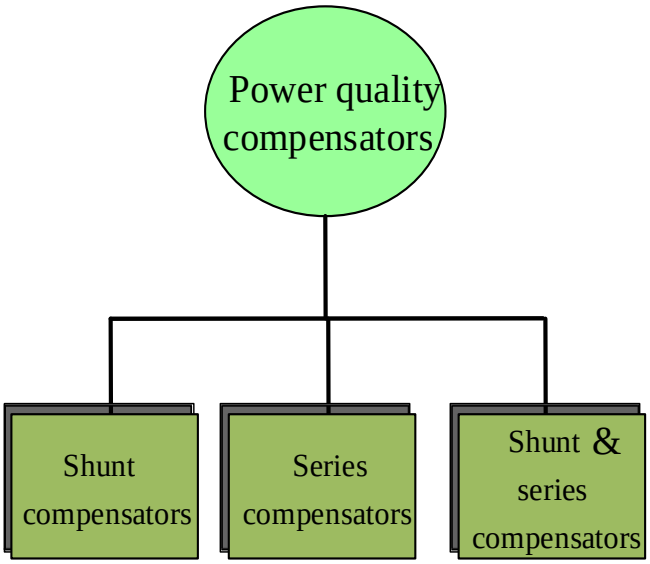

Fig. 1.5 Classifications of PQ compensators

The power quality compensators are classified into three types those are shunt, series and shunt &series compensators to improve the power quality of the system.

1.1.4 DSTATCOM Structure, topology, classification

Number of switching elements, isolation provided by transformers, and other

factors can be used to categorize the DSTATCOM topologies. These DSTATCOMs are designed to reach the necessities of 3P3W.

A. 3-Phase 3-Wire DSTATCOM

3P3W DSTATCOM is utilized for enhancement of PQ in 3P3W EPDS for the compensation of customer loads. The classifications of 3P3W DSTATCOM topologies are shown in Fig. 1.6.

Bhim singh et al. outlines various DC-DSTATCOMs structures, and how they work together for power quality enhancement [5].

The VSI-based DSTATCOMs are two types i) non-isolated VSI ii) isolated VSI

1) Direct Coupled DSTATCOM (DC-DSTATCOM): The DC-DSTATCOM is shown in fig 1.6. The literature proposes a topology based on a 3-leg VSI. The two-leg VSI with split capacitor topology has advantageous because it requires fewer switching components. However, the control & regulation of equal dc potentials of capacitors & necessity of more dc bus potentials are main demerits.

2) Inductively Coupled DSTATCOM (IC-DSTATCOM): The IC-DSTATCOM is shown in fig 1.6. Three 1-phase VSIs as 3-phase DSTATCOM is used, however the usage of additional elements made this configuration have less common. Here the transformer kVA rating identical to the essential reactive power insertion is necessary. Yet, the inductive transformer creates separation between load and system & gives the elasticity to use an "off-the-shelf" VSI for the preferred function. Different configurations are possible by using number of transformers may in this DSTATCOM.

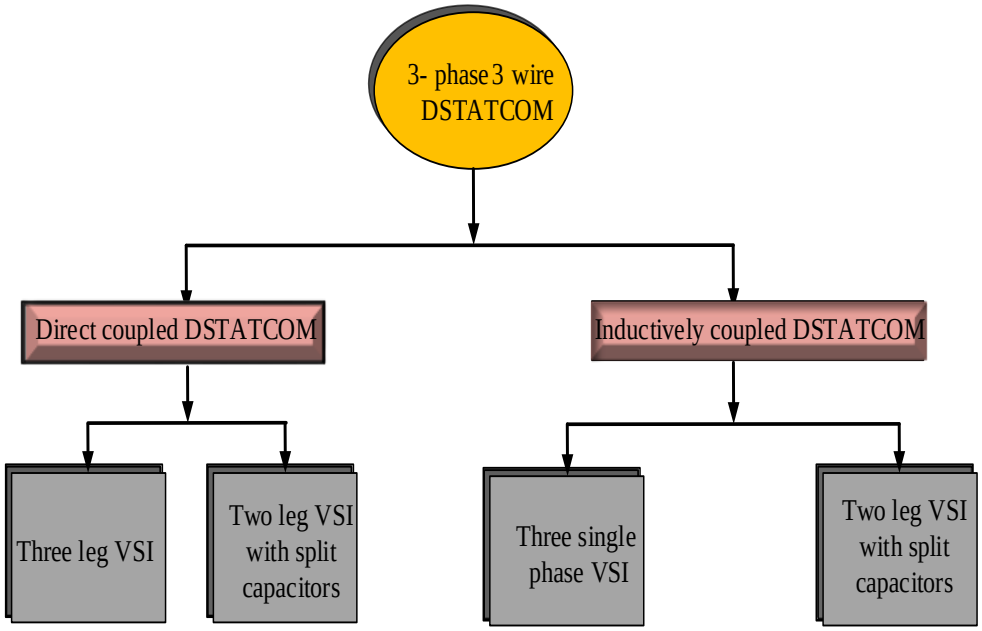

Fig. 1.6 Classification of DSTATCOM

1.15 Comparison between DC and IC – DSTATCOM

Table 1.1 Comparisons between DC and IC – DSTATCOM

DC-DSTATCOM	IC-DSTATCOM
1. The DSTATCOM is connected directly at the PCC 2. There is a chance of short circuit due to direct contact. 3. Due to the short circuit system efficiency will reduce 4. Does not provide optimized active and reactive power flow at the PCC 5. The compensator current is more 6. %THD is more 7. Here there is no IFCT. 8. Less protection	1. The DSTATCOM is jointed Inductively at the PCC through IFCT 2. The possibility of short circuit is less due to IFCT. 3. It maintains better efficiency. 4. The optimized active and reactive power flow are obtained due to the IFCT. 5. The compensator current is less 6. %THD is less 7. The IFCT is to damp-out the harmonic resonance in between source and filtering side. Drooping structure down time-cost will improve 8. It provides flexible protection against of harmonic current.

1.1.6 Direct coupled DSTATCOM

Of course, lot of researchers are done very good research on DC-DSTATCOM with self-supported capacitance. The main advantages of DC-DSTATCOM: (i) It achieves reduced static error and quick convergence characteristics, (ii) The features like heftiness, tracking & adaptive capabilities under adjustable loading periodicity are obtained. But in DC-DSTATCOM, the PCC possesses various severities because of direct connection of DSTATCOM, supply and load. Hence, flow of short circuit current, poor protection, some thermal losses are occurred. Because the PCC is in close contact with the source, load, and DSTATCOM in DC-DSTATCOM, it is subjected to additional stress. As a result, there are increased opportunities for short circuit currents to flow, insufficient protection, and thermal losses, among other things.

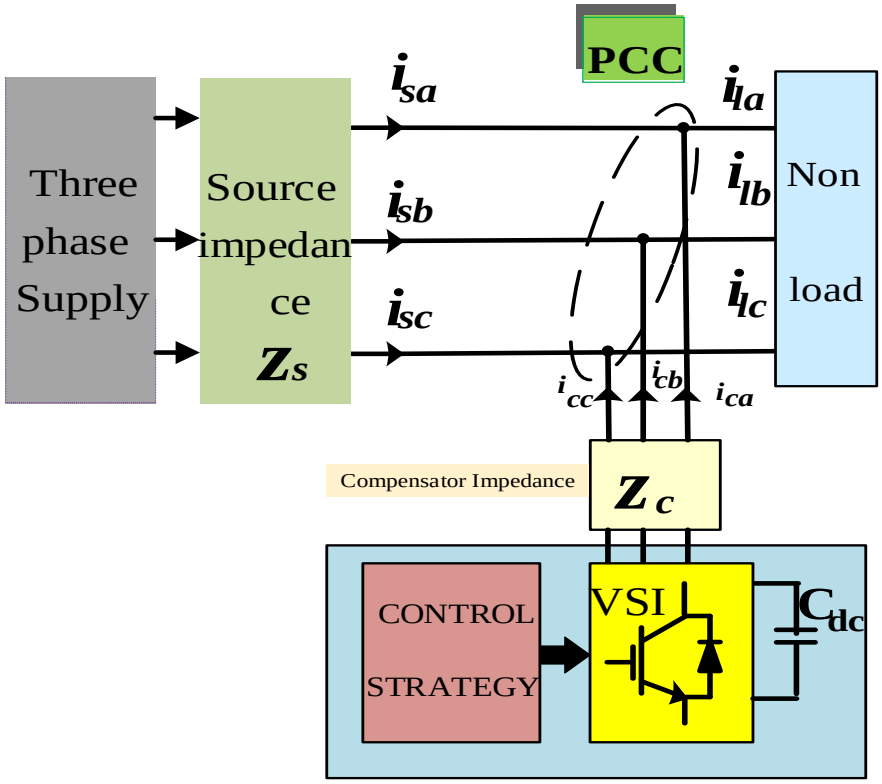

Fig. 1.7 DC-DSTATCOM

1.1.7 Inductively coupled DSTATCOM

As the aforementioned DC-DSTATCOM undergoes further development, the requirement for an IC-DSTATCOM is expected to increase, allowing it to function more effectively in practise. Here the transformer kVA rating identical to the essential reactive power insertion is necessary. Yet, the inductive transformer creates separation between load and system. DC-DSTATCOM can be configured in different ways by using number of transformers.

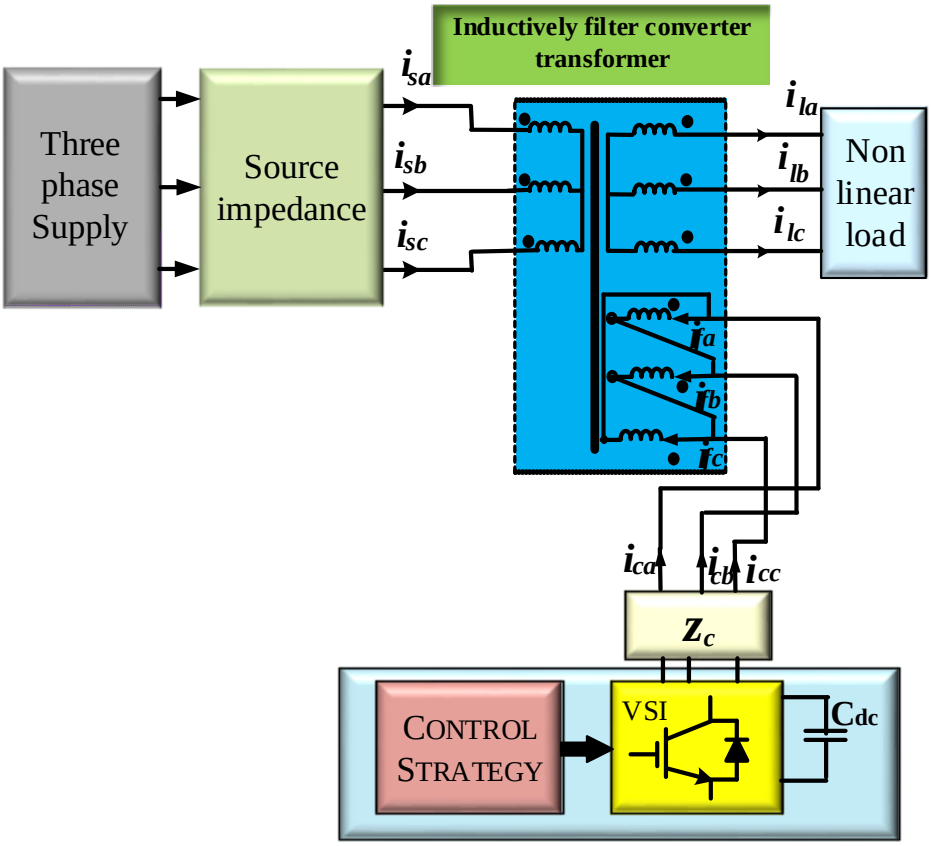

Fig. 1.8 IC-DSTATCOM

1.1.8 DC-DSTATCOM using conventional control technique

Synchronous Reference frame (SRF): In 3-phase, this is widely used theory but phase, frequency & amplitude values are not provided. It will only provide averages. The major function of this technique is to discover the voltage& frequency at PCC. The current component is extracted to implement this control method. The base current is utilized to fix the triggering of DSTATCOM. The controller removes dc elements so non-dc elements are isolated from base signal.

Instantaneous Reactive power Theory (IRPT): Akagi first proposed the concept of IRPT in 1983. The estimation of instantaneous active & reactive power in α –β frame & the subsequent conversion of 3-phase quantities to 2-phase numbers form the basis of the theory. This proposed algorithm has 3-phase load currents & 3-phase load potentials are attached at the PCC.

Model predictive control (MPC): This theory is very popular algorithm for regulating PQ issues & also speedy-transient reaction. Including this, During potential spikes and dips, DC-DSTATCOM keeps the load potential steady at 1p.u. SAPF are utilized to improve the PCC potential, which makes system management more challenging..

Sliding Mode Controller (SMC): This controller is employed in DC-DSTATCOM current regulation, regulate the potential & to compensate load output current harmonics. To achieve the essential results in system, a discontinuous control signal is created using the SMC method.

Adaptive Neuro-Fuzzy Interference System (ANFIS): ANFIS control mechanism is implemented for 3-stage DSTATCOM to mitigate present-day PQ difficulties. ANFIS-LMS based control calculation is used to compare the dynamic & receptive force segments.

1.1.9 DC-DSTATCOM using artificial intelligence technique

The conventional *icosϕ* technique possesses a clustered weight in active and reactive part.

(i) The employment of a filter to obtain a noise-free weight, however, is an additional load with no guarantee of yielding a tuned value. These demerits of conventional *icosϕ* technique are overcome by suggested technique.

(ii) DBSCAN stands for density-based spatial clustering of applications with noise

(iii) This method was chosen because it is more efficient in terms of processing speed, memory usage, accuracy, power consumption, responsiveness, and ease of implementation.

1.1.10 IC-DSTATCOM using conventional control technique

The proposed scheme provides flexibility for further improvement for connecting additional converters. Improving the IFCT's compensation and stability structured a well-thought-out plan for matching the impedance of the DC-DSTATCOM and the converting transformer. Balancing of supply current, input supply current harmonics drop, balancing of load at output, improvent in power factor (pf), potential control are all examples of efficiency improvements. The following remarks are inference from the proposed IC-DSTATCOM scheme in accordance with the standard set by IEC- 61000-1& IEEE-2030-7-2018 grid data.

(i) Good convergence performance is obtained.

(ii) The main features of this algorithm are enhanced tracking, adaptive, and compensatory capacities.

(iii) The anticipated structure supports for accomplishing the numerous PQ issues like harmonics reduction, healthier potential regulation, PF rectification, load equalizing and reduction in DC link voltage etc.

(iv) It also provides the healthier protection over the harmonics.

(v) It is capable to restructure the additional parameters for improved version of algorithm.

1.1.11 various control strategies of IC-DSTATCOM:

Mainly there are two varieties of control strategies used for IC-DSTATCOM such as conventional & adaptive techniques. The different conventional control techniques are SRF theory, instantaneous reactive power theory, freeze power theory, $i\cos\varphi$ technique and so on. Likewise the different adaptive control technique such as artificial neural network technique, adaptive least mean square technique, and different types of kalmon's filtering technique are there. Hence in our work $i\cos\varphi$ control technique is chosen from conventional and DBSCAN control technique is chosen from adaptive control techniques for better comparison which are discussed in the chapters 3, 4, 5 respectively.

1.1.12 IC-DSTATCOM using Artificial intelligence technique:

This inductively coupled topology is made some advancement by using artificial intelligence technique in the place of conventional technique. The suggested AI controllers for DC-DSTATCOM are NN based one-cycle controllers. The PQ issues are generally rising due to the existence of uneven loads. An improved source current waveform can be generated using ANN and ANFIS-based approaches, which can also be used to determine & display non-direct frameworks & consequently better PQ.

1.1.13 DBSCAN Control algorithm:

Density-Based Spatial Clustering of Applications with Noise is a widely used clustering algorithm in data mining and machine learning.

Working:

Density-Based Clustering: DBSCAN means clusters as dense regions of data points divided with areas of lowest point density. Unlike some other clustering algorithms like K-Means, DBSCAN does not require specifying the number of

clusters beforehand.

Core Points: In DBSCAN, a core point is has at least a minimum number of other data points within a certain radius (specified by another parameter, often denoted as **`eps`** or ε) around it. These core points are considered the "seeds" of clusters.

Density-Reach ability: A point A is said to be density-reachable from a point B when there is a chain of data points connecting them, where each point in the chain is within ε distance of the previous point. This defines the notion of connectivity between points.

Density-Connected: Two points are density-connected when there exists a common data point from which they are both density-reachable. Density-connected points belong to the same cluster.

Implementation issues:

1. Choosing parameters

2. Scalability

3. Handling high dimensional data

4. Sensitivity to density

Table 1.1 Comparative analyses between different control strategies for DSTATCOM

S.No	Control algorithms	Advantages	Disadvantages
1	Synchronous reference frame Theory	(i) This technique is engaged for both reactive power compensation & harmonics attenuation. (ii) Enhanced performance to achieve UPF.	(i) PLL's functioning is sluggish & causes some delays in computation. (iii)Mathematical analysis is more & not fit for 3P4W systems
2	Instantaneous Reactive power Theory	(i) It has good Computational Complexity, (ii) Requires sophisticated conversion in addition to handling with the power components	(i) Filtering power signals with a LPF causes computation delays. (ii) This concept derives immediate active and reactive powers from volt signals.

3	Model Predictive Control	(i) To mitigate the existing PQ issues, MPC of NNPC DSTATCOM is deployed & to keep the potential stable across each flying capacitor. (ii) This algorithm has a low barrier to entry and delivers satisfactory dynamic and steady-state responses.	(i) The cost function is modified by adding weights for two extra constraints.
4	Sliding Mode Controller	(i) SMC strengthens the system's resistance to fluctuations and external shocks, keeping it stable. (ii) The source current's harmonics can be eliminated with this.	(i)Because of resonance issues & rigid correction in this filters, CPDs are accessible now to address PQ problems.
5	ANFIS algorithm	(i) Under both static and fluctuating loads, ANFIS-LMS performs admirably. (ii) This algorithm has been tested & shown to successfully perform potential regulation, load balancing, harmonic distortion & UPF.	(i) It does not perform well under non-ac potentials.
6	Artificial Intelligence Based Controllers	(i) This helps with current-related PQ problems & reactive power adjustment. (ii) quicker reactions, small size	(i) High cost of implementation (ii) Lack of creativity

The comparison table motivates in the research study to analyze the behavior for IC-DTATCOM by using conventional and adaptive techniques. This adaptive technique is selected based upon better convergence characteristics, parallel processing, flexibility, robust nature, self-organization properties.

CHAPTER-2

CHAPTER 2

LITERATURE REVIEW

A custom power specification may include provisions for (i) zero power disturbance (ii) healthy potential regulation including short interval drops or bloats (iii) zero harmonic voltage & (iv) Non linear loads without any effect on input potential. DSTATCOM is a CPD utilized for PQ change within dissemination framework. Over the last decade, there is lot of research works are implemented on DC-DSTATCOM to improve the power quality in EPDS. Different control techniques are implemented for healthy operation of DC-DSTATCOM. Initially conventional techniques like SRF, IRPT, *icosø* are implemented and got satisfactory results in direct DC-DSTATCOM, and then AI techniques are incorporated to get the efficient results. After that researchers take look into IC-DSTATCOM with conventional and AI techniques.

2.1 Working of DSTATCOM

In general, the DC-DSTATCOM is regarded as DSTATCOM to understand the working principle of DC-DSTATCOM the following points are explained

(i) The DC-DSTATCOM is a shunt compensator which is used to supply or absorb the reactive power.

(ii) When DC-DSTATCOM connected at the PCC for the capacitive load it absorbs the reactive power, where-as for inductive load the DC-DSTATCOM supplies the reactive power.

(iii) This DC-DSTATCOM can be used for both load and source side compensation.

(iv) For the load side compensation source current is taken as the reference & the THD of the load current will be reduced.

(v) For the source side compensation load current is taken as the reference & the THD of the source current will be reduced.

2.2 DSTATCOM with conventional techniques

M.Mangaraj et al. shows how *icosø* and naive back propagation-based *icosø* control techniques can be compared to one another in DC-DSTATCOM evaluations for 3P3W EPDS [30]. Harmonic elimination has been used to prove

how well a design performs under both constant and variable loads over time. NBP controlled *icosø* technique based DC-DSTATCOM performs better than *icosø* technique.

Bhim singh et al. outlines various DC-DSTATCOMs structures, and how they work together for power quality enhancement. This paper is aimed to explore a broad perspective on DC-DSTATCOMs to researchers [5].

M.Mangaraj et al. shows how *icosø* and conjugate gradient back propagation-based icosø control techniques can be compared to one another in DC-DSTATCOM evaluations [31]. From all comparisons CGBP based *icosø* control technique can be provide better economical solution for PQ issues with effectively.

M.Mangaraj et al. illustrates two special compensation algorithms are assessed for the analysis of 3P3W potential source converter-based DC-DSTATCOM [32]. Those are *icosϕ* control technique & Levenberg– Marquardt back propagation-based *icosϕ* control technique. Using the LMBP method, the system's PQ is improved by retaining a less potential across the capacitor. This technique accomplishes lessening in the size of the DC-DSTATCOM.

Bhim singh et al. describes a comprehensive review of active filter configurations, control strategies, selection of components, other related economic and technical considerations, and their selection for specific applications [72]. It is aimed at providing a broad perspective on the status of AF technology to researchers.

M.Mangaraj et al. illustrates a simple positive sequence detector based control strategy is used [34]. As the load currents are unbalanced and distorted, therefore the voltages at PCC are unbalanced and distorted. If these PCC voltages are used for generating the filter current references, the control strategy results in erroneous compensation. To eliminate this restriction of the control strategy; positive sequence voltages of the PCC voltages are extracted and provide reference supply current by using such type of control algorithm for DC-DSTATCOM.

Bhim singh et al. describes the *icosø* method is customized for regulating the DC-DSTATCOM for pf modification and zero potential regulation at PCC with indirect current control technique [26].

M.Mangaraj et al. illustrates a hybrid method named quasi-Newton back-

propagation based *icosϕ* control algorithm [35]. Its framework is based on biological concepts such as input neuron, target neuron, and weight adjustment & its parallel computing, learning capacity make it more appealing.

M.Mangaraj et al. describes a dual potential source inverter-based DC-DSTATCOM to develop the PQ of power system [42]. The reactive power is regulated by a pair of two levels VSI in the projected DC-DSTATCOM. One is main VSI and the other is auxiliary VSI. The *icosϕ* control structure is engaged to feed the reference source currents.

S.Puspanjali et al. proposes a hybrid synchronous reference frame method has been proposed for the DSTATCOM to enhance the compensation performance [13]. This controller is designed in such a way that it generates the reference with respect to the change in load to reject the harmonics.

M.Mangaraj et al. describes a back to back connected ZSI is presented for PQ upgrading in an EPDS [51]. The modulation index and possible boost inversion capabilities of BB-ZSI are both quite high.

M. K. Mishra et al. describes a single VSC with a battery–super capacitor energy storage system combines the operation of DSTATCOM and UPS [53]. The system mitigates the load current harmonics, unbalance, and reactive power during normal voltages.

M.Mangaraj et al. describes a control strategy named naive back propagation standard *icosϕ* is executed in DC-DSTATCOM [63]. Conducted a comparison between the proposed & *icosϕ* method under different load condition to examine the DC-DSTATCOM in the 3P3W EPDS. The outcomes prove the superiority of the proposed method over the conventional one.

M. K. Mishra et al. describes a dual voltage source inverter (DVSI) scheme. The proposed scheme is comprised of two inverters, which enables the microgrid to exchange power generated by the distributed energy resources (DERs) and also to compensate the local unbalanced and nonlinear load.

S.B Karanki et al. describe a topology for DC-DSTATCOM with non-stiff source [1]. The proposed topology allows for a lower dc-link potential in DC-DSTATCOM without sacrificing compensatory capability. In addition to the shunt filter capacitor and the interconnecting inductor, a series capacitor is used.

A.Devanshu et al. developed a device called DC-DSTATCOM and its control

is implemented [8]. For the elimination of current harmonics of a 3P3W EPDS, a rectified resistive & inductive load is used. Here they are used SRF control theory.

Q.Liu et al. proposes an inductive filtering-based parallel operating transformer with a shared filter to improve the PQ at the grid-connected step-up station of a wind farm [9]. The proposed transformer together with the shared filter has the merits of less installation space, higher equipment utilization, and better filtering performance compared with the conventional scheme.

T.M.Tamiz et al. proposes a HAPF has been used in EPDS [11]. A HAPF is designed to improve the filtering performance of the passive filter and reduce the VA rating of the active filter. In this proposed filter to operate the active filter in variable harmonic conductance mode a seventh harmonic tuned passive filter is connected in series with the active filter. The results obtained from both the model are compared. It is effective in improving the THD for current and voltage from 8.38% to 2.64% and 8.32% to 3.15%.

E.Lei et al. proposes an improved transformer winding tap injection DSTATCOM for medium-potential reactive power reparation [14]. For closed-loop control of current, a nonlinear passivity-based control method is developed & a 3-layer potential balancing regulating strategy is applied to stable the dc capacitor potential.

B.Nageswar rao et al. recommends a concept for SAPF using a single power source fed to a cascaded multilevel inverter with 3-φ transformers [17]. Apart from traditional transformer based topologies, the required number of transformers is substantially reduced, resulting in less space requirement, which leads to low cost and simple control system.

Yong Li et al. recommends an industrial DC supply system with the 4-winding inductively filtered rectifier transformer. Which may efficiently address the PQ issues plaguing the majority of high-power rectifier systems [18].

J.Yu et al. recommends an impedance-match design format of the enhanced IAPF, which is good to enhance compensation accuracy, perturbation rejection ability and stability, is proposed for EPDS connected with nonlinear loads [19]. The topology that consists of an IFCT and a SAPF is proposed.

S.D.Swain et al. recommends a new controller design using sliding-mode controller-2 is proposed to make the Hybrid Series Active Power Filter (HSAPF)

more robust and stable [21]. An accurate averaged model of a three-phase HSAPF is also derived.

Yong Li et al. recommended an IAPF method to comprehensively improve the PQ for the EPDS (nonlinear load) connected to the network [22]. A unique filtering mechanism of the IAPF method is revealed in theory.

P.W.Sun et al. recommended this paper presents a new type of cascade inverter based on dual buck topology and phase-shift control scheme [25]. Compared to traditional cascade inverters, it has much enhanced system reliability thanks to no shoot-through problems and lower switching loss with the help of using power MOSFETs.

A.Chandra et al. recommends a control structure for a 3-phase SAPF to control load potential, remove harmonics, good source PF, and stable the non-linear loads [80]. A carrier wave PWM controller is applied over the base & actual supply currents to produce gate signals to IGBTs.

C.Kumar et al. describes a new control-algorithm-based multifunctional DC-DSTATCOM is proposed to operate in potential control mode under stiff source [90]. This scheme provides fast potential regulation at the load terminal during potential disturbances & protects critical loads.

M.V Manoj et al. present a dual voltage source inverter scheme to enhance the PQ and reliability of the micro-grid system [7]. The proposed scheme is comprised of two inverters, which enables the micro-grid to exchange power generated by the distributed energy resources and also to compensate the local unbalanced and nonlinear load. The control algorithms are developed based on instantaneous symmetrical component theory.

H. Myneni et al. proposes a simple control algorithm for LCL-filter-based DC-DSTATCOM for PQ improvement [15]. The proposed algorithm is able to operate DSTATCOM in both current control mode and POTENTIAL control mode by controlling PCC voltage. Achieved THDs of 3.3%.

In grid-connected systems, HRES such as photovoltaic systems, wind turbines, and battery energy storage systems are producing PQ issues. To address such challenges in the HRES system, G.S Rao et al. is suggested an Atom Search Optimization in conjunction with a Unified Power Flow Controller [33].

A. Michaelides et al. examines the possibility to exploit the inductance of

wound aluminum foil capacitors in order to realize an integrated component [6].

P.Salameran et al. proposes a control algorithm for a three-phase hybrid power filter is proposed. It is constituted by a series active filter and a passive filter connected in parallel with the load [23].

A.Tiwari et al. manages operation and control of a dispersion static synchronous compensator (DSTATCOM) for power quality change in offbeat machinebased disseminated era as the nonconcurring generator has poor voltage regulation exceptionally, throughout top burden conditions [27].

2.3 DSTATCOM with AI techniques

M.Mangaraj et al. illustrate the relative evaluation of DC-DSTATCOM with Adaptive Least Mean Square and Hebbian least mean square (HLMS) scheme for 3P3W EPDS [24]. As a result of this analysis, the HLMS controller will consistently outperform under all loading scenarios.

M.Mangaraj et al. describes the system performance, including DC-DSTATCOM using both ALMS and Kernel Hebbian Least Mean Square (KHLMS) control techniques [41]. The competencies of KHLMS over ALMS control algorithm based on its leaning pattern are discussed in terms of various PQ issues. Experimental results showed that the proposed KHLMS could improve the robustness of PQ under the different event of loading than ALMS algorithm.

M.Mangaraj et al. describes a ANN-based control scheme is used for the VSI and merged with an suitable transformer to improve the shunt compensation ability & reliable operation [51].

S.R.Arya et al. designed a 3-leg VSC based DC-DSTATCOM is implemented by using ANN based control algorithm for harmonics suppression, load balancing & potential regulation in 3P3W system with a battery energy storage system [44].

M.Mangaraj et al. describes a control approach is implemented to investigate the performance of a DC-DSTATCOM in a 3-phase balanced nonlinear load fed by a 3-phase AC [65].

M.Mangaraj et al. worked to conceptualize and simulate a VSI based DC-DSTATCOM for a 3-phase AC feeds to all loads [93]. NN based DC-DSTATCOM was implemented, to keep proper DC link potential.

Density-based spatial clustering of applications with noise (DBSCAN) is a

typical kind of algorithm based on density clustering in unsupervised learning. It can cluster data of arbitrary shape and also identify noise samples in the dataset. W.Lai et al. proposed to optimize the DBSCAN parameters [37]. Multi-verse optimizer algorithm, a special variable updating method with excellent optimization performance, is selected and improved for optimizing the parameters of DBSCAN.

S.R.Arya et al. deals with leaky least mean square-based control algorithm for a 3-phase DC-DSTATCOM to lessen reactive power, harmonics, load un-balancing [45]. The proposed scheme is executed to removal of adjusted weights of active & reactive power elements.

Bhim singh et al. outlines various DC-DSTATCOMs structures, and how they work together for power quality enhancement. This paper is aimed to explore a broad perspective on DC-DSTATCOMs to researchers [96].

T.Ouyang et al. proposes a new rule-based modeling approach, which utilizes DBSCAN-based information granules to construct the rules [36]. First, bear in mind the advantages of density-based clustering; this is proposed to generate data structures.

M.Srinivas et al. deals with LMS–LMF based control scheme [43]. The suggested control method combines features found in the LMF and the LMS, It aids in quick, precise responses because to a robust structure.

R.K.Agarwal et al proposes an application of a least mean-square (LMS)-based neural network structure [61]. This admittance LMS-based NN structure has a simple architecture which reduces the computational complexity and burden which makes it easy to implement.

A.K Panda et al. proposes new hybrid control technique called gradient descent back propagation (GDBP)-based *icosø* for a three phase two-level distribution static compensator (DSTATCOM) to perform the functions [38]

Mustakim et al. conducted two experiments, first experiment is Density-Based Spatial Clustering of Applications with Noise (DBSCAN) without dimensional reduction and second experiment is DBSCAN clustering with dimensional reduction using Principal Component Analysis (PCA) [47].

M.Mangaraj et al describes the Hebbian least mean square controller is

employed on the various aspects such as, weight updating, direct and quadrature unit voltage template, active and reactive part of reference supply currents and switching signal generation [52].

Badoni et al. proposes the real-time implementation of a three-phase distribution static compensator (DSTATCOM) using adaptive neurofuzzy inference system least-mean-square (ANFIS-LMS)-based control algorithm for compensation of current-related power quality problems

2.4 Research Gaps and motivation

(i) Most of the control strategies like SRF, IRPT, *icosø* and AI based algorithm for two levels DC-DSTATCOM have been designed for low and medium voltage application which were reported in many research works.

(ii) Above all techniques are developed for direct coupled structure. But these methods are also facing different problems like additional losses, temperature increase, vibration, and noise.

(iii) To enhance the performance of DSTATCOM, there is a necessity to develop an IC-DSTATCOM.

(iv) To achieve better operation of IC-DSTATCOM, the weights- updating algorithm can be included in the traditional neural network technique.

(v) Keeping all these motivation in mind some design approaches with adaptive control algorithm is selected on the basis of voltage regulation, potential balancing, source current harmonics reduction, power factor improvement for the different load changing condition

2.5 Research objectives

(i) To identify and develop a control scheme for existing DC-DSTATCOM structure for inductively coupled loads.

(ii) Implementation of AI based techniques for the identified control scheme.

(iii) To achieve the Proposed IC-DSTATCOM in generating switching signals followed by the extraction of reference currents for the harmonic reduction in distribution network.

(iv) To analyze and compare IC-DSTATCOM with minimum dc-link voltage for shunt compensation in distribution network.

CHAPTER-3

CHAPTER 3

VSI BASED DSTATCOM USING *ICOSϕ* CONTROL TECHNIQUE

3.1. Introduction

The proportion of Power Electronics & Microprocessor based non linear load in the EPDS has been increasing in recent years. Including these, Electric Vehichle charging station, electric traction as well as renewable energy system are also playing a growing role in the EPDS. Hence, improvement for sustainability and flexibility of EPDS is very challenging and important task for such scenarios. As a result, possibility of quality power delivery to the consumers using improved technology will make EPDS very attractive.

Of course, lot of researchers are done very good research on DC-DSTATCOM with self-supported capacitance. The main advantages of DC-DSTATCOM: (i) It achieves reduced static error and quick convergence characteristics, (ii) The features like robustness, tracking capabilities under adjustable loading periodicity are obtained. But in DC-DSTATCOM, the point of common coupling (PCC) possesses various severities due to the direct connection of DSTATCOM, supply and load. Hence, flow of short circuit current, poor protection, some thermal losses are occurred.

Due to these drawbacks of DC-DSTATCOM, nowadays the development was started in the area of IC- DSATCOM. It is obtained by connecting the non-linear loads to the source through a coupling transformer. It bears number of merits such as less switching stress, flexibility, controllability, improved balance voltage at PCC, increasing the compensation capability, and different possible combinations for extension etc. DC-DSTATCOM design considerations suggest that split capacitor architecture and self-supported capacitors work well for 3P3W EPDS. But, The 3-leg VSC architecture is frequently proposed because of its own widespread acceptance in the literature.

As the aforementioned DC-DSTATCOM undergoes further development, the requirement for an IC-DSTATCOM is expected to increase, allowing it to function more effectively in practise. Here the transformer kVA rating identical to the essential reactive power insertion is necessary. Yet, the inductive transformer creates separation between load and system. DC-DSTATCOM can be configured in different ways by using number of transformers.

The projected techniques provides flexibility for further improvement for connecting additional inverters & loads. Improving the IFCT's compensation & stability structured a well-thought-out plan for matching the impedance of the DC-DSTATCOM and the converting transformer. Balancing of supply current, input supply current harmonics drop, balancing of load at output, improvent in power factor (pf), potential control are all examples of efficiency improvements.

The filtering system is completed by subsequent generalized mathematical structure using $icos\emptyset$ algorithm using MATLAB/ Simulink.The subsequent conclusions can be drawn from the proposed IC-DSTATCOM scheme's control algorithm;

- Improved convergence performance can be achieved.
- This algorithm's most notable features are its enhanced tracking, adaption & compensation abilities.
- Suggested structure for accomplishing the number of PQ issues those are harmonics drop, helthier potential regulation, pf modification and lesser DC link potential of the IC-DSTATCOM etc.

3.2. MODELING OF THE PROPOSED IC-DSTATCOM

The arrangement of the 3P3W EPDS with DC-DSTATCOM and IC-DSTATCOM are portrayed in Fig.3.1 & 3.2 respectively. The DC-DSTATCOM which covers of a stable 3-phase supply, DSTATCOM, 3-phase non-linear load. Whereas The IC-DSTATCOM which consists of a balanced 3-phase supply, converter transformer DSTATCOM, three-phase non-linear load. The VSI linked at PCC of EPDS is exposed in Fig. 3.3. A customized technique of DC-DSTATCOM & IC-DSTATCOM are utilized as a compensator to moderate the PQ disputes. triggering signals for the IGBTs of both compensator are engendered by the $icos\phi$ technique.

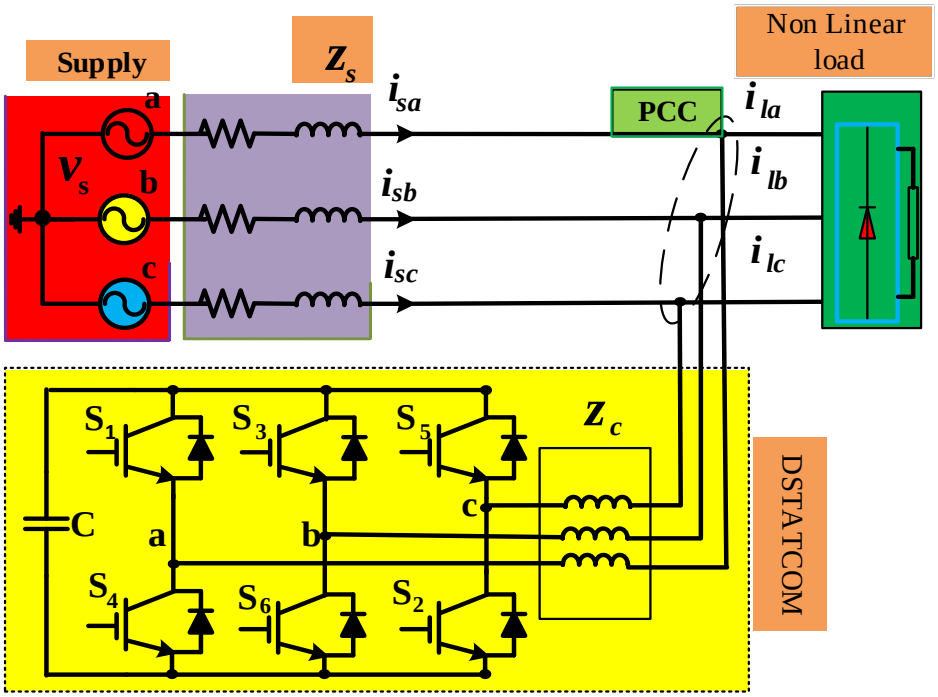

Fig. 3.1 EPDS with DC- DSTATCOM

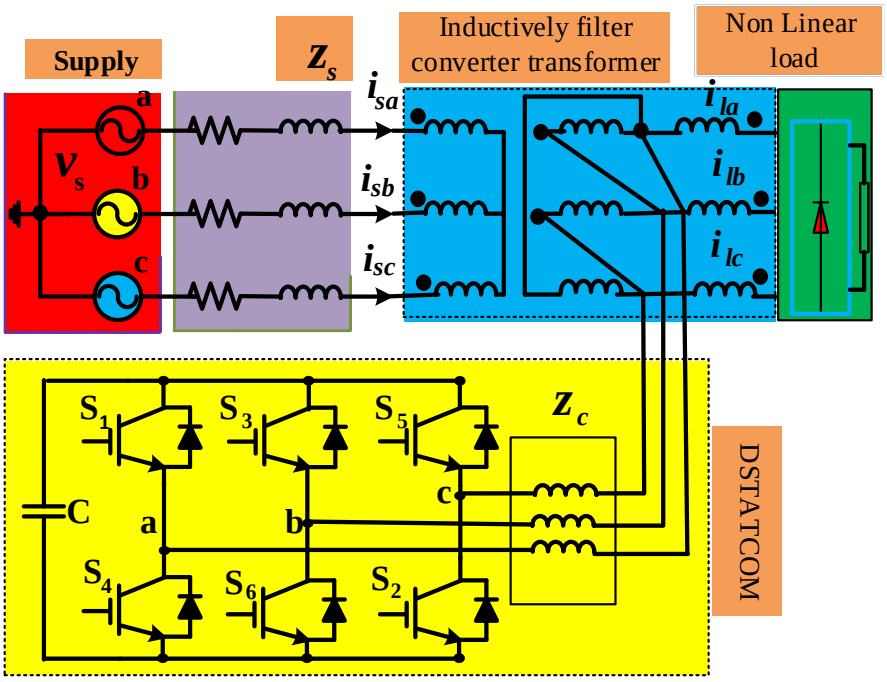

Fig. 3.2 EPDS with IC- DSTATCOM

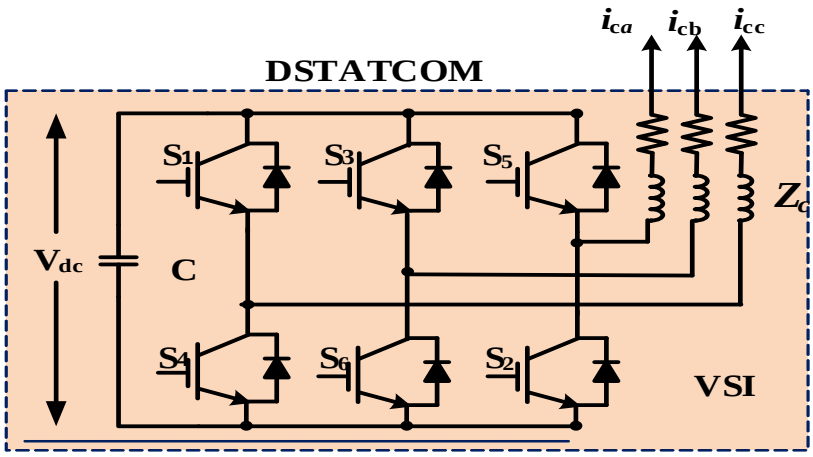

Fig. 3.3 Two-level self-supported capacitor supported VSC based DSTATCOM

The study's main goal is to pick the scrupulous structure by applying *icosϕ* control algorithm.

3.3 MODELLING AND DESIGN OF INDUCTIVE TRANSFORMER

The full winding structure of projected IC-DSTATCOM was exposed in Fig.3.1. The projected IC-DSTATCOM arranges inductively filter converting transformer (IFCT), DSTATCOM consisting VSC & load. The IFCT plan has three winding which are used to connect DSTATCOM and non-linear load. In 3 windings, the primary winding (PW) allotted to grid with star connection, secondary side winding (SW) allocated to non-linear load with star connection & the filtering winding (FW) allocated to DSTATCOM with delta type wiring. The special winding of IFCT aimed to get the balanced potential between grids, DSTATCOM & load. In the following sections, we'll learn deeper about the IFCT's mathematical model and filtering method.

The voltage balance mathematical equation is shown below, [19]

$$\begin{cases} N_1 \mathrm{i}_{\mathrm{ap}} + N_2 \mathrm{i}_{\mathrm{as}} + N_3 \mathrm{i}_{\mathrm{af}} = 0 \\ N_1 \mathrm{i}_{\mathrm{bp}} + N_2 \mathrm{i}_{\mathrm{bs}} + N_3 \mathrm{i}_{\mathrm{bf}} = 0 \\ N_1 \mathrm{i}_{\mathrm{cp}} + N_2 \mathrm{i}_{\mathrm{cs}} + N_3 \mathrm{i}_{\mathrm{cf}} = 0 \end{cases} \quad (3.1)$$

As per KCL, the current equations are written as [19]

$$\begin{cases} \mathrm{u}_{\mathrm{abf}} = (i_{zb} - i_{za}) * Z_o \\ \mathrm{u}_{\mathrm{bcf}} = (i_{zc} - i_{zb}) * Z_o \\ \mathrm{u}_{\mathrm{caf}} = (i_{za} - i_{zc}) * Z_o \end{cases} \quad (3.2)$$

$$\begin{cases} \mathrm{i_{ap}} = (u_{sa} - u_{apo})/Z_{line} \\ \mathrm{i_{bp}} = (u_{sb} - u_{bpo})/Z_{line} \\ \mathrm{i_{cp}} = (u_{sc} - u_{cpo})/Z_{line} \\ \mathrm{i_{as}} = i_{al} + i_{zal} \\ \mathrm{i_{bs}} = i_{bl} + i_{zbl} \\ \mathrm{i_{cs}} = i_{cl} + i_{zcl} \\ \mathrm{i_{ap}} + i_{bp} + i_{cp} = 0 \\ \mathrm{i_{as}} + i_{bs} + i_{cs} = 0 \\ \mathrm{i_{af}} + i_{bf} + i_{cf} = 0 \\ \mathrm{i_{af}} = i_{cf} + i_{cat} = i_{cf} + i_{ra} + i_{za} \\ \mathrm{i_{bf}} = i_{af} + i_{cbt} = i_{af} + i_{rb} + i_{zb} \\ \mathrm{i_{cf}} = i_{bf} + i_{cct} = i_{bf} + i_{rc} + i_{zc} \end{cases} \tag{3.3}$$

$$\begin{cases} \mathrm{u_{apo}} - \dfrac{\mathrm{N_1}}{\mathrm{N_3}}\mathrm{u_{abf}} = \mathrm{i_{ap}z_p} - \dfrac{\mathrm{N_1}}{\mathrm{N_3}}\mathrm{i_{af}z_f} \\ \mathrm{u_{bpo}} - \dfrac{\mathrm{N_1}}{\mathrm{N_3}}\mathrm{u_{bcf}} = \mathrm{i_{bp}z_p} - \dfrac{\mathrm{N_1}}{\mathrm{N_3}}\mathrm{i_{bf}z_f} \\ \mathrm{u_{cpo}} - \dfrac{\mathrm{N_1}}{\mathrm{N_3}}\mathrm{u_{caf}} = \mathrm{i_{cp}z_p} - \dfrac{\mathrm{N_1}}{\mathrm{N_3}}\mathrm{i_{cf}z_f} \end{cases} \tag{3.4}$$

As per multi-winding transformer theory,the potential transfer equations are obtained in eqn 3.4 [19].

3.4 PROPOSED *ICOSϕ* CONTROL METHOD

The constructed control scheme is structured in Fig. 3.4. To feed the reference input supply current, which aims for a good pf and harmonics distortion, the 3-phase non-linear output current is used. The gate signals are generated with the help of *icosϕ* controller for switching operation of inverter. Fig 3.5 depicts the *icosϕ* control algorithm's internal control signal.The gate signals are generated in 4 stages for controlling the DC-DSTATCOM as well as IC-DSTATCOM

(i) The base quantity of the 3-ϕ output load currenti_L is figured by means of fourier system.

(ii) The method used to generate the active & the reactive components of load output current is described.

(iii) The output ampers' active & reactive parts are used after the topology to breed the reference supply currents.

(iv) The sum of the output current's active and reactive components was fed to the HCC, which powers the switching pulses..

In terms of fundamental output current, i_{lap} can be stated as the active power component as

$$\begin{bmatrix} i_{lap} \\ i_{lbp} \\ i_{lcp} \end{bmatrix} = \begin{bmatrix} Re(i_{la}) \\ Re(i_{lb}) \\ Re(i_{lc}) \end{bmatrix} = \begin{bmatrix} i_{la}cos\phi_{la} \\ i_{lb}cos\phi_{lb} \\ i_{lc}cos\phi_{lc} \end{bmatrix} \quad (3.5)$$

The weighted mean worth of the real active power module w_p

$$w_p = \left(\frac{i_{la}cos\phi_{la}+i_{lb}cos\phi_{lb}+i_{lc}cos\phi_{lc}}{3}\right) \quad (3.6)$$

The 'Q' component can be stated

$$\begin{bmatrix} i_{laq} \\ i_{lbq} \\ i_{lcq} \end{bmatrix} = \begin{bmatrix} Im(i_{la}) \\ Im(i_{lb}) \\ Im(i_{lc}) \end{bmatrix} = \begin{bmatrix} i_{la}sin\phi_{la} \\ i_{lb}sin\phi_{lb} \\ i_{lc}sin\phi_{lc} \end{bmatrix} \quad (3.7)$$

The weighted mean worth of reactive power module w_q

$$w_q = \left(\frac{i_{la}sin\phi_{la}+i_{lb}sin\phi_{lb}+i_{lc}sin\phi_{lc}}{3}\right) \quad (3.8)$$

The v_{de} is fed to PI controller & its output is equated

$$w_{dp} = k_{pdp}v_{de} + k_{idp}\int v_{de}dt \quad (3.9)$$

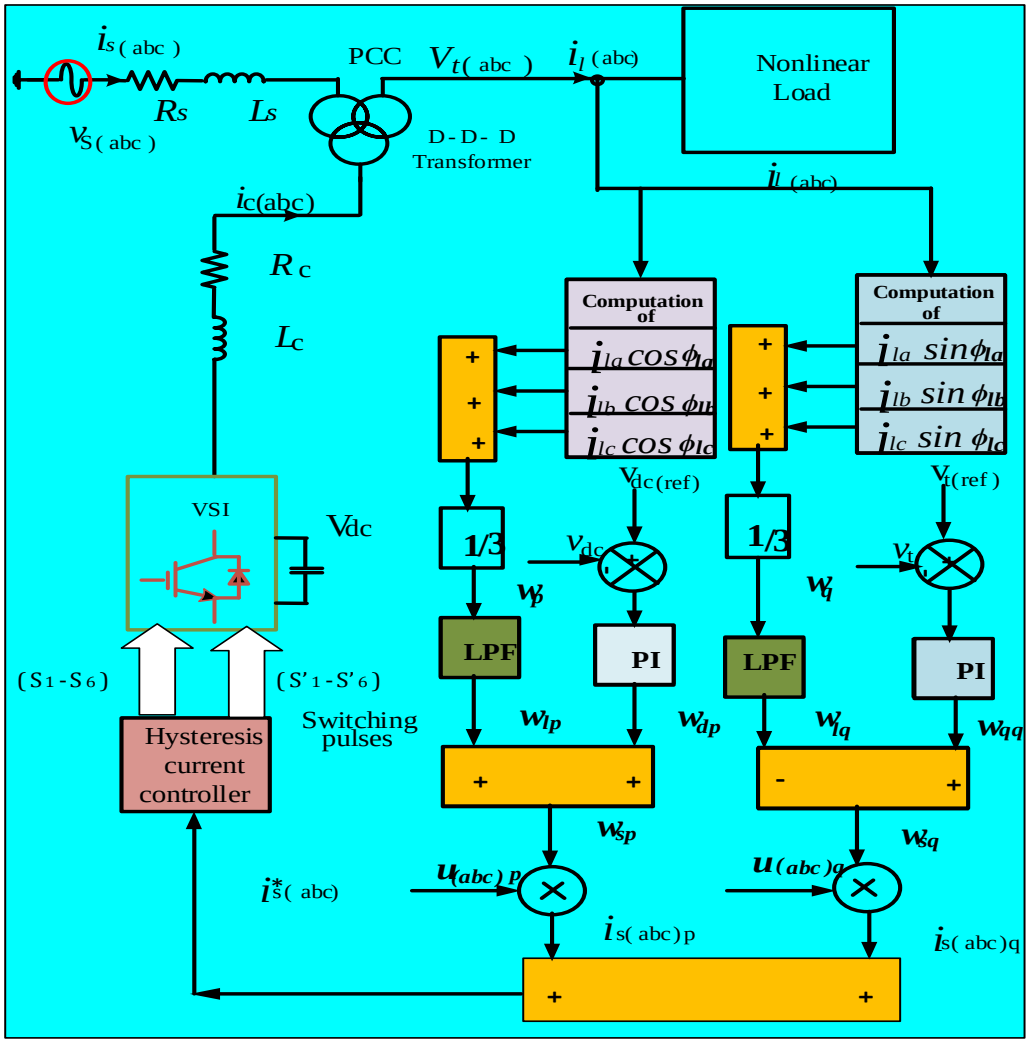

Fig. 3.4 Switching signals generation for IC-DSTATCOM

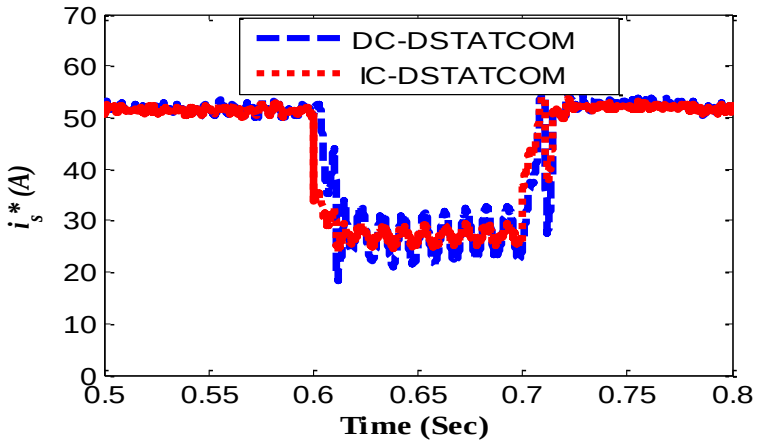

Fig. 3.5 inside control signal of the control technique

The median value of active & reactive weighted modules is 'w_p', 'w_q'correspondingly. The'w_p', 'w_q' are the clustered weight and no assurance to give an adjusted value. These boundaries are overwhelmed by suggesting the LPF exposed in the Fig. 3.4. These masses are handled from LPF & mitigate larger harmonics element. Thus, the tuned mass active element (w_{spt}) & reactive element (w_{sqt}) of the output current are attained. At last, the advised commanding scheme is directed to bring a filtered and adjusted mass. The adjusted mass is less disturbed with noise so it become more stable & also fit to any disturbance occupied on the network, with the PCC's compensated current can be immunized. The overall active elements of reference supply input current.

$$w_{spt} = w_{dp} + w_{lp} \tag{3.10}$$

In the identical way, the entire reactive factors can be computed

$$w_{sqt} = w_{qq} - w_{lq} \tag{3.11}$$

A low frequency pass filter which cut of rate was 20.5 Hz applied for filtering of output current.

Instantneous worth of input currents i_{sp}, is stated as

$$\begin{bmatrix} i_{sap} \\ i_{sbp} \\ i_{scp} \end{bmatrix} = w_{spt} \begin{bmatrix} u_{ap} \\ u_{bp} \\ u_{cp} \end{bmatrix} \tag{3.12}$$

Instantneous worth of reactive supply currents i_{sq}, can be stated as

$$\begin{bmatrix} i_{saq} \\ i_{sbq} \\ i_{scq} \end{bmatrix} = w_{sqt} \begin{bmatrix} u_{aq} \\ u_{bq} \\ u_{cq} \end{bmatrix} \tag{3.13}$$

Atlast the refernce input currents can be illustrated as

$$\begin{bmatrix} i_{sa}^{*} \\ i_{sb}^{*} \\ i_{sc}^{*} \end{bmatrix} = \begin{bmatrix} i_{sap} \\ i_{sbp} \\ i_{scp} \end{bmatrix} + \begin{bmatrix} i_{saq} \\ i_{sbq} \\ i_{scq} \end{bmatrix} \tag{3.14}$$

Both the actual & base input currents ($i_{sa,}i_{sb}, i_{sc}$), ($i_{sa}^{*}, i_{sb}^{*}, i_{sc}^{*}$) of corresponding phases are matched, and then errors are sent to HCC. It is widely applied here due to: simple to develop & diminishes the hardware complications. The following is the procedure to be followed:

When$i_{sa} < i_{sa}^{*}$, $s_1$is ON and s_4 is OFF (ii) when$i_{sa} > i_{sa}^{*}$, $s_1$is OFF and s_4 ON

3.5 SIMULATION OUTCOMES & ANALYSIS:

The EPDS is fed by a sinusoidal balanced potential 230V/phase with an input inductance 2mH and an input resistance 0.5Ω. The constraints taken for the simulation of both DC-DSTATCOM & IC-DSTATCOM using icos$\boldsymbol{\phi}$ algorithm is given in the Table-3.2. Simulation outcomes are structured by MATLAB and the outcomes are validating to picking the right technique for EPDS. The performance of IC-DSTATCOM for PQ betterment, equated with DC-DSTATCOM, which is structured here in the following sub-sections

3.5.1 Simulation results of DC-DSTATCOM

The DC- DSTATCOM is avoiding output load output current deviations with great %THD to pass into supply path & enlightening the pf. The proposed DC-DSTATCOM controller's effectiveness and feasibility have been demonstrated in various scenarios. . It was tested in response to a 0.6-second spike in the mean DC-link potential of the VSC (681 to 750 V). The steady-state & transitory reaction of VSI is showed in Fig. 3.6 (a), from up to down supply potential, supply current, output current, DTATCOM current & DC-link potential.

Hence, DC-DSTATCOM can be improved power factor and diminished THD at source side. Later parallel compensation, the PF is progressed to 0.94 & THD% is 4.51 which portrayed in Fig. 3.6 (b). The output current THD% 27.91 portrayed in Fig. 3.6 (c).

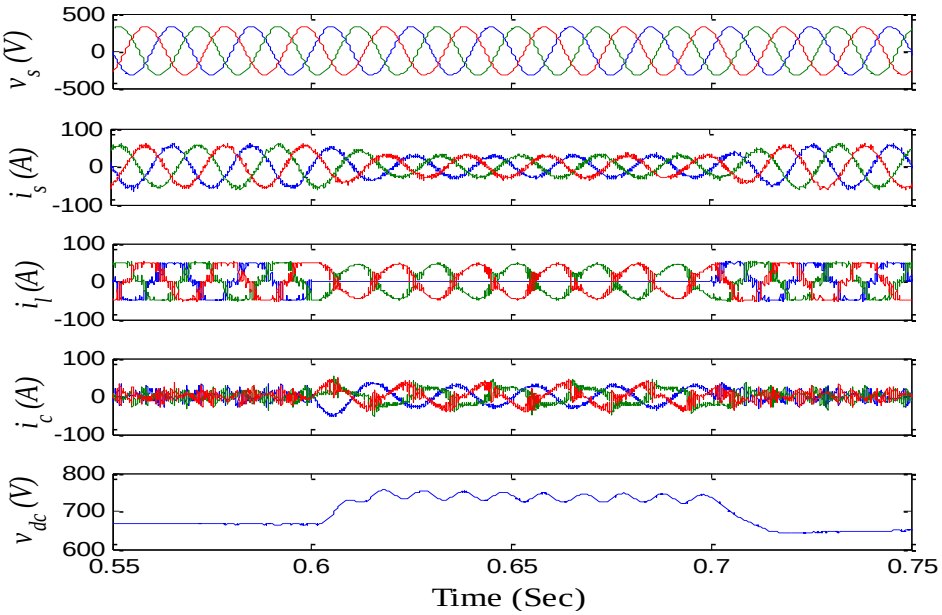

Fig. 3.6 a Waveform of three phase input potential, supply current, output current, DSTATCOM current & DC potential with DC- DSTATCOM.

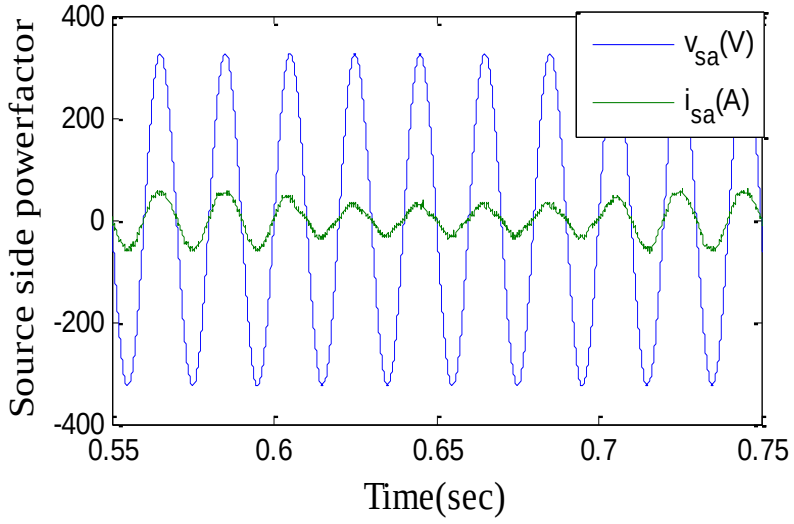

Fig. 3.6 b Source side powerfactor with DC- DSTATCOM

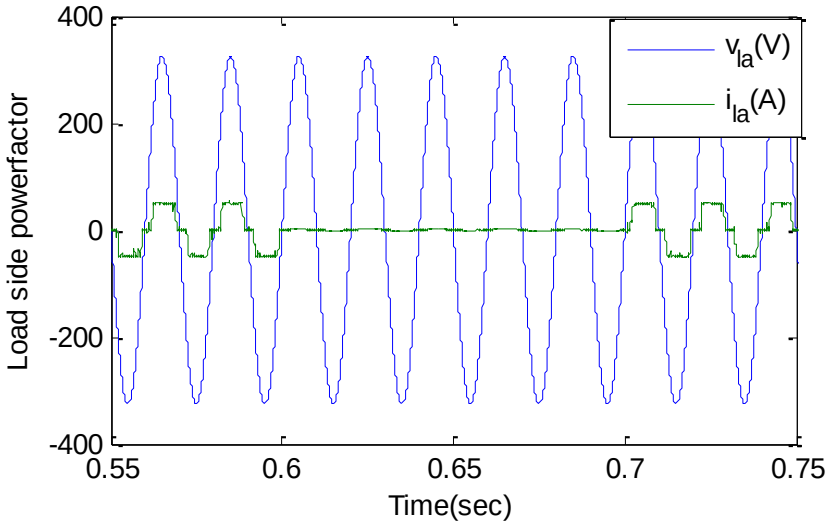

Fig. 3.6 c Load side powerfactor with DC- DSTATCOM

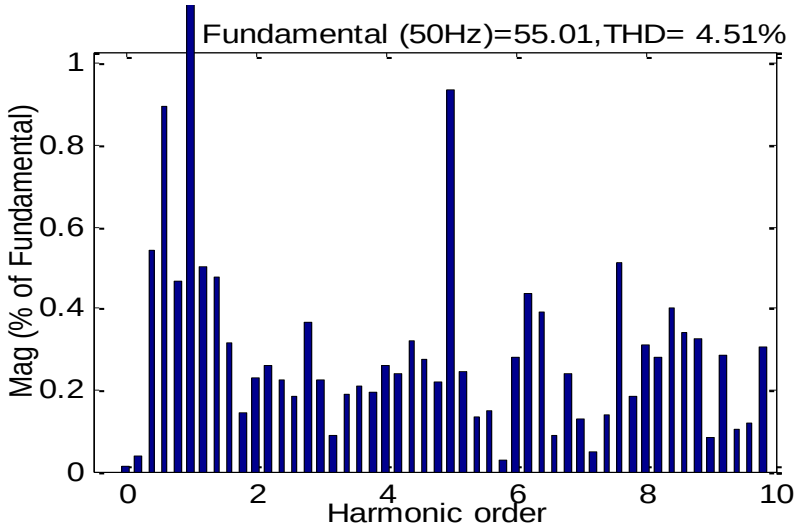

Fig. 3.6 d Source current THD with DC- DSTATCOM

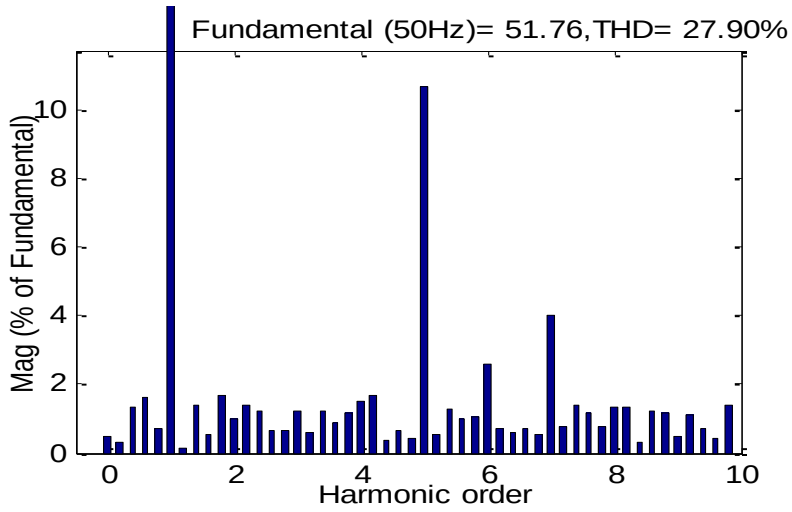

Fig. 3.6 e Load current THD with DC- DSTATCOM

The THD is the measurement of harmonics distortion & it is defined as a ratio of RMS values of n^{th} component to the fundamental component

$$\text{THD} = \frac{\sqrt{I_1^2+I_2^2+I_3^2+----+I_n^2}}{I_1}$$

The procedure to find out the THD to show source harmonics component is evaluated as follows

(i) The simulation study is analyzed for x axis from 0.55 to 0.75 sec

(ii) The THD is calculated by using graphical user interface (GUI) for 10 cycles which starts from 0.55 sec. or for 5 cycles which starts from 0.65 sec.

3.5.2 Simulation results of IC- DSTATCOM

The proposed IC- DSTATCOM controller's effectiveness and feasibility have been demonstrated in various scenarios. . It was tested in response to a 0.6 sec spike in the mean DC potential of VSC (600 to 680V). The steady-state & transient reaction of IC- DSTATCOM characteristics were indicated in Fig. 3.7 (a).

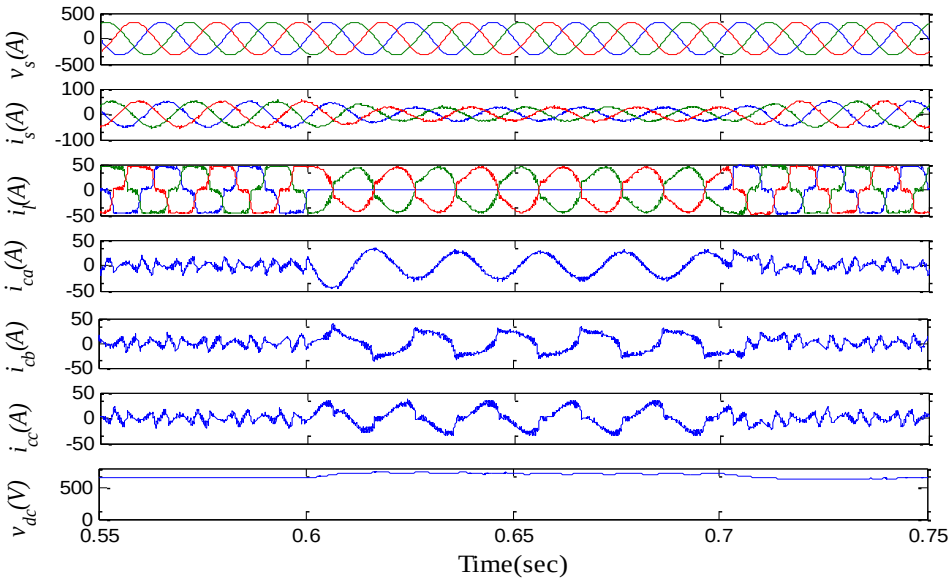

Fig. 3.7 a Waveform of three phase input potential, supply current, output load current, DSTATCOM current, DC-link potential with IC-DSTATCOM

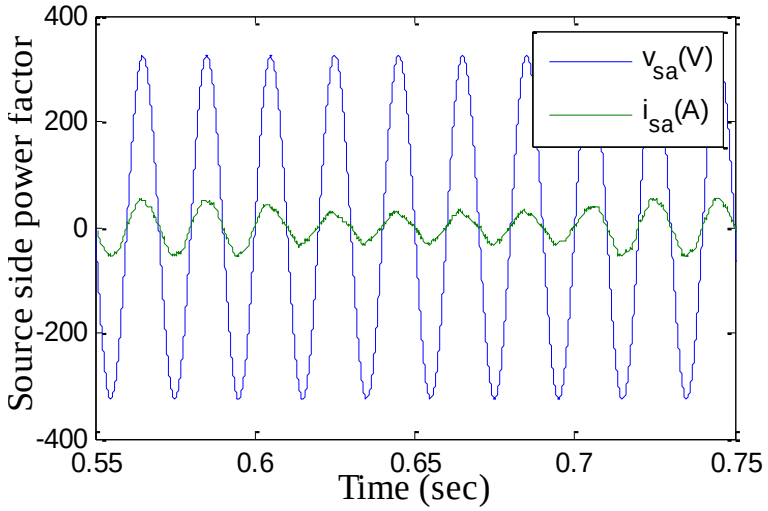

Fig. 3.7 b Source side powerfactor with IC-DSTATCOM

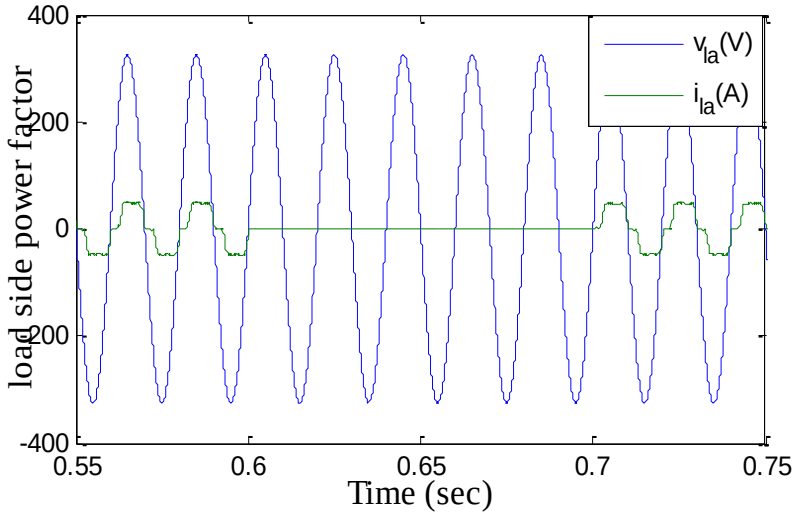

fig. 3.7 c Load side powerfactor with IC-DSTATCOM

All the subplots are arranged in the order of up to down wise like supply potential, input supply current, load output current, DSTATCOM current, DC potential. The proposed IC-DSTATCOM affords a healthy pf and supply current THD percentage. Later parallel compensation, the P.F is reached to 0.99 & THD% dropped to 3.57 depicted in Fig. 3.7 (b). The output current THD% 27.91 in Fig.3.7(c). The analysis of both DC-DSTATCOM and IC-DSTATCOM are indicated in Table-3.1. The proposed IC-DSTATCOM filtered a greatly polluted supply current harmonics of the EPDS as compared to other.

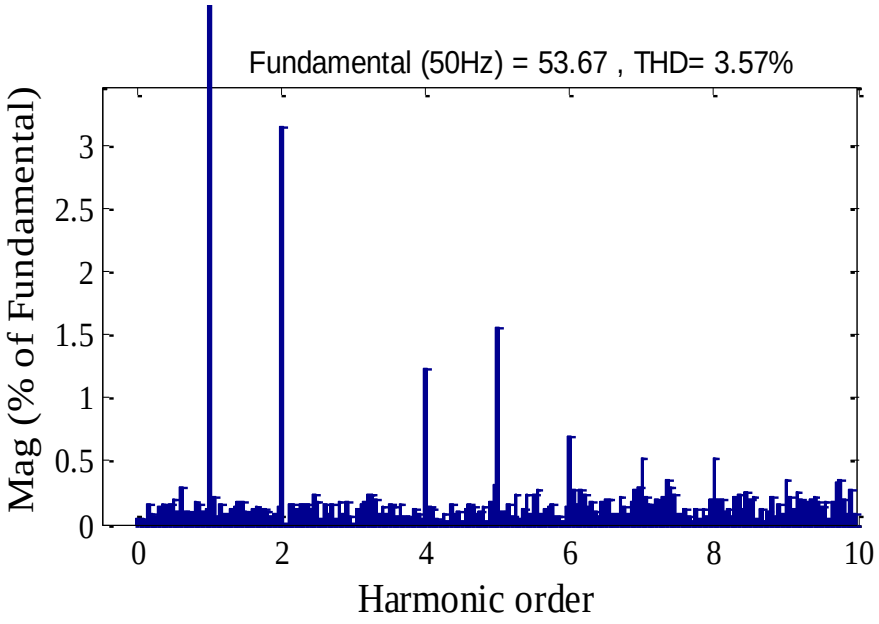

Fig. 3.7 d Source current THD with IC-DSTATCOM

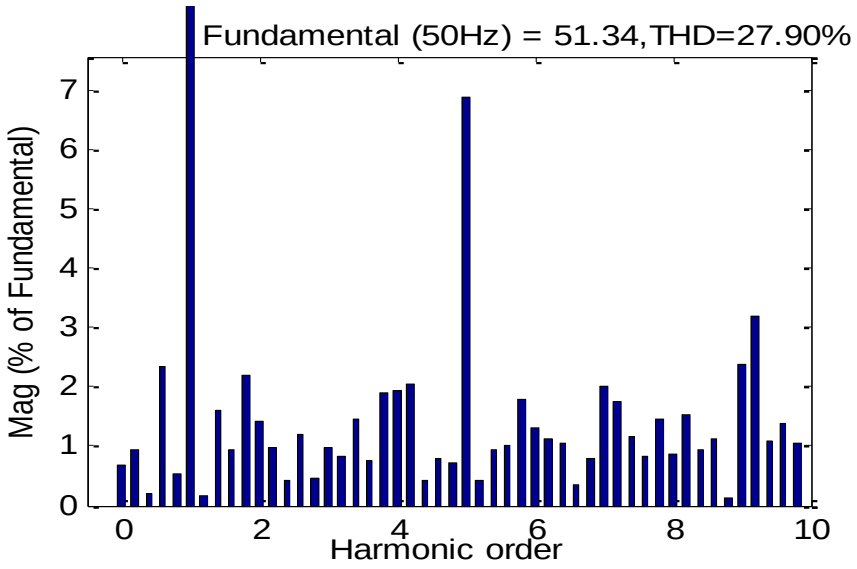

Fig. 3.7 e Load current THD with IC-DSTATCOM

Table.3.1 Performance parameter of DC-DSTATCOM and IC-DSTATCOM

Performance parameter	DSTATCOM at PCC	
	DC-DSTATCOM	IC-DSTATCOM
i_s(A), %THD	55.01, 4.51	53.67, 3.57
v_s (V), %THD	321.5, 2.24	321.2, 1.43
i_l (A), %THD	51.76, 27.90	51.34 ,27.90
Power Factor	0.94	0.99

The controller parameters are selected as a base study in this research. The same parameters are utilized from the previous published reference work as presented in [19].

Table.3.2 Simulation formation parameters

Symbol	Definition	Value
v_s	3- phase supply potential	230V/phase
f_s	Frequency	50Hz
R_s	Input resistance	0.5Ω
L_s	Input inductance	2mH
K_{pr}	'P' controller of AC	0.2
K_{ir}	'I' controller of AC	1.1
v_{dc}	DC potential	600V
C_{dc}	Capacitor	2000μF
K_{pa}	'P' controller of DC	0.01
K_{ia}	'I' controller of DC	0.05
R_c	VSC resistance	0.26Ω
L_c	VSC inductance	1.5mH

Table.3.3 Basic name plate rating parameters of the IFCT

	Grid side	Load side	Filtering side
Wiring scheme	**Wye**	**Wye**	**Wye**
Power and frequency	**10kV, 50 Hz**	**10kV, 50 Hz**	**10kV, 50 Hz**
Voltage (ph-ph), R, and L	**230V, 0.002 (pu), 0.08 (pu)**	**230V, 0.002 (pu), 0.08 (pu)**	**230V, 0.002 (pu), 0.08(pu)**
Magnetic resistance, reactance	**500Ω,100Ω**	**500 Ω,100Ω**	**500 Ω,100Ω**

Table.3.4 Measured active & reactive power of IFCT

Grid side	**Active power reactive power**	**26 kW 1.388 kVAR**
Load side	**Active power reactive power**	**15 kW 1.388 kVAR**
Filtering side	**Active power reactive power**	**24 kW 570 VAR**

3.6 Analysis and calculation of kVA rating, DF, HCR, DIN, FF, RF, HF and C-Message weights

3.6.1 Analysis of kVA rating

The Volt ampere (VA) rating=$\sqrt{3} * \frac{v_{dc}}{\sqrt{2}} * \frac{I_f}{\sqrt{2}}$

Where $v_{dc}$the DC is link potential of VSI & I_f is the inverter current

DC-DSTATCOM = $\sqrt{3} * \frac{535}{\sqrt{2}} * \frac{12.5}{\sqrt{2}} = 5.794\ kVA$

IC-DSTATCOM = $\sqrt{3} * \frac{535}{\sqrt{2}} * \frac{10.5}{\sqrt{2}} = 4.867$kVA

3.6.2 Calculation of Derating Factor (DF)

DF= 1-efficiency Efficiency = $\frac{\text{output power}}{\text{input power}} * 100$

kVA rating of DC-DSTATCOM = 5.79 kVA, power factor cosϕ = 0.97

kW output of the CDC-DSTATCOM = kVA* cosϕ

= 5.794*0.97 = 5.62 kW

Power losses of CDC-DSTATCOM = $3I_f^2 * R_c$

I_f is the inverter current= 12.5 A, R_c= 0.25 Ω

$3I_f^2 * R_c$ = 3*$12.5^2 * 0.25$ = 117.18 W

Power input = output power + losses

= 5620+117.18 = 5737.18 W = 5.737 kW

DC-DSTATCOM = $\frac{\mathbf{5.62}}{\mathbf{5.737}} * 100$ = 97.65%

DF of DC-DSTATCOM = 1- 0.97 = 0.03

kVA rating of IC-DSTATCOM = 4.867 kVA, power factor cosϕ = 0.99

kW output of the CDC-DSTATCOM = kVA* cosϕ

4.867*0.99 = 4.81 kW

I_f is the inverter current= 10.5 A, R_c= 0.25 Ω

$3I_f^2 * R_c$ = 3*$10.5^2 * 0.25$ = 82.68 W

Power input = output power + losses

= 4810 + 82.68 = 4892.68 W = 4.89 kW

IC-DSTATCOM = $\frac{4.81}{4.89} * 100$ = 98.36%

DF of IC-DSTATCOM = 1- 0.983 = 0.017

3.6.3 Harmonic compensation ratio (HCR)

The HCR of DC-DSTATCOM is calculated as

HCR= $\frac{\text{THD\% after compensation}}{\text{THD\% before compensation}} = \frac{4.05}{27.90} = 0.145$

Similarly, the HCR of IC-DSTATCOM is given as

HCR= $\frac{THD\%\ after\ compensation}{\text{THD\% before compensation}} = \frac{3.14}{27.90} = 0.11$

3.6.4 Distortion index (DIN)

Taylor series expansion for small ranks of harmonics is below

= THD (1- $\frac{1}{2}$ (THD))

DIN for DC-DSTATCOM = 4.05(1- $\frac{1}{2}$ 4.05) = -4.15

DIN for IC-DSTATCOM = 3.14 (1- $\frac{1}{2}$ 3.14) = -1.78

3.6.5 Form factor (FF)

The form factor is defined as FF = $\frac{I_{rms}}{I_{avg}}$

FF for DC-DSTATCOM =

I_{rms}= 39.21 A $I_{rms} = \frac{\pi}{2\sqrt{2}} I_{avg}$

I_{avg}=35.30A FF= $\frac{39.21}{35.30}$= 1.11

FF for IC-DSTATCOM =

I_{rms}= 37.9 A $I_{rms} = \frac{\pi}{2\sqrt{2}} I_{avg}$

I_{avg}=34.12A FF= $\frac{37.9}{34.12}$= 1.11

3.6.6 Ripple factor (RF)

RF for DC-DSTATCOM = $\sqrt{(FF^2) - 1}$= $\sqrt{(1.11^2) - 1}$ = 0.48

RF for IC-DSTATCOM = $\sqrt{(FF^2) - 1}$= $\sqrt{(1.11^2) - 1}$ = 0.48

3.6.7 Harmonic factor (HF)

The HF of the h_{th} harmonic, $HF_h = \frac{I_{rms}^{(h)}}{I_{rms}^{(1)}}$

HF for DC-DSTATCOM = $\frac{39.21}{53.25} = 0.736$

HF for IC-DSTATCOM=$\frac{37.9}{52.42}$ = 0.72

3.6.8 C-Message weights

The C-Message weighted is C= $\frac{\sqrt{\sum_{i=1}^{\infty}(C_i I^{(i)})^2}}{I_{rms}}$

C-Message weights for DC-DSTATCOM = $\frac{39.21^2}{53.25^2}$ = 0.5

C-Message weights for IC-DSTATCOM = $\frac{37.9^2}{52.42^2}$ = 0.5

Table.3.5 Comparative study on kVA rating, DF, HCR, DIN, FF, RF, HF and C-Message weight of DC-DSTATCOM and IC-DSTATCOM

Sl. No.	Types of configurations	Analysis of KVA rating	DF	HCR	DIN	FF	RF	HF	C-message weight
1	**DC-DSTATCOM**	5.794	0.03	0.145	-4.15	1.11	0.48	0.736	0.5
2	**IC-DSTATCOM**	4.867	0.017	0.112	-1.78	1.11	0.48	0.72	0.5

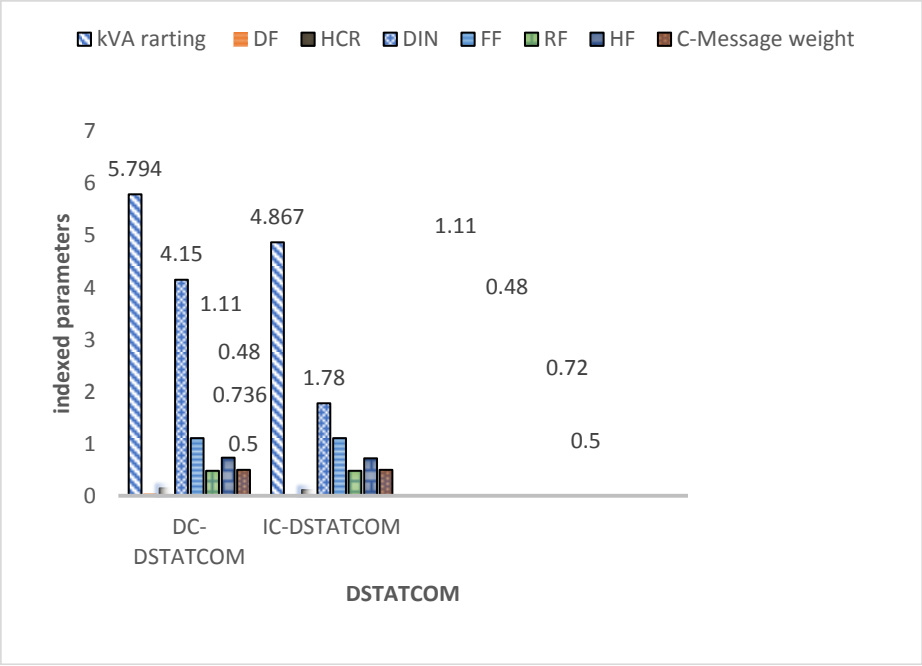

Fig. 3.8 Bar chart for the indexed parameter

3.7 Chapter summary:

The present study is dealt on both DC-DSTATCOM and IC-DSTATCOM topologies for Improvements of PQ. In the proposed configuration, the total output power is provided due to proper coordination of coupled transformer and interfacing impedance of VSC. The following objectives are achieved below:

(i) It consumes low power with better Reliability due to the reduction of the filter size.

(ii) The diminished component stress, effortless continuance, modularity & interleaving are deliberated are the advantages of projected architecture.

(iii) Apart from these, the effectiveness like harmonics restriction, good pf, & regulation with different PQ parameter indices are presented and compared as per IEC- 61000-1 & IEEE-2030-7-2018 value.

The proposed topology can be utilized for multi-inverter, renewable sources and new intelligent controller for further.

CHAPTER-4

CHAPTER 4

Cascaded VSI based DSTATCOM using *icosϕ* control algorithm

4.1. Introduction

The prime motivation of EPDS is attracted to the consumers and service provider to offer secure, consistent, quality, effective & reasonable source of energy. Therefore, the EPDS must be well-thought-out, well-designed & safely operated. When in operation, EPDS often experiences a higher number of failures and disturbances. Increase in demands, less long standing plan, open access to consumers, minimum security, nonlinear loads, unplanned load switching are the reasons for degrading quality of supply.

As a result, experts in the field of power system operation require innovative methods for enhancing PQ performance. With this motivation for improving the PQ performance in the EPDS, the DSTATCOM is the important choice for current related PQ issues. Even though, DSTATCOM is playing an important role in the EPDS, still, on the other side of the coin, diversification of the DSTATCOM is a growing role for the modern EPDS. Hence, the challenging task is to provide flexibility and sustainability for all above scenarios. Pertinent selection of voltage source inverter (VSI), extension of VSI, design of control algorithm, IFCT design, impedance matching are the major research areas for the improvement of the PQ. From last three decades, most of the researchers and several R&Ds focused on different CPDs to neutralize the PQ based problems. All the CPDs perform flexible, reliable and quick reaction to inject reactive power at PCC of system. In cascaded direct coupled DSTATCOM (CDC-DSTATCOM) the PCC experiences more stress because of direct contact between supply, load & DSTATCOM. Hence, more chances to flow of short circuit currents, poor protection, and thermal losses etc. Also it causes to increase harmonic loss, noise and mechanical imbalance. Hence, the new step has to be taken to overcome the demerits of CDC-DSTATCOM. Hence, the research direction is motivated to step forward for the remedial solution by using IFCT. The purpose of IFCT to introduce in this study, to damp out the harmonic's resonance in between source and filtering side, which further does not allow the harmonics to flow in to the source side. So that, PQ improvement with stable operation will be achieved.

First of all, this chapter is dealt with the design of CDC-DSTATCOM for EPDS. Later to this, the IFCT is introduced with CDC-DSTATCOM to behave as an inductive medium between source and load. In addition to this, another set of similar kind of VSI is connected in cascade through the suitable value of inductor in every phase to justify the recommended topology for the EPDS. It bears number of merits such as less switching stress, improved balance voltage at PCC, increasing the compensation capability, and other different combinations are possible. In view of the design of DSTATCOM, two levels VSC are considered for 3P3W EPDS. This 3-leg VSI technique is widely put onward due to its own reputation in the literature. The projected topology affords flexibility for future improvement for connecting additional converters and loads.

For healthier operation of DSTATCOM, The filtering system is completed by subsequent generalized mathematical structure using $icos\emptyset$ algorithm using MATLAB/ Simulink. The below comments are inferenced from the proposed CIC-DSTATCOM scheme in accordance with the standard set by IEC- 61000-1 & IEEE-2030-7-2018 data.

(i) Good convergence performance is obtained.

(ii) The main features of this algorithm are enhanced tracking, adaptive, and compensatory capacities.

(iii) The anticipated structure supports for accomplishing the numerous PQ issues like harmonics reduction, healthier potential regulation, PF rectification, load equalizing and reduction in DC link voltage etc.

(iv) It also provides the flexible support against of harmonics over current.

(v) It is capable to restructure the additional parameters for improved version of algorithm.

4.2 MODELING OF THE PROPOSED CIC-DSTATCOM

The arrangement of the 3P3W EPDS with CDC-DSTATCOM and CIC-DSTATCOM are shown in Fig.4.1 & 4.2 respectively. The CDC-DSTATCOM which consists of balanced 3-phase supply, DSTATCOM, non-linear load (uncontrolled rectifier), whereas the CIC-DSTATCOM which consists of a stable 3-phase supply, converter transformer DSTATCOM, 3-phase non-linear load. The VSI based DSTATCOM associated at PCC of EPDS is exposed in Fig.4.3. An adapted technology CDC-DSTATCOM & CIC-DSTATCOM utilized as like compensator to lessen the

power system issues. The triggering pulses of the both compensators are created by icosϕ control technique. This study's goal is to employ this control algorithm in order to choose a reliable method.

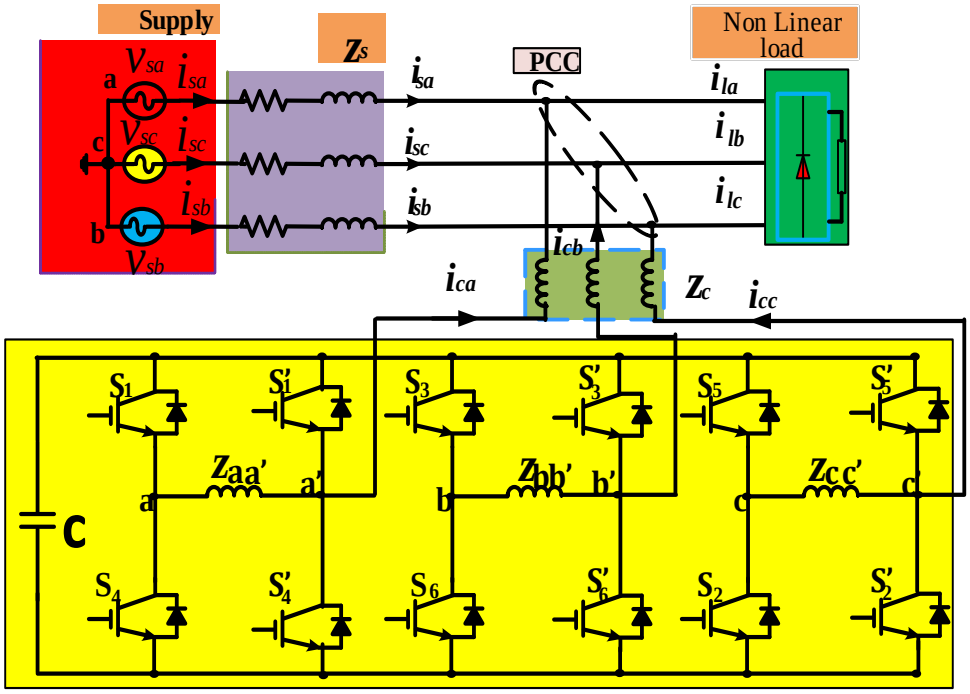

Fig. 4.1 EPDS with CDC- DSTATCOM.

The proposed cascaded module includes 12 semiconductor switches and placed together with an appropriate connection with inductor linking which is shown in fig.2. as shown in fig S_1 – S_6 switches are selected for one limb whereas S_1^1 – S_6^1 are chosen for other limb to accommodate the voltage balancing and reducing switching stress, consequently each limb of full bridge inverter is achieved bipolar output in this inverter, inductors (Z_{AA}^1, Z_{bb}^1, Z_{cc}^1) are used to enable the bidirectional current flow and block positive off state voltage.

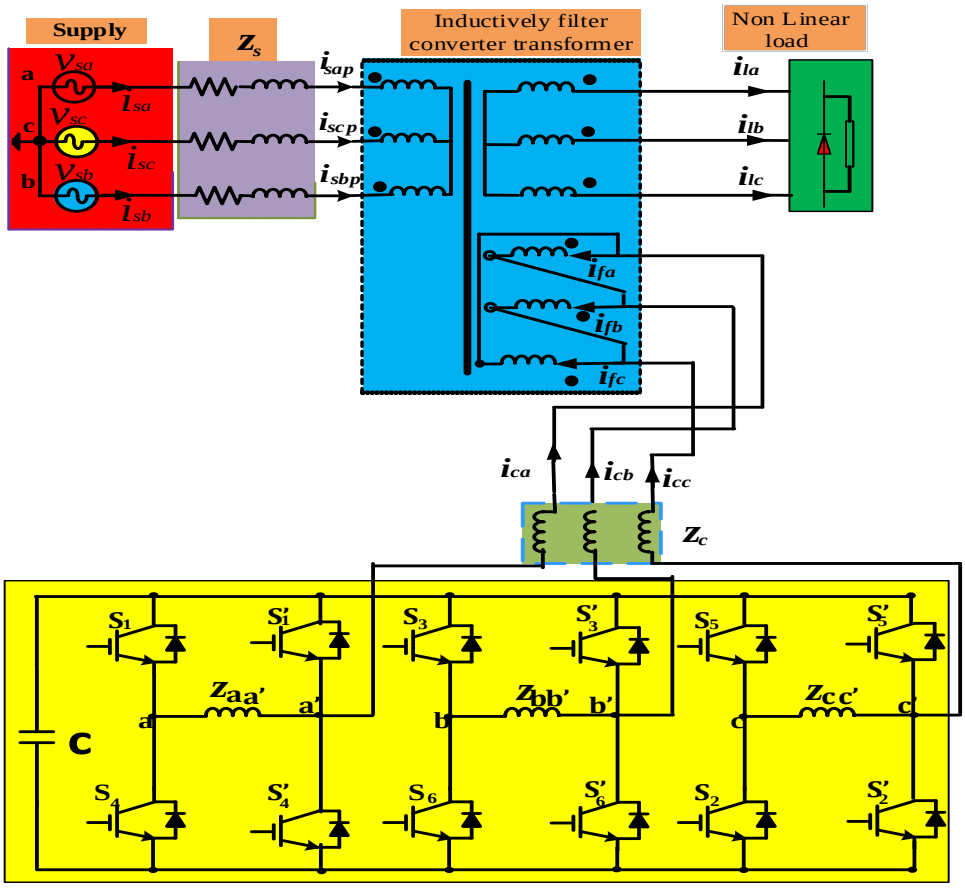

Fig. 4.2 EPDS with CIC- DSTATCOM

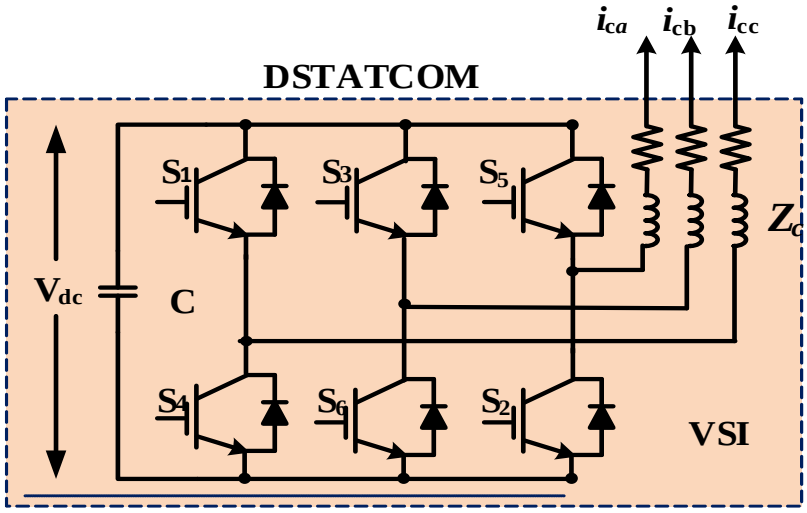

Fig. 4.3 Two-level self-supported capacitor supported VSI based DSTATCOM

4.3 MODELLING AND DESIGN OF INDUCTIVE TRANSFORMER

The three-phase harmonic equivalent circuit of the specified CIC-DSTATCOM is structured in Fig-4.2; from this we can get clear idea about connection structure of IFCT at PCC. Both voltages and currents have their fundamental and harmonic components. The suggested CIC-DSTATCOM constitutes IFCT, DSTATCOM & load. The CDC-DSTATCOM & non-linear load both are coupled to the IFCT's three winding. The star-wired primary winding (PW), the star-wired secondary winding (SW), and the delta-wired third winding filtered winding (FW) is linked with CDC-DSTATCOM. The purpose of the specialized IFCT winding is to achieve a potential equilibrium among the grid, the load, and the DSTATCOM. In the following sections, we'll learn deeper about the IFCT's mathematical model and filtering method.

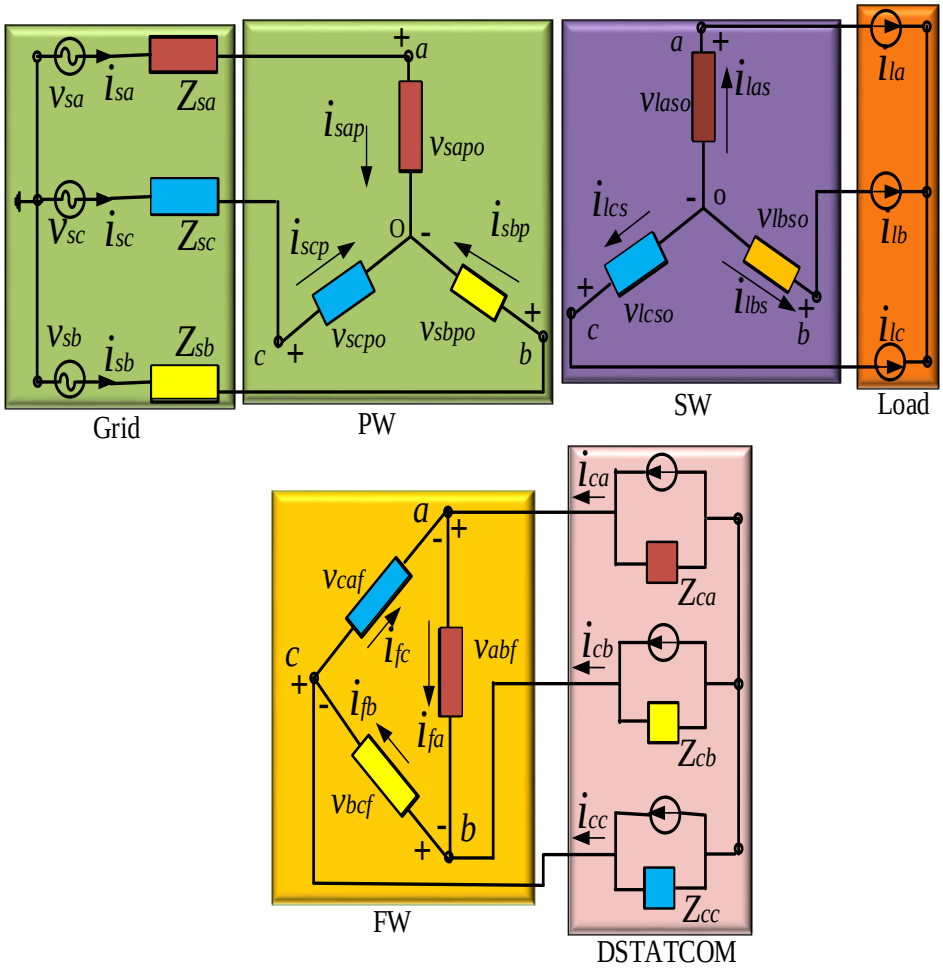

Fig.4.4 Equivalent circuit of proposed DSTATCOM

The voltage balance equation of PW, SW and FW is expressed as [19],

$$\begin{cases} N_1 \mathrm{i}_{\mathrm{sap}} + N_2 \mathrm{i}_{\mathrm{las}} + N_3 \mathrm{i}_{\mathrm{caf}} = 0 \\ N_1 \mathrm{i}_{\mathrm{sbp}} + N_2 \mathrm{i}_{\mathrm{lbs}} + N_3 \mathrm{i}_{\mathrm{cbf}} = 0 \\ N_1 \mathrm{i}_{\mathrm{scp}} + N_2 \mathrm{i}_{\mathrm{lcs}} + N_3 \mathrm{i}_{\mathrm{ccf}} = 0 \end{cases} \quad (4.1)$$

According to KCL, the current equations in the primary side of the IFCT are written as

$$\begin{cases} \mathrm{i}_{\mathrm{sap}} = (v_{sa} - v_{sapo})/Z_{sa} \\ \mathrm{i}_{\mathrm{sbp}} = (v_{sb} - v_{sbpo})/Z_{sb} \\ \mathrm{i}_{\mathrm{scp}} = (v_{sc} - v_{scpo})/Z_{sc} \end{cases} \quad (4.2)$$

According to KCL, the current equations in the secondary side of the IFCT (load side) are written as

$$\begin{cases} \mathrm{i}_{\mathrm{la}} = i_{las} + i_{caf} \\ \mathrm{i}_{\mathrm{lb}} = i_{lbs} + i_{cbf} \\ \mathrm{i}_{\mathrm{lc}} = i_{lcs} + i_{cbf} \end{cases} \quad (4.3)$$

The current balance equations are shown below [19]:

$$\begin{cases} \mathrm{i}_{\mathrm{sap}} + i_{sbp} + i_{scp} = 0 \\ \mathrm{i}_{\mathrm{las}} + i_{lbs} + i_{lcs} = 0 \\ \mathrm{i}_{\mathrm{caf}} + i_{cbf} + i_{ccf} = 0 \end{cases} \quad (4.4)$$

The total compensating current equations at filter side are written as [19]

$$\begin{cases} \mathrm{i}_{\mathrm{caf}} = i_{ca} + i_{fa} \\ \mathrm{i}_{\mathrm{cbf}} = i_{cb} + i_{fb} \\ \mathrm{i}_{\mathrm{ccf}} = i_{cc} + i_{fc} \end{cases} \quad (4.5)$$

4.4 ICOSϕ CONTROL STRUCTURE

The regulated assembly of the structure is shown in Fig.4.4. Owing to its rapid & strong dynamic reaction the *icosϕ* structure is chosen to provide gate signals to switches. Inside control signal of *icosϕ* scheme is shown in Fig. 4.6. The gate signals used to operate the DSTATCOM are created using a four-stage process.

(i) In order to calculate the most basic quantity of the III-phase output load current, Fourier blocks are used.

(ii) Active and reactive load output current are generated via the same control method.

(iii) Base input currents are generated using re-active & active elements of the output currents in accordance with the algorithm.

(iv) Each switching signal is produced by totaling the active & reactive components of the output current that are provided to the hysteresis current controller (HCC).

Numerous measures are being enacted to reduce emissions of undesirable gases and the Here, i_{lap} denotes the active power element of basic load output current is articulated as

$$\begin{bmatrix} i_{lap} \\ i_{lbp} \\ i_{lcp} \end{bmatrix} = \begin{bmatrix} Re(i_{la}) \\ Re(i_{lb}) \\ Re(i_{lc}) \end{bmatrix} = \begin{bmatrix} i_{la}cos\phi_{la} \\ i_{lb}cos\phi_{lb} \\ i_{lc}cos\phi_{lc} \end{bmatrix} \quad (4.6)$$

The weighted mean worth of the real active power element w_p

$$w_p = \left(\frac{i_{la}cos\phi_{la}+i_{lb}cos\phi_{lb}+i_{lc}cos\phi_{lc}}{3}\right) \quad (4.7)$$

In the similar way we can express the reactive power component

$$\begin{bmatrix} i_{laq} \\ i_{lbq} \\ i_{lcq} \end{bmatrix} = \begin{bmatrix} Im(i_{la}) \\ Im(i_{lb}) \\ Im(i_{lc}) \end{bmatrix} = \begin{bmatrix} i_{la}sin\phi_{la} \\ i_{lb}sin\phi_{lb} \\ i_{lc}sin\phi_{lc} \end{bmatrix} \quad (4.8)$$

The weighted mean worth of the reactive power component w_q

$$w_q = \left(\frac{i_{la}sin\phi_{la}+i_{lb}sin\phi_{lb}+i_{lc}sin\phi_{lc}}{3}\right) \quad (4.9)$$

The median worth of active & reactive weighted modules is 'w_p', 'w_q'correspondingly. The'w_p', 'w_q' are the clustered mass & there is assurance to give an adjusted worth. The LPF, as depicted in Fig.4.5, is proposed as a means of overcoming these limitations. With LPF applied, these sonic parameters dampen the greater-order harmonics. Thus, the tuned weight active element (w_{spt}) & reactive element (w_{sqt}) of output current are reached. At last, the advised control procedure is aimed to get a filtered and adjusted mass. In addition, the modified weight is less susceptible to noise and, as a result, becomes steady and adaptable to any network disturbance, which assists to vaccinate the correct compensator current at coupling point. The accumulation of PI controllers output & weighted mean worth of active power element w_p grants the overall active elements of the reference supply input current.

The controller's output can be outright as

$$w_{dp} = k_{pdp}v_{de} + k_{idp}\int v_{de}dt \quad (4.10)$$

$$w_{spt} = w_{dp} + w_{lp} \quad (4.11)$$

In similar way, the overall reactive components are outright

$$w_{sqt} = w_{qq} - w_{lq} \tag{4.12}$$

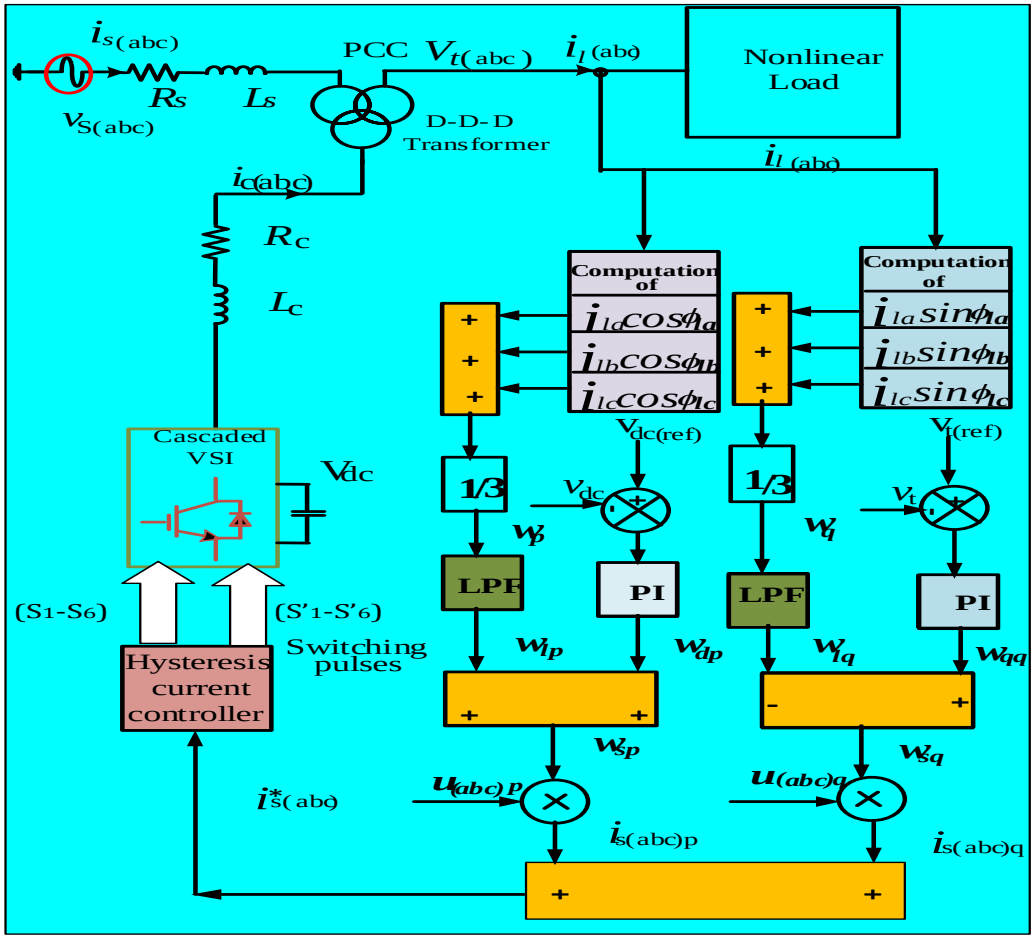

Fig. 4.5 Switching signals generation for CIC-DSTATCOM

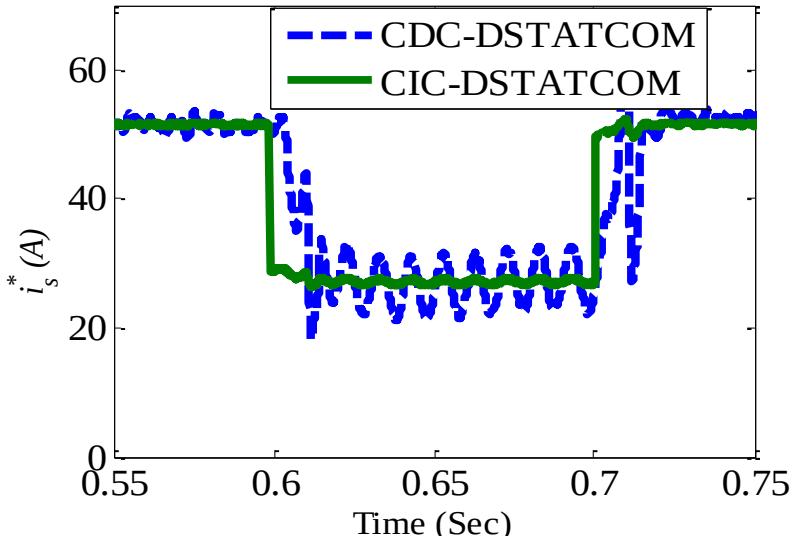

Fig. 4.6 Inner signal of the control algorithm

A low pass filter which cut of rate is 20.1 Hz utilized for load output current.

Instantneous worth of active supply currents i_{sp}, can be figured as

$$\begin{bmatrix} i_{sap} \\ i_{sbp} \\ i_{scp} \end{bmatrix} = w_{spt} \begin{bmatrix} u_{ap} \\ u_{bp} \\ u_{cp} \end{bmatrix} \tag{4.13}$$

Instantneous worth of the reactive supply currents i_{sq}, can be figured as

$$\begin{bmatrix} i_{saq} \\ i_{sbq} \\ i_{scq} \end{bmatrix} = w_{sqt} \begin{bmatrix} u_{aq} \\ u_{bq} \\ u_{cq} \end{bmatrix} \tag{4.14}$$

The refernce supply currents are illustrated as

$$\begin{bmatrix} i_{sa}^{*} \\ i_{sb}^{*} \\ i_{sc}^{*} \end{bmatrix} = \begin{bmatrix} i_{sap} \\ i_{sbp} \\ i_{scp} \end{bmatrix} + \begin{bmatrix} i_{saq} \\ i_{sbq} \\ i_{scq} \end{bmatrix} \tag{4.15}$$

Together the actual supply currents ($i_{sa,} i_{sb}, i_{sc}$) & the origin supply currents ($i_{sa}^{*}, i_{sb}^{*}, i_{sc}^{*}$) are compared, next, the Hysteresis current controller (HCC) receives error value based on the current flow. Its operation as follows:

(i) when $i_{sa} < i_{sa}^{*}$, s_1 ON & s_4 is OFF

(ii) when $i_{sa} > i_{sa}^{*}$, s_1 OFF & s_4 turn ON

These outputs are utilized to breed the triggering pulses of both CDC-DSTATCOM & CIC-DSTACOM.

4.5 SIMULATION OUTCOMES & ANALYSIS:

The performance of EPDS with topologies are demonstrated using MATLAB/Simulink studies. Identical operating conditions and system parameters are considered to perform computer simulations. The suggested $icos\emptyset$ mechanism is implemented for reference current generation for appropriate switching pulses to the both varieties of topologies. The system parameters are listed in Table 4.2. Both the balanced and unbalanced performance of CIC-DSTATCOM and CDC-DSTATCOM based EPDS are analyzed here in the below sub-sections.

4.5.1 Simulation results of CDC-DSTATCOM

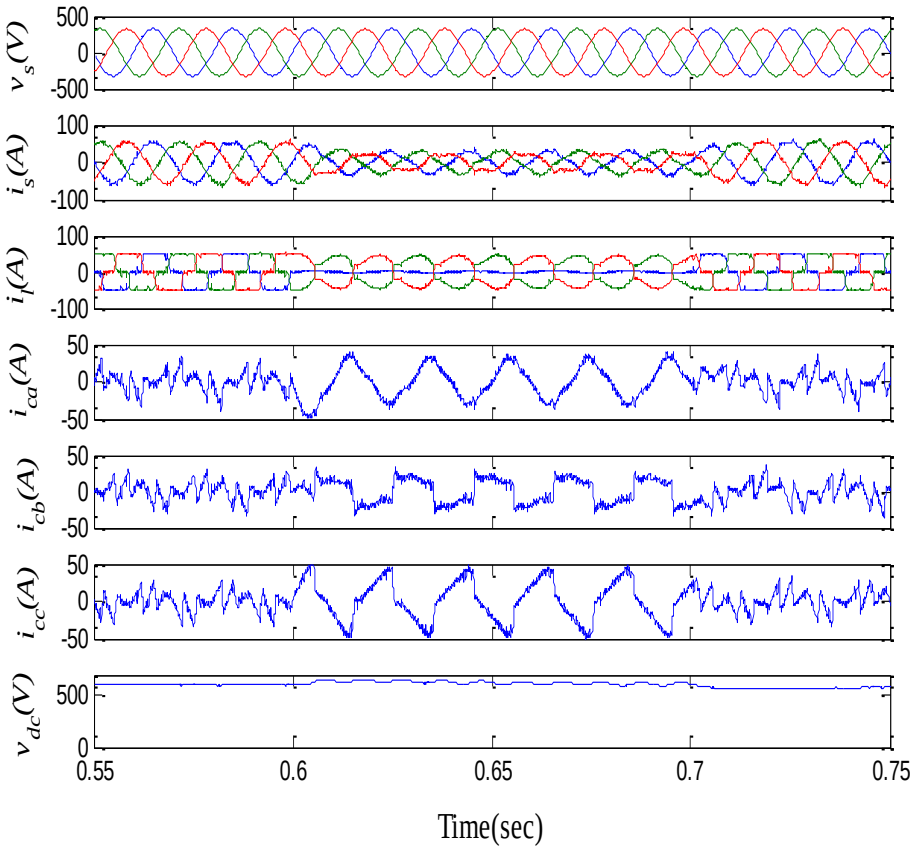

Fig. 4.7 a Simulation wave shape of (top to down) III- phase input potential, supply current, output current, DSTATCOM current & DC- link potential with CDC-DSTATCOM.

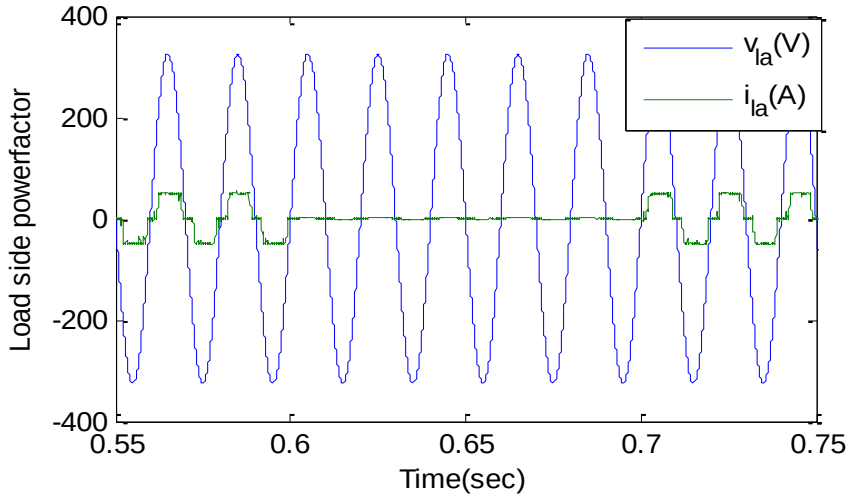

Fig.4.7 b Load side powerfactor with CDC- DSTATCOM

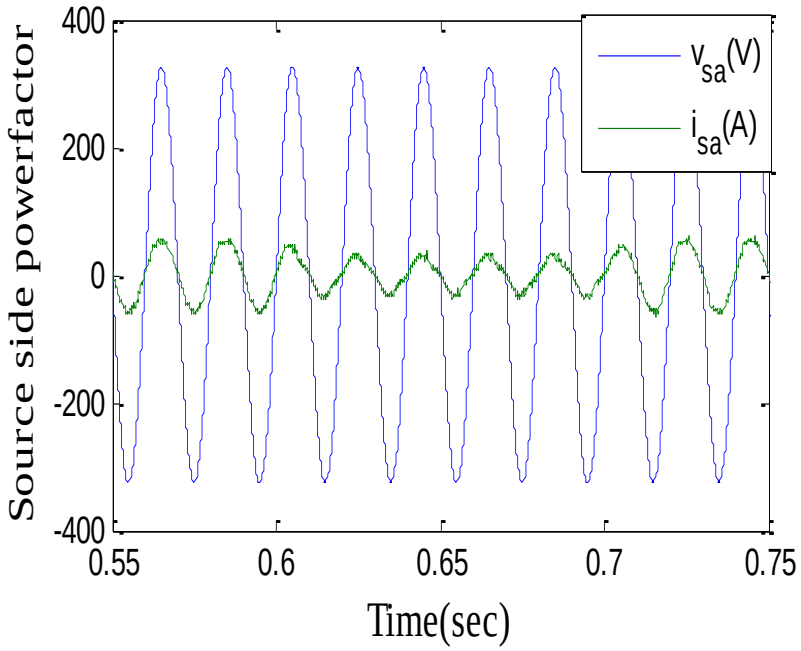

Fig. 4.7 c Source side powerfactor with CDC-DSTATCOM

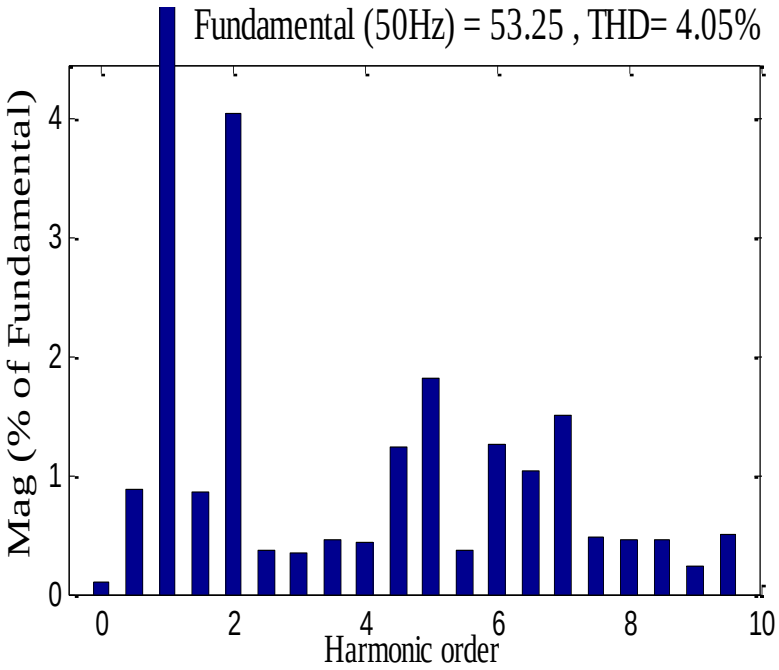

Fig.4.7 d Source current THD with CDC- DSTATCOM

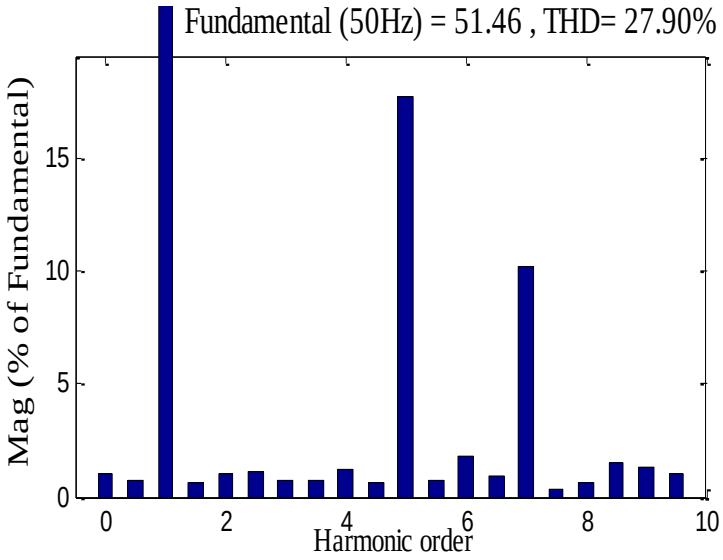

Fig. 4.7 e Load current THD with CDC- DSTATCOM.

The simulation study is analyzed during 0.55 Sec to 0.75 Sec to maintain the uniformity. But unbalanced performance is chosen during a step drop in a-phase loading in between 0.6 Sec to 0.7 Sec. In the Fig. 4.7 b, the significant improvement of power factor (p.f) at source side is achieved 0.94 under this situation, whereas, Fig. 4.7 c shows the low power factor at load side. Figure 4.7d shows a 4.05% THD in the source current, while Figure 4.7e shows a 27.90% THD in the load current at the output. This indicates the significant supply current harmonics discount based on IEEE-2030-7-2017 & IEC-61000-1 standard. The voltage regulation is maintained due to 535V desired and uniform DC link potential. Finally, 320V is keep up at PCC for satisfying the voltage balancing.

4.5.2 Simulation outcomes of CIC- DSTATCOM

The presentation of the CIC- DSTATCOM based EPDS at both balanced and unbalanced loading is depicted in Fig.4.8 a. In this figure, several subplots such as supply potential, supply input current, load output current, DSTATCOM current & DC potential is constructed. The simulation study was analyzed during 0.55 Sec to 0.75 Sec to maintain the uniformity. But unbalanced performances are chosen during a step drop in a-phase loading in between 0.6 Sec to 0.7 Sec.

In the Fig. 4.8 b, the significant improvement of power factor (p.f) at source side is achieved 0.99 under this situation, whereas, Fig. 4.8 c shows the low pf at load side. The source current THD% is 3.14 which depicted in Fig.4.8 d, whereas the load current THD% is 27.90 which is shown in Fig.4.8 e.

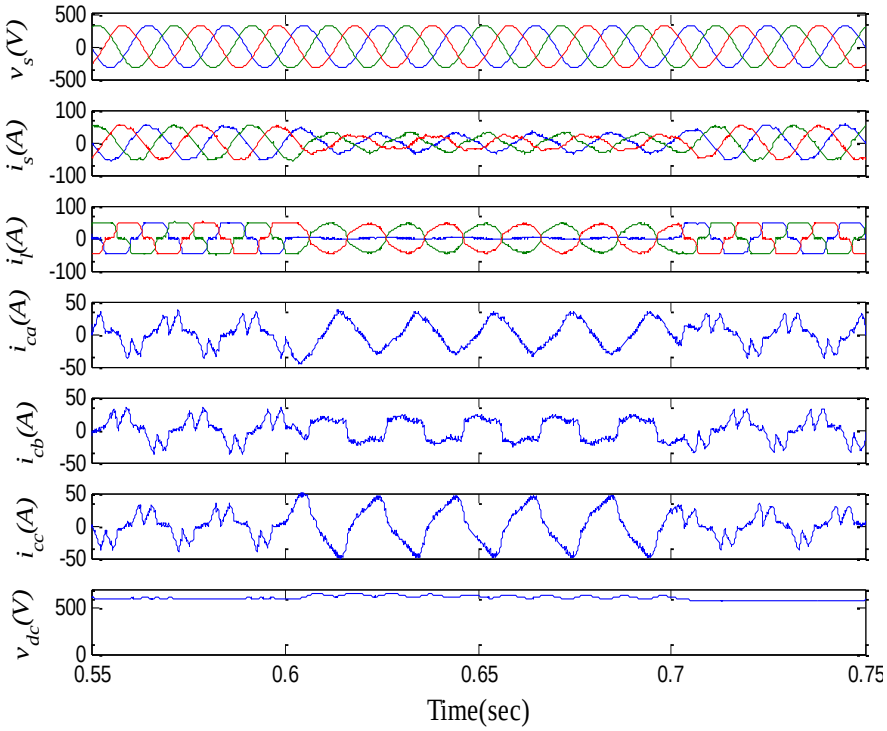

Fig. 4.8 a Simulated wave shape (top to down) III- phase input potential, supply current, output current, DSTATCOM current, DC-link potential with CIC-DSTATCOM

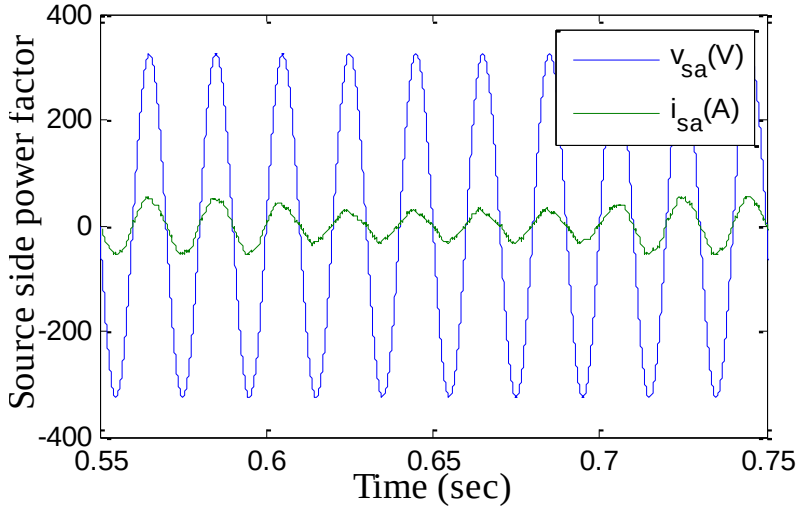

Fig. 4.8 b Source side powerfactor with CIC-DSTATCOM

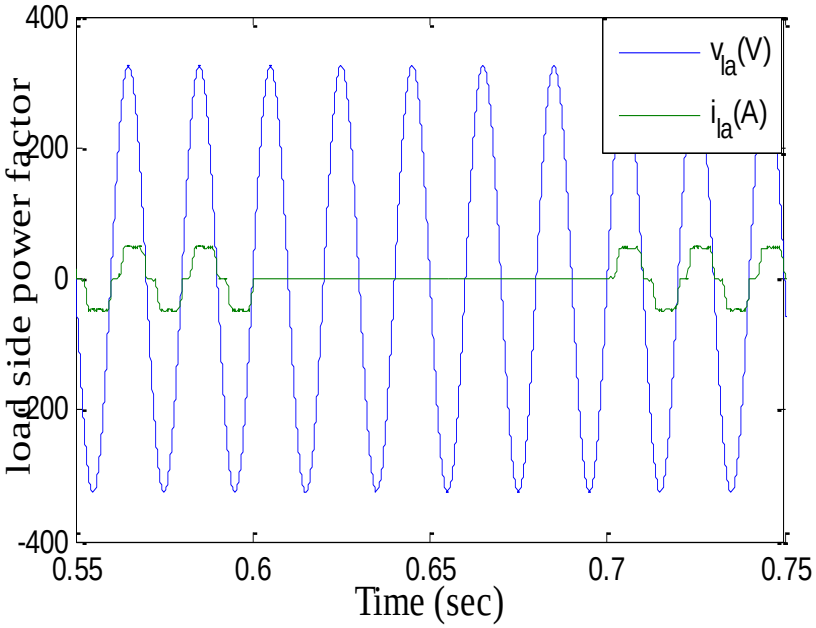

Fig. 4.8 c Load side powerfactor with CIC-DSTATCOM

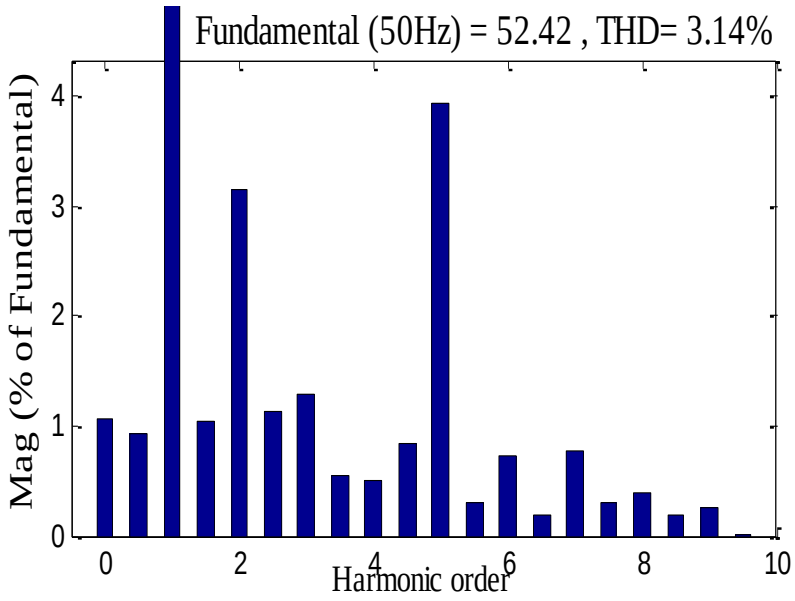

Fig. 4.8 d Source current THD with CIC-DSTATCOM

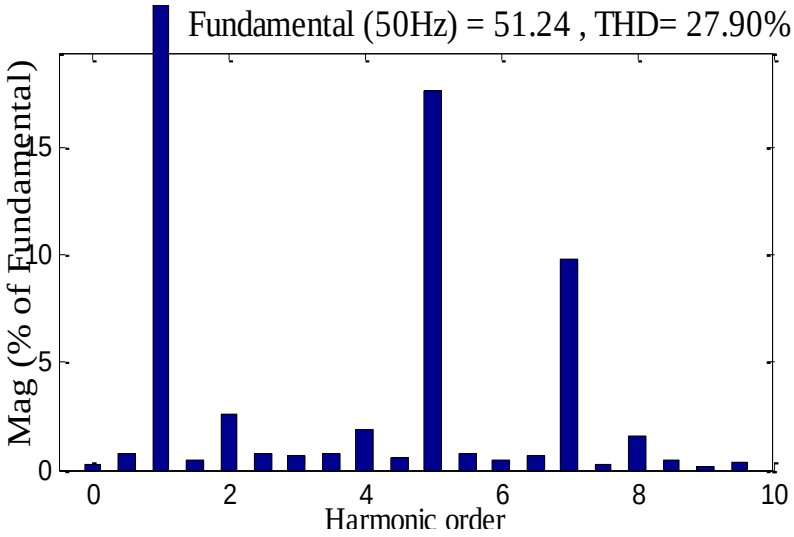

Fig. 4.8 e Load current THD with CIC-DSTATCOM

Table.4.1 Performance parameter of CDC-DSTATCOM and CIC-DSTATCOM

Performance parameter	**DSTATCOM at PCC**	
	CDC-DSTATCOM	**CIC-DSTATCOM**
i_s**(A), %THD**	53.25, 4.05	52.42, 3.14
v_s **(V), %THD**	321.4, 2.23	321, 1.42
i_l **(A), %THD**	51.46, 27.90	51.24, 27.90
Power Factor	0.94	0.99

Table.4.2 Simulation formation parameters

Symbol	Definition	Value
v_s	3- phase supply potential	230V/ph
f_s	Frequency	50Hz
R_s	Input resistance	0.5Ω
L_s	Input inductance	2mH
K_{pr}	AC 'P' controller	0.2
K_{ir}	'I' controller	1.1
v_{dc}	DC potential	600V
C_{dc}	Capacitor	2000µF
K_{pa}	'P' controller of DC	0.01
K_{ia}	'I' controller of DC	0.05
R_c	VSC resistance	0.26Ω
L_c	VSC inductance	1.5mH

Table.4.3 Basic rating parameters of the IFCT

	Grid side	Load side	Filtering side
Wiring scheme	**Wye**	**Wye**	**Delta**
Nominal power and frequency	**10kV, 50 Hz**	**10kV, 50 Hz**	**10kV, 50 Hz**
Voltage (ph-ph), R, and L	**230V, 0.002 (pu), 0.08 (pu)**	**230V, 0.002 (pu), 0.08 (pu)**	**230V, 0.002 (pu), 0.08 (pu)**
Magnetic resistance	**500 Ω**	**500 Ω**	**500 Ω**
Magnetic inductance	**500 Ω**	**500 Ω**	**500 Ω**

Table.4.4 Measured active & reactive power of IFCT

Grid side	**Active power** **reactive power**	**26 kW** **1.388 kVAR**
Load side	**Active power** **reactive power**	**15 kW** **1.388 kVAR**
Filtering side	**Active power** **reactive power**	**24 kW** **570 VAR**

4.6 Analysis and calculation of kVA rating, DF, HCR, DIN, FF, RF, HF and C-Message weights of CDC-DSTATCOM and CIC-DSTATCOM

4.6.1 kVA rating

The Volt ampere (VA) rating=$\sqrt{3} * \frac{I_f v_{dc}}{\sqrt{2}}$

CDC-DSTATCOM = $\sqrt{3} * \frac{12.5(535)}{\sqrt{2}} = 8.19\ kVA$

CIC-DSTATCOM = $\sqrt{3} * \frac{10.5(535)}{\sqrt{2}} = 6.88$kVA

4.6.2 De-rating Factor (DF)

DF=1-efficiency

kVA rating of CDC-DSTATCOM = 5.79 kVA, cosϕ = 0.97

kW output of the CDC-DSTATCOM = kVA* cosϕ = 5.794*0.97 = 5.62 kW

Power losses of CDC-DSTATCOM = $3I_f^2 * R_c$

I_f = 12.5 A, R_c= 0.25 Ω

$3I_f^2 * R_c$ = 3*$12.5^2 * 0.25$ = 117.18 W

Power input = output power + losses = 5620+117.18 = 5737.18 W = 5.737 kW

Efficiency of CDC-DSTATCOM = $\frac{\mathbf{5.62}}{\mathbf{5.737}} * 100$ = 97.65%

DF of CDC-DSTATCOM = 1- efficiency = 1- 0.97 = 0.03

For CIC-DSTATCOM

kVA rating of CIC-DSTATCOM = 4.867 kVA, power factor cosϕ = 0.99

kW output of the CDC-DSTATCOM = kVA* cosϕ = 4.867*0.99 = 4.81 kW

I_f is the inverter current= 10.5 A, R_c= 0.25 Ω

$3I_f^2 * R_c$ = 3*$10.5^2 * 0.25$ = 82.68 W

Power input = output power + losses = 4810 + 82.68 = 4892.68 W = 4.89 kW

Efficiency of CIC-DSTATCOM = $\frac{4.81}{4.89} * 100$ = 98.36%

DF of CIC-DSTATCOM = 1- efficiency = 1- 0.983 = 0.017

4.6.3 Harmonic compensation ratio (HCR)

The HCR of CDC-DSTATCOM is calculated as follows

HCR= $\frac{\text{THD\% after compensation}}{\text{THD\% before compensation}} = \frac{4.05}{27.90} = 0.145$

Similarly, the HCR of CIC-DSTATCOM is given as

HCR= $\frac{THD\%\ after\ compensation}{\text{THD\% before compensation}} = \frac{3.14}{27.90} = 0.112$

4.6.4 Distortion index (DIN)

Taylor series expansion for small ranks of harmonics is below

DIN = THD (1- $\frac{1}{2}$ (THD))

DIN for CDC-DSTATCOM = 4.05(1- $\frac{1}{2}$ 4.05) = -4.15

DIN for CIC-DSTATCOM = 3.14 (1- $\frac{1}{2}$ 3.14) = -1.78

4.6.5 Form factor (FF)

The form factor is defined as FF = $\frac{I_{rms}}{I_{avg}}$

FF for CDC-DSTATCOM =

I_{rms}= 39.21 A $I_{rms} = \frac{\pi}{2\sqrt{2}} I_{avg}$ I_{avg}=35.30A FF= $\frac{39.21}{35.30}$= 1.11

FF for CIC-DSTATCOM =

I_{rms}= 37.9 A I_{avg}=34.12A

FF= $\frac{37.9}{34.12}$= 1.11

4.6.6 Ripple factor (RF)

RF= $\frac{I_{AC}}{I_{DC}}$

RF= $\frac{\sqrt{(I_{rms})^2-(I_{DC})^2}}{I_{DC}}$= $\sqrt{(FF^2)-1}$

RF for CDC-DSTATCOM = $\sqrt{(FF^2)-1}$= $\sqrt{(1.11^2)-1}$ = 0.48

RF for CIC-DSTATCOM = $\sqrt{(FF^2)-1}$= $\sqrt{(1.11^2)-1}$ = 0.48

4.6.7 Harmonic factor (HF)

The HF = $\frac{I_{rms}^{(h)}}{I_{rms}^{(1)}}$

HF for CDC-DSTATCOM = $\frac{39.21}{53.25} = 0.736$

HF for CIC-DSTATCOM=$\frac{37.9}{52.42}$ = 0.72

4.6.8 C-Message weights

The C-Message weight is C= $\frac{\sqrt{\sum_{i=1}^{\infty}(C_i I^{(i)})^2}}{\sqrt{\sum_{i=1}^{\infty}(I^{(i)})^2}}$ C= $\frac{\sqrt{\sum_{i=1}^{\infty}(C_i I^{(i)})^2}}{I_{rms}}$

C-Message weights for CDC-DSTATCOM = $\frac{39.21^2}{53.25^2}$ = 0.5

C-Message weights for CIC-DSTATCOM = $\frac{37.9^2}{52.42^2}$ = 0.5

Table.4.5 Comparative study on kVA rating, DF, HCR, DIN, FF, RF, HF and C-Message weight of CDC-DSTATCOM and CIC-DSTATCOM

Sl. No.	Types of configurations	Analysis of KVA rating	DF	HCR	DIN	FF	RF	HF	C-message weight
1	CDC-DSTATCOM	8.19	0.03	0.145	-4.15	1.11	0.48	0.736	0.5
2	CIC-DSTATCOM	6.88	0.017	0.112	-1.78	1.11	0.48	0.72	0.5

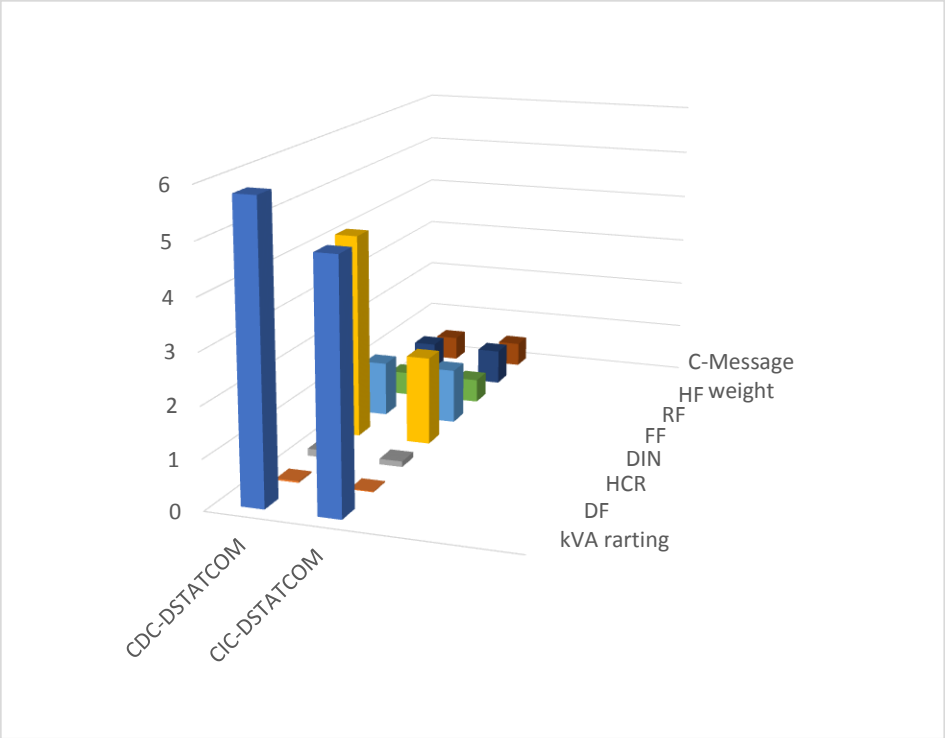

Fig. 4.9 Bar chart for the indexed parameters

Finally, the bar chart for the indexed parameters is in Fig. 4.9, it is concluded that the suggested study reveals the applicability and suitability for the PQ improvement.

4.7 Chapter Summary

In this research work, two different types of CIC-DSTATCOM and CDC-DSTATCOM topologies are presented. The cascaded DSTATCOM mainly composed of a number of identical H-bridge power cells connected in cascade The key features of the projected topology is highlighted as below:

(i) The Performance observed from the suggested topology is suitable from the application prospective of industrial and power utility sectors.

(ii) The cascaded IC-DSTATCOM which having less manufacturing cost, and having less THD.

(iii) The power cells are connected in cascade to produce high voltages which eleminates the problems of equal voltage sharing for series connected devices.

(iv) Inclusion of IFCT caused to improve the output AC voltage at inverter side.

(v) The advantages like low voltage stress, less switching loss and higher efficiency are observed.

Apart from these above mentioned merits, load balancing, source current harmonics elimination (% THD at source side 3.14), voltage regulation, pf improved to 0.99 are obtained based on benchmark worth of IEC- 61000-1& IEEE-2030-7-2018 code. The simulation analysis is carried out for the selection of topology among two approaches under unavoidable circumstances of loading. With these benefits, a thorough real time analysis will be the key features for the future work.

CHAPTER-5

CHAPTER 5

DBSCAN Based inductively coupled DSTATCOM for PQ improvement

5.1. Introduction

The prime objective of the EPDS based on the present situation is to offer secure, consistent, quality, effective & reasonable source of energy to the consumers. As a result, the EPDS must be appropriately planned, designed, and operated in a safe manner. EPDS is generally prone to greater number of failures and disturbances during process. Increased demand, a less long-lasting plan, open access to consumers, a minimum level of security, nonlinear loads, and unexpected load switching are all contributing factors to deteriorating supply quality. As a result, power system operators require innovative strategies for increasing PQ performance.

The DSTATCOM is an important choice for current PQ concerns because of this incentive to improve PQ performance in the EPDS. Despite the fact that DSTATCOM plays an important part in the EPDS, diversification of the DSTATCOM is becoming a rising role for the modern EPDS. As a result, the difficult issue is to provide flexibility and long-term viability for all of the above possibilities. Important voltage source inverter (VSI) selection, VSI extension, control algorithm design, IFCT design, and impedance matching are the primary study areas for PQ improvement.

For the past three decades, most academics and R&D firms have worked on various custom power devices (CPD) to alleviate PQ-related issues. All CPDs inject reactive power at PCC in a flexible, reliable, and rapid manner. Because the PCC is in close contact with the source, load, and DSTATCOM in DC-DSTATCOM, it is subjected to additional stress. As a result, there are increased opportunities for short circuit currents to flow, insufficient protection, and thermal losses, among other things.

To solve the shortcomings of DC-DSTATCOM, a new step must be made. As a result, the research direction is encouraged to move forward with a corrective approach based on IFCT. First and foremost, the design of DC-DSTATCOM for EPDS is the subject of this chapter. Later, with DC-DSTATCOM, the IFCT is introduced to act as an inductive medium between the source and the load. It has a variety of advantages, including reduced switching stress, improved PCC balancing voltage, increased compensation capabilities, and other conceivable combinations. For 3P3W EPDS, two

levels VSC are considered due to the design element of the DSTATCOM. Due of its popularity in the literature study, this three-leg VSI topology is widely advocated. The proposed architecture allows for future flexibility in terms of adding more converters and loads.

Traditional high-voltage transmission line monitoring systems focus entirely on AC measurements via voltage transformers (VTs) & current transformers (CTs), ignoring the DC components flowing on lines. Nonlinear loads (or) overloading transformers, may also cause harmonics to flow in the grid. Most of data is constantly collected from many sections of the EPDS. ML is a powerful mathematical method for analyze this data and offering useful imminent to system operatives so they may make quick and efficient judgments.

In this chapter we are incorporating Density based spatial clustering and noise (DBSCAN) for PQ improvement. EPDS are one of the most promising segments, with a massive quantity of underutilized data. The available datasets can be used to analyze a variety of power system planning, operation, monitoring, and economics problems. Power grids are complex nonlinear arrangements, and cutting-edge machine learning tools can aid in the analysis and modeling of their behavior.

Due to a lack of data and computational power in previous decades, machine learning (ML) did not gain widespread use in the business. Many practical uses of machine learning in power systems are now possible thanks to recent advances in computing knowledge & the distribution of improved meter infrastructures & Phasor measuring components. Load prediction, EPDS irregularity detection, security review, optimal power flow, fault identification, improving grid resiliency, & detecting frequency events are just a few of the promising applications of machine learning.

The filtering mechanism of DSTATCOM is carried out utilizing a broader mathematical approach and the DBSCAN algorithm in MATLAB/ Simulink for a healthier functioning. According on the benchmark of IEC-61000-1 & IEEE-2030-7-2018 codes, the following observations can be drawn from the proposed IC-DSTATCOM method.

(i) It is possible to achieve good convergence results.

(ii) This algorithm's main features are enhanced tracking, compensatory and adaptive capabilities.

(iii) The suggested approach enables many PQ problems, such as harmonic drop, improved potential control, healthy power factor, output load balancing, and lower DC link voltage, among others.

(iv) It also has a flexible harmonics over current protection feature.

(v) It has the ability to reorganise more parameters for a better algorithm version.

5.2. Modeling of the proposed IC-DSTATCOM

The arrangement of the 3P3W EPDS with DC-DSTATCOM and IC-DSTATCOM are exposed in Fig.5.1 & 5.2 respectively. The DC-DSTATCOM which contains of balanced 3-ϕ supply, DSTATCOM, 3-ϕ non-linear load, whereas the IC-DSTATCOM which contains of a balanced 3-ϕ supply, converter transformer DSTATCOM, 3-ϕ non-linear load. The VSI dependent DSTATCOM linked at PCC of EPDS is exposed in Fig.5.3. A customized methodology of DC-DSTATCOM & IC-DSTATCOM are utilised as a compensator to overcome the PQ difficulties. The triggering pulses of both compensators are produced by DBSCAN control technique.

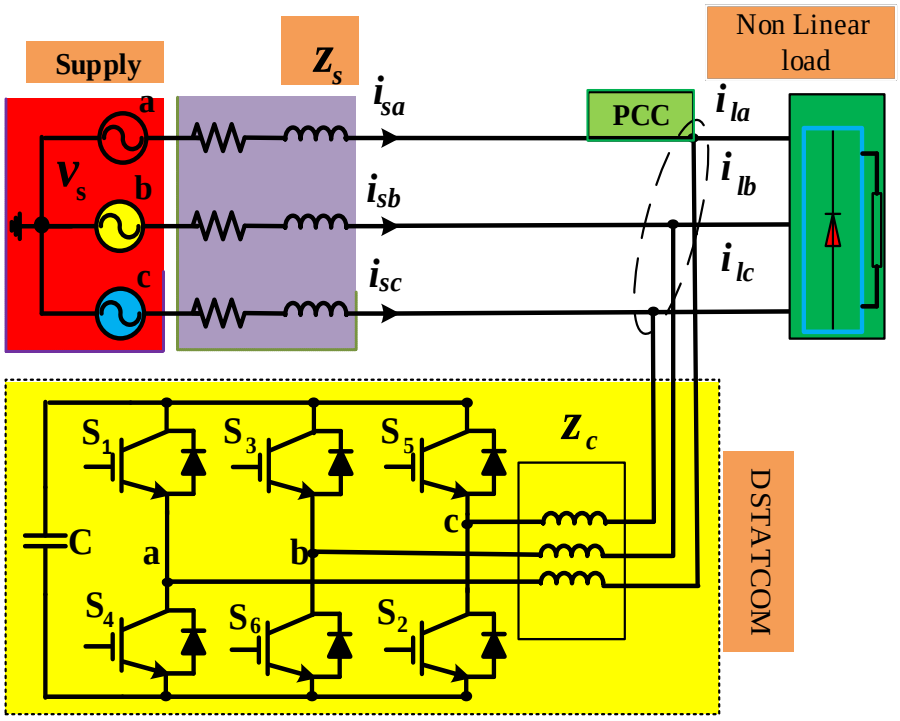

Fig.5.1 EPDS with DC- DSTATCOM

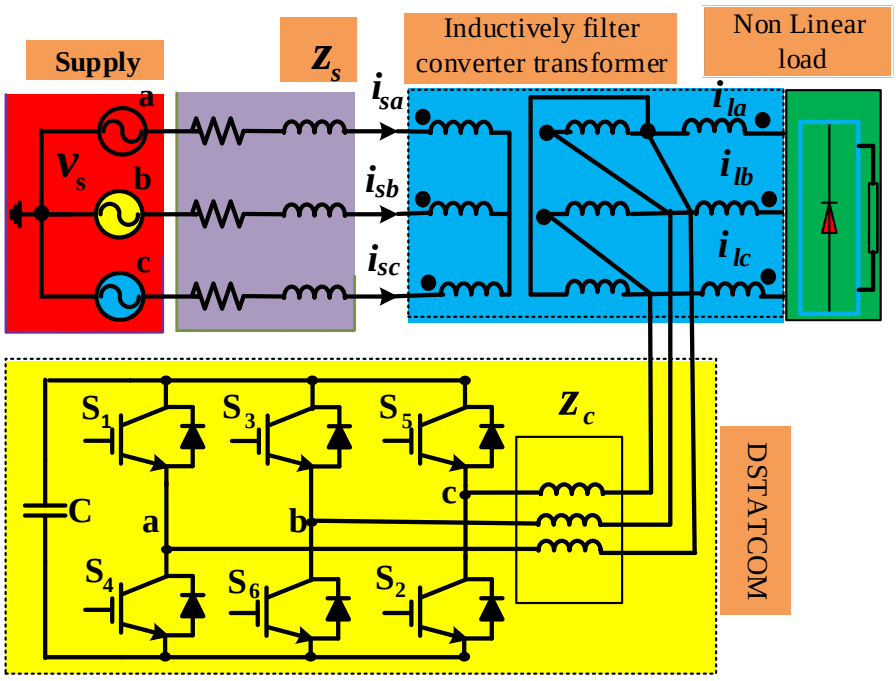

Fig.5.2 EPDS with IC- DSTATCOM

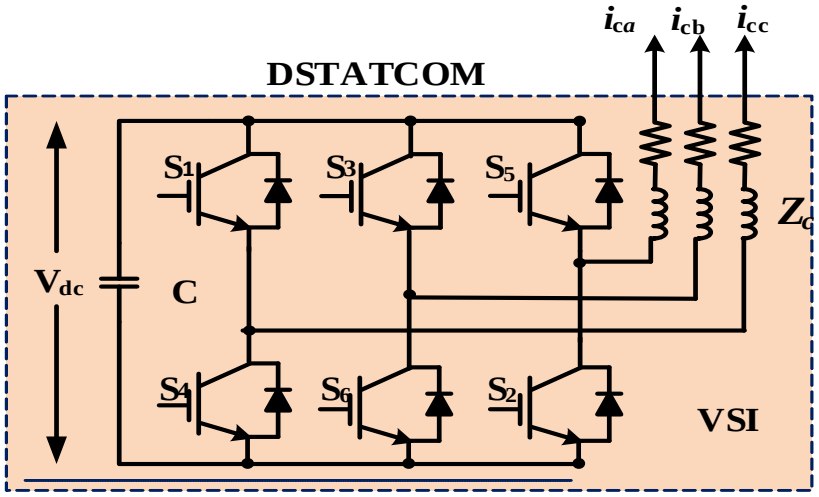

Fig. 5.3 Two-level self-supported capacitor supported VSI based DSTATCOM

The prime agenda of this work is to choose a scrupulous outline by DBSCAN control topology.

5.3. Novelties of the proposed topology

Below, we elaborate on the many ways in which the suggested approach differs from DC- DSTATCOM:

(i) *Response and reaction time:* The proposed DSTATCOM possesses better response and reaction time.

(ii) *Component extraction:* the proposed method has the capability to extract demanded time domain component for both harmonics and inter harmonics.

(iii) *Reduced computation time:* This technique is designed to fit parallel processing structure for each time domain component to reduce the computation time.

(iv) *Dynamic operation of inverter*: AS VSC is operated by DBSCAN algorithm, the Hysteresis current controller (HCC) processes the Analog signal to convert in to digital signals for the generation of the firing pulses for different loading scenarios.

(v) *Increase in system efficiency:* The system efficiency is increased due to less iteration process is involved in the DBSCAN algorithm.

(vi) *Discount in %THD of the input current:* %THD of supply & output currents are 2.94% & 26.69% correspondingly gained from IC-DSTATCOM. while, the %THD of the input & output currents are 4.00% & 26.32% correspondingly gained from DC-DSTATCOM.

5.4. Modelling and design of inductive transformer

The full winding structure of projected IC-DSTATCOM was exposed in Fig.5.1. The projected IC-DSTATCOM arranges inductively filter converting transformer (IFCT), DSTATCOM containing VSC & load. The IFCT plan has three winding which are used to connect DSTATCOM and non-linear load. In 3 windings, the primary winding (PW) allotted to grid with star connection, secondary side winding (SW) allocated to non-linear load with star connection & the filtering winding (FW) allocated to DSTATCOM with delta type wiring. The special winding of IFCT aimed to get the balanced potential between grids, DSTATCOM & load. In the following sections, we'll learn deeper about the IFCT's mathematical model and filtering method [19].

$$\begin{cases} N_1 \mathrm{i}_{\mathrm{ap}} + N_2 \mathrm{i}_{\mathrm{as}} + N_3 \mathrm{i}_{\mathrm{af}} = 0 \\ N_1 \mathrm{i}_{\mathrm{bp}} + N_2 \mathrm{i}_{\mathrm{bs}} + N_3 \mathrm{i}_{\mathrm{bf}} = 0 \\ N_1 \mathrm{i}_{\mathrm{cp}} + N_2 \mathrm{i}_{\mathrm{cs}} + N_3 \mathrm{i}_{\mathrm{cf}} = 0 \end{cases} \quad (5.1)$$

$$\begin{cases} \mathrm{i_{ap}} = (u_{sa} - u_{apo})/Z_{line} \\ \mathrm{i_{bp}} = (u_{sb} - u_{bpo})/Z_{line} \\ \mathrm{i_{cp}} = (u_{sc} - u_{cpo})/Z_{line} \\ \mathrm{i_{as}} = i_{al} + i_{zal} \\ \mathrm{i_{bs}} = i_{bl} + i_{zbl} \\ \mathrm{i_{cs}} = i_{cl} + i_{zcl} \\ \mathrm{i_{ap}} + i_{bp} + i_{cp} = 0 \\ \mathrm{i_{as}} + i_{bs} + i_{cs} = 0 \\ \mathrm{i_{af}} + i_{bf} + i_{cf} = 0 \\ \mathrm{i_{af}} = i_{cf} + i_{cat} = i_{cf} + i_{ra} + i_{za} \\ \mathrm{i_{bf}} = i_{af} + i_{cbt} = i_{af} + i_{rb} + i_{zb} \\ \mathrm{i_{cf}} = i_{bf} + i_{cct} = i_{bf} + i_{rc} + i_{zc} \end{cases} \tag{5.2}$$

$$\begin{cases} \mathrm{u_{abf}} = (i_{zb} - i_{za})/Z_o \\ \mathrm{u_{bcf}} = (i_{zc} - i_{zb})/Z_o \\ \mathrm{u_{caf}} = (i_{za} - i_{zc})/Z_o \end{cases} \tag{5.3}$$

$$\begin{cases} \mathrm{u_{apo}} - \dfrac{\mathrm{N_1}}{\mathrm{N_3}}\mathrm{u_{abf}} = \mathrm{i_{ap}z_p} - \dfrac{\mathrm{N_1}}{\mathrm{N_3}}\mathrm{i_{af}z_f} \\ \mathrm{u_{bpo}} - \dfrac{\mathrm{N_1}}{\mathrm{N_3}}\mathrm{u_{bcf}} = \mathrm{i_{bp}z_p} - \dfrac{\mathrm{N_1}}{\mathrm{N_3}}\mathrm{i_{bf}z_f} \\ \mathrm{u_{cpo}} - \dfrac{\mathrm{N_1}}{\mathrm{N_3}}\mathrm{u_{caf}} = \mathrm{i_{cp}z_p} - \dfrac{\mathrm{N_1}}{\mathrm{N_3}}\mathrm{i_{cf}z_f} \end{cases} \tag{5.4}$$

5.4.1. Mathematical demonstrating of the DBSCAN by PI controller

The whole topology in addition with complete mathematical modeling engaged in the evaluation of switching pulse production is in Fig. 5.3. The total strategy procedure is articulated below:

$$w_{pa}(n+1) = w_{pa}(n) + \mu_k e_k i_{La} u_{pa} - \sum_{1}^{n} w_{pa}(n)\xi_k \Big/ \sum_{1}^{n} w_{pa}(n) \tag{5.5}$$

$$w_{pb}(n+1) = w_{pb}(n) + \mu_k e_k i_{Lb} u_{pb} - \sum_{1}^{n} w_{pb}(n)\xi_k \Big/ \sum_{1}^{n} w_{pb}(n) \tag{5.6}$$

$$w_{pc}(n+1) = w_{pc}(n) + \mu_k e_k i_{Lc} u_{pc} - \sum_{1}^{n} w_{pc}(n)\xi_k \Big/ \sum_{1}^{n} w_{pc}(n) \tag{5.7}$$

$$w_{qa}(n+1) = w_{qa}(n) + \mu_k e_k i_{La} u_{qa} - \sum_{1}^{n} w_{qa}(n)\xi_k \Big/ \sum_{1}^{n} w_{qa}(n) \qquad (5.8)$$

$$w_{qb}(n+1) = w_{qb}(n) + \mu_k e_k i_{Lb} u_{qb} - \sum_{1}^{n} w_{qb}(n)\xi_k \Big/ \sum_{1}^{n} w_{qb}(n) \qquad (5.9)$$

$$w_{qc}(n+1) = w_{qc}(n) + \mu_k e_k i_{Lc} u_{qc} - \sum_{1}^{n} w_{qc}(n)\xi_k \Big/ \sum_{1}^{n} w_{qc}(n) \qquad (5.10)$$

5.4.2. The median of the weighting values for active & reactive components

The average quantity (w_p) of active weight measures of 3-phases is computed as like below:

$$w_p = \frac{w_{pa} + w_{pb} + w_{pc}}{3} \qquad (5.11)$$

The average quantity (w_q) of re-active weigh measures of 3-phases is computed as like below:

$$w_q = \frac{w_{qa} + w_{qb} + w_{qc}}{3} \qquad (5.12)$$

5.4.3. Computation of in-phase & quadrature unit potential template

The in-phase unit potential templates *(u_{pa}, u_{pb}, u_{pc})* are the relation of phase potentials & amplitude of PCC potential (v_t) estimated as follows

$$u_{pa} = \frac{v_{sa}}{v_t}, u_{pb} = \frac{v_{sb}}{v_t}, u_{pc} = \frac{v_{sc}}{v_t} \qquad (5.13)$$

Likewise, the quadrature unit potential patterns (u_{qa}, u_{qb}, u_{qc}) are the relations of phase potentials shown below:

$$\left.\begin{aligned} u_{qa} &= \frac{u_{pb} + u_{pc}}{\sqrt{3}} \\ u_{qb} &= \frac{3u_{pa} + u_{pb} - u_{pc}}{2\sqrt{3}} \\ u_{qc} &= \frac{-3u_{pa} + u_{pb} - u_{pc}}{2\sqrt{3}} \end{aligned}\right\} \qquad (5.14)$$

Where v_t can be expressed as

$$v_t = \sqrt{\frac{2(v_{sa}^2+v_{sb}^2 + v_{sc}^2)}{3}} \quad (5.15)$$

5.4.4. Assessment of active module of base supply currents

The DC potential error is written as

$$v_{de} = v_{dc\,(ref)} - v_{dc} \quad (5.16)$$

The PI controller's output is written as

$$w_{cp} = k_{pa} v_{de} + k_{ia} \int v_{de} dt \quad (5.17)$$

The overall active modules of origin supply current is found by totaling both w_{cp}, w_{ap}

It can be written as

$$w_{sp} = w_{ap} + w_{cp} \quad (5.18)$$

5.4.5 Assessment of active module of base supply currents

The AC potential error is written as

$$v_{te} = v_{t\,(ref)} - v_t \quad (5.19)$$

The possible expression for the PI controller's output is

$$w_{cq} = k_{pr} v_{te} + k_{ir} \int v_{te} dt \quad (5.20)$$

The overall reactive modules of the origin supply current is found by deducting PI controller's output from the mean weight of active module of output current. It can be written as

$$w_{sq} = w_{rq} - w_{cq} \quad (5.21)$$

5.4.6 Assessment of switching arrangement

The instant base active module is written as:

$$i_{aa} = w_{sp} u_{pa},\ i_{ab} = w_{sp} u_{pb},\ i_{ac} = w_{sp} u_{pc} \quad (5.22)$$

Likewise, the instant base reactive module is Written as:

$$i_{ra} = w_{sq} u_{qa}, i_{rb} = w_{sq} u_{qb}, i_{rc} = w_{sq} u_{qc} \quad (5.23)$$

The reference input source currents are equated like

$$i_{sa}^* = i_{aa} + i_{ra}, i_{sb}^* = i_{ab} + i_{rb}, i_{sc}^* = i_{ac} + i_{rc} \quad (5.24)$$

The both (i_{sa}, i_{sb}, i_{sc}) & ($i^*_{sa}, i^*_{sb}, i^*_{sc}$) are compared then error values are sent to HCC. Their outputs are fed to $\mathbf{T_1}$ -$\mathbf{T_6}$ insulated-gate bipolar transistors (IGBTs) used in the voltage source converter (VSC).

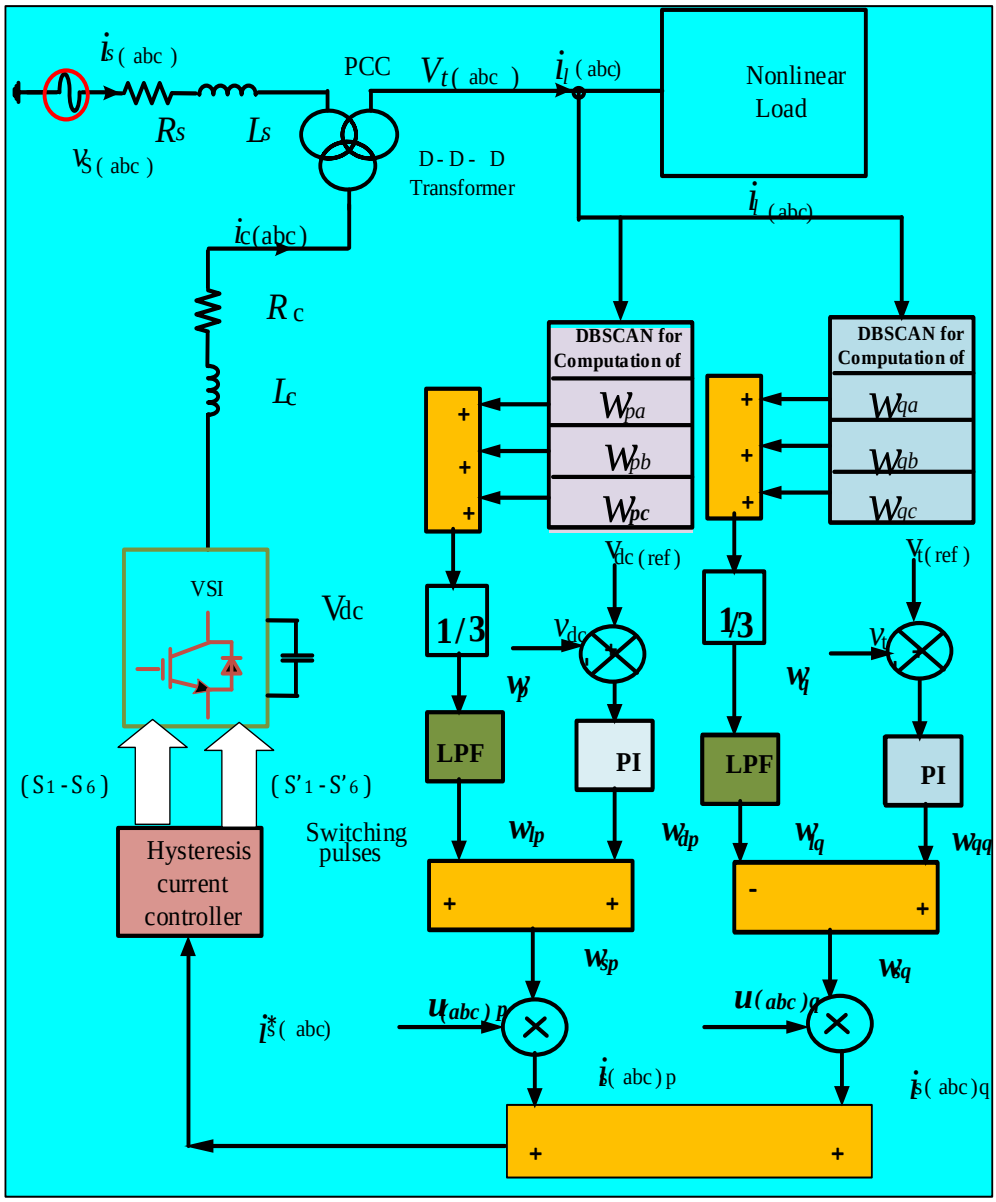

Fig. 5.4 Switching signals production by DBSCAN control algorithm for IC-DSTATCOM

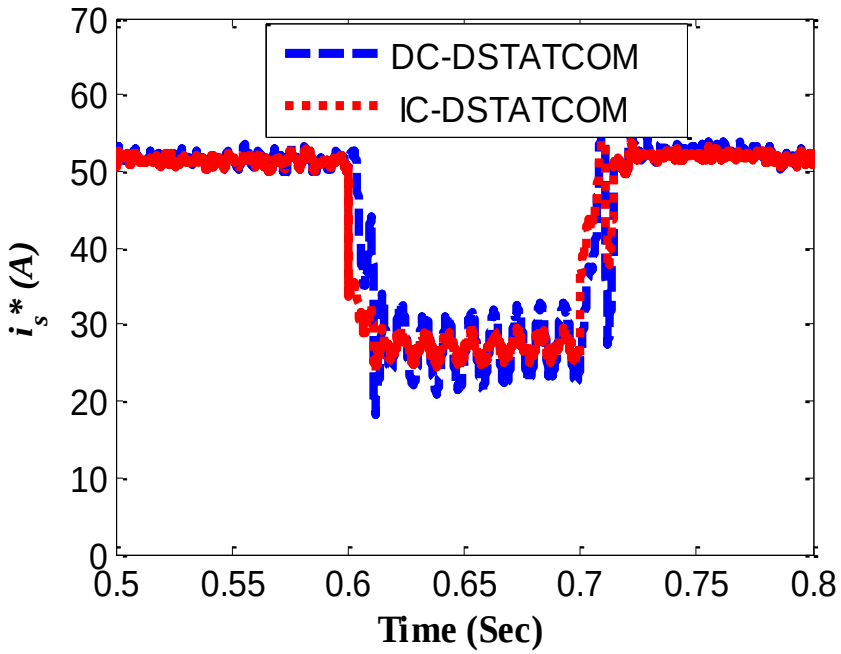

Fig. 5.5 Internal signal of the control structure

5.5. SIMULATION OUTCOMES & ANALYSIS

The performance of EPDS with topologies are demonstrated using MATLAB/Simulink studies. Identical operating conditions and system parameters are considered to perform computer simulations. The suggested DBSCAN mechanism is implemented for reference current generation for appropriate switching pulses to the both varieties of topologies. The system parameters are listed in Table 5.2. Both the balanced and unbalanced performance of IC-DSTATCOM and DC-DSTATCOM based EPDS are analyzed here in the below sub-sections.

5.5.1 Simulation results of DC-DSTATCOM

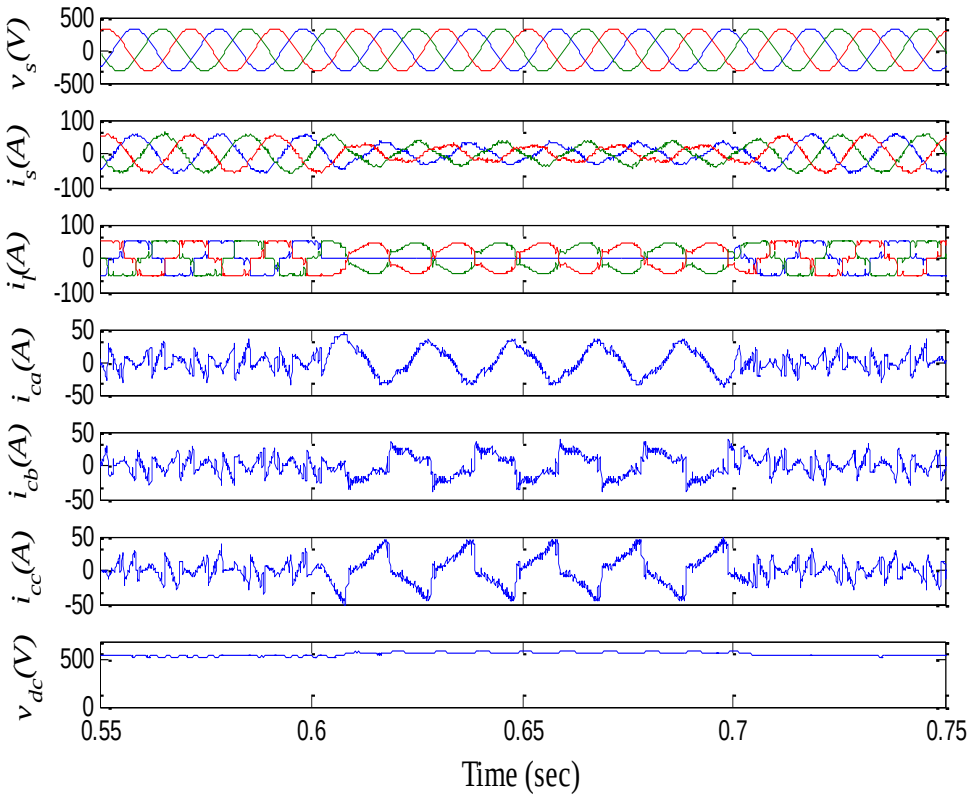

Fig. 5.6 a Simulation waveform of source potential, supply current, output current, DSTATCOM current and DC potential with DC- DSTATCOM.

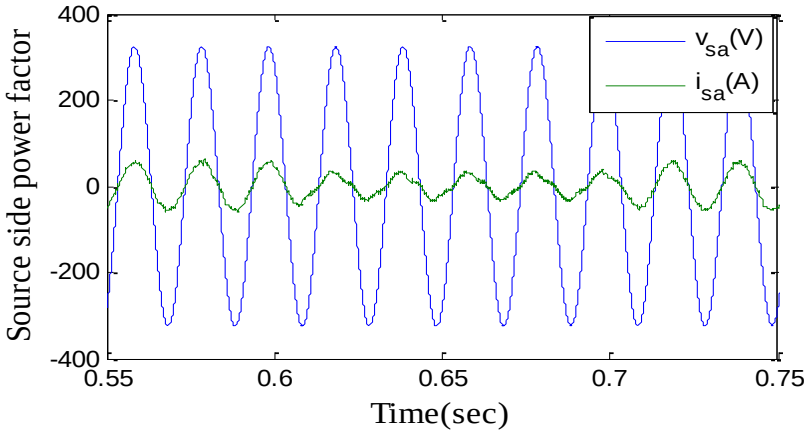

Fig.5.6 b Source side powerfactor with DC- DSTATCOM

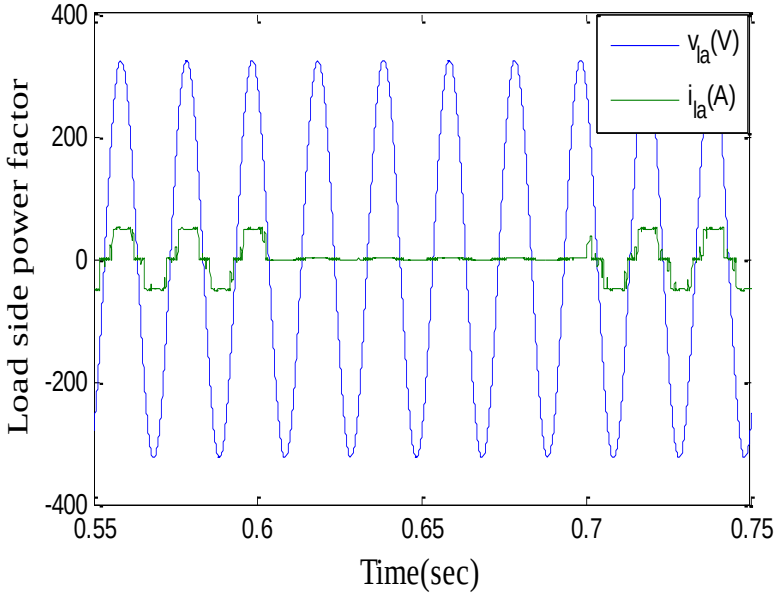

Fig. 5.6 c Load side powerfactor with DC- DSTATCOM

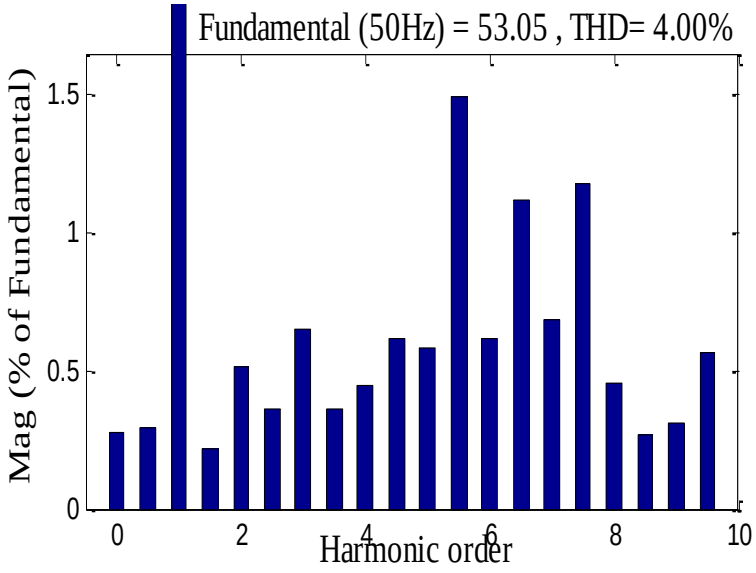

Fig.5.6 d Source current THD with DC- DSTATCOM

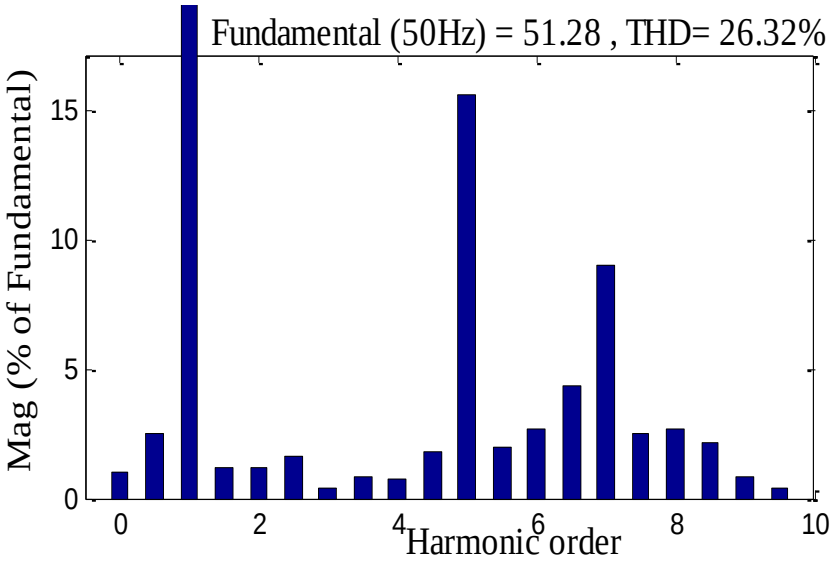

Fig. 5.6 e Load current THD with DC- DSTATCOM

To verify the PQ performance during the un-balanced loading condition, DBSCAN based direct coupled DSTATCOM is considered. The simulation time in between 0.55S and 0.75S for this Power Distribution system (PDS) is chosen. Here, the load is turn inactive in any-phase with opening the CB at 0.6 & turn active at 0.7 Sec. as described in fig 5.6 a. For this particular event, time in varying load is maintained all over the mentioned simulation time, as depicted in fig. 5.6 a. Several sub figures are set on the single plot to show the behavior of supply potential (vs), load output current (i_l), source current (is), DSTATCOM current (ica, icb, icc) & respective DC potential (vdc) respectively. By considering a-phase supply voltage and corresponding current, the power factor of the supply side is observed and shown in Fig.5.6. b. From this figure, the source side power factor is maintained to improve and maintained at p.f 0.97. The harmonics mitigation performance of the source & load current are exposed in the fig.5.6 d. & fig.5.6 e. respectively. In fig.5.6 e. the THD of the load current is greatly distorted and whose THD is 26.32%, whereas source current is improved with reduced THD-4% The potential THD is maintained with a smaller worth than the requirement of the IEC-61000-3-2 & IEEE-519-2018 standard (i.e., THD < 5%). In addition, this control scheme maintains load balancing and voltage regulation as shown in Fig.5.6 a. Therefore, it can be said that the imposed scheme is fit for the upgrading of the PQ in the EPDS.

5.5.2 Simulation results of IC- DSTATCOM

To validate the PQ performance during the unbalanced loading, DBSCAN based inductively coupled DSTATCOM is considered. The simulation time in between 0.55S and 0.75S for this Power Distribution system (PDS) is chosen. Here, the load is turn in active in any-phase with opening the CB at 0.6 & turn active at 0.7 Sec. as described in fig 5.7 a. For this particular event, time varying load is maintained all over the mentioned simulation time, as depicted in fig.5.7 a. Several sub figures are set on the single plot to show the behavior of supply potential (vs), load output current ($\boldsymbol{i_l}$), source current (is), DSTATCOM current (ica, icb, icc) and respective DC potential (vdc) respectively. By considering a-phase supply potential & corresponding current, the PF of the supply side is observed and shown in Fig. 5.7 c from this figure, the source side power factor is maintained to improve and maintained at p.f 0.99. The harmonics mitigation performance of the input & load output current is exposed in the fig.5.7 d & fig.5.7 e correspondingly. In fig.5.7 e the THD of the load output current is greatly distorted and whose THD is 26.69%, whereas source current is improved with reduced THD 2.94%, The potential THD worth is maintain with a less value than the requirement of the IEC-61000-3-2 & IEEE-519-2017 standard (i.e., THD < 5%). In addition, this control scheme maintains load balancing and voltage regulation as shown in Fig.5.7. a. Therefore, it can be said that the projected scheme is fit for the development of the PQ in the PDS. Because of the 535V desired and consistent DC link potential, the potential regulation is maintained. Finally, 320V is maintained at PCC to meet the voltage balancing requirements.

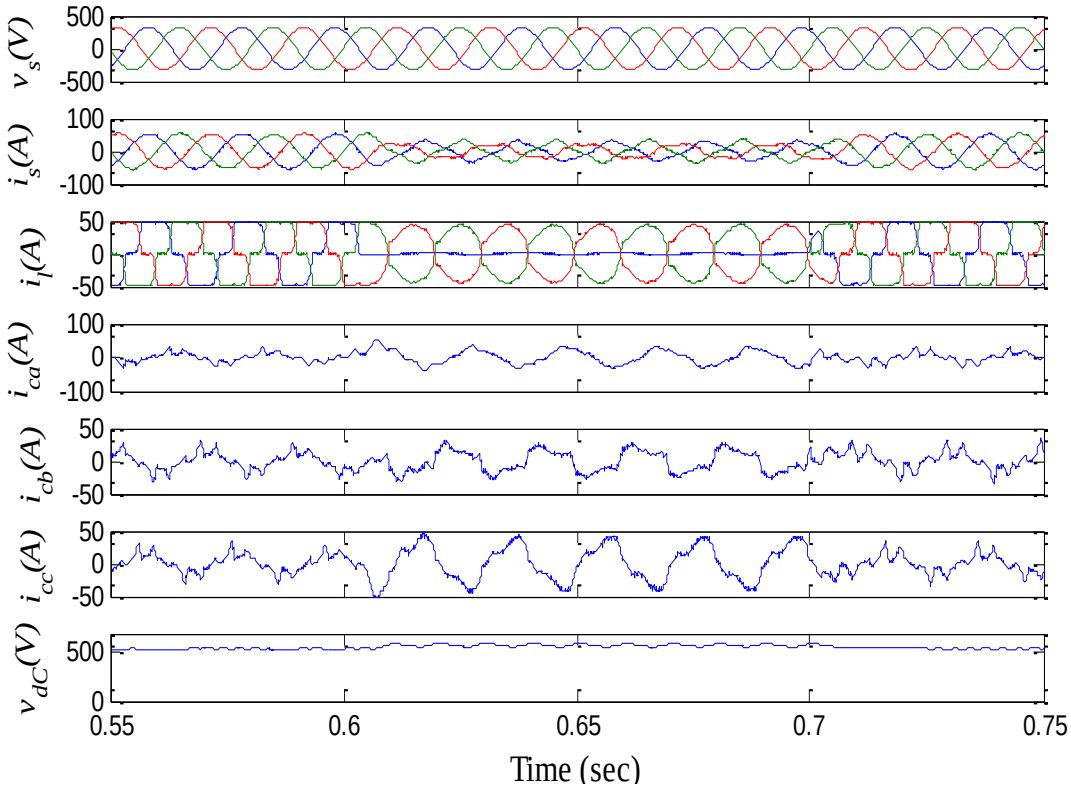

Fig. 5.7 a Simulated 3-phase supply potential, supply current, output current, DSTATCOM current, DC potential with IC-DSTATCOM

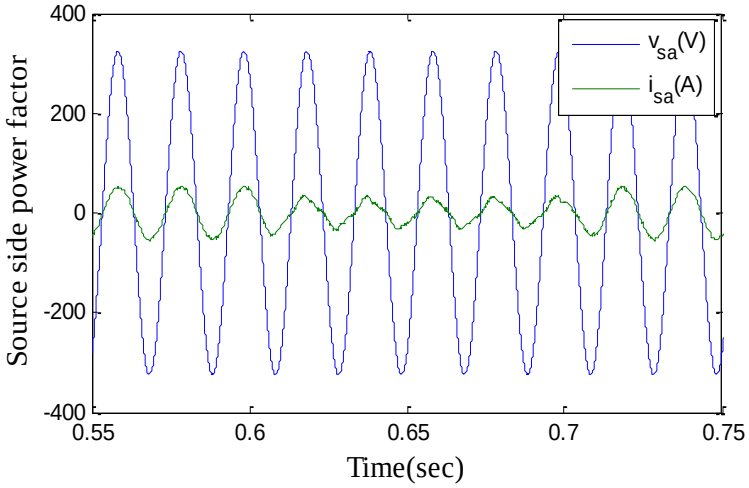

Fig. 5.7 b Source side powerfactor with IC-DSTATCOM

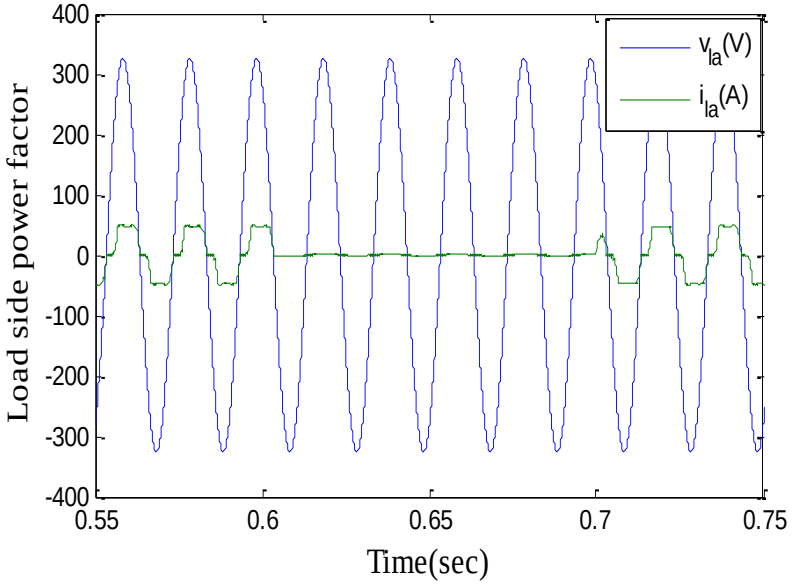

Fig. 5.7 c Load side powerfactor with IC-DSTATCOM

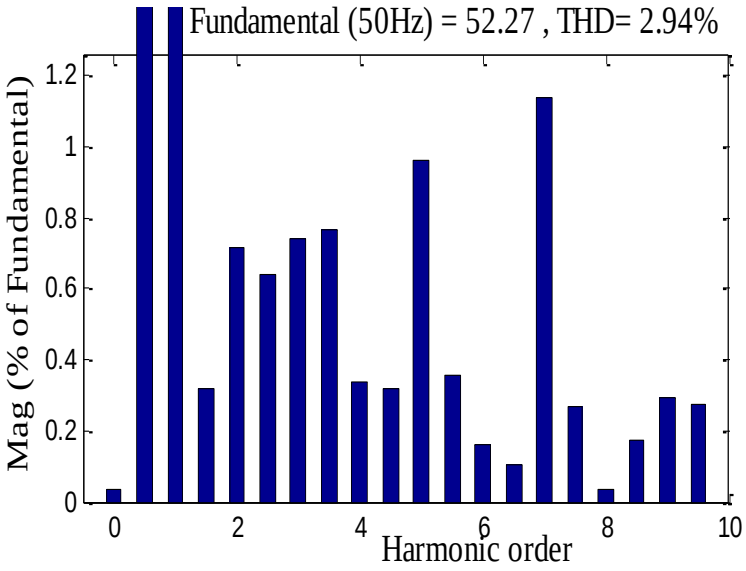

Fig. 5.7 d Source current THD with IC-DSTATCOM

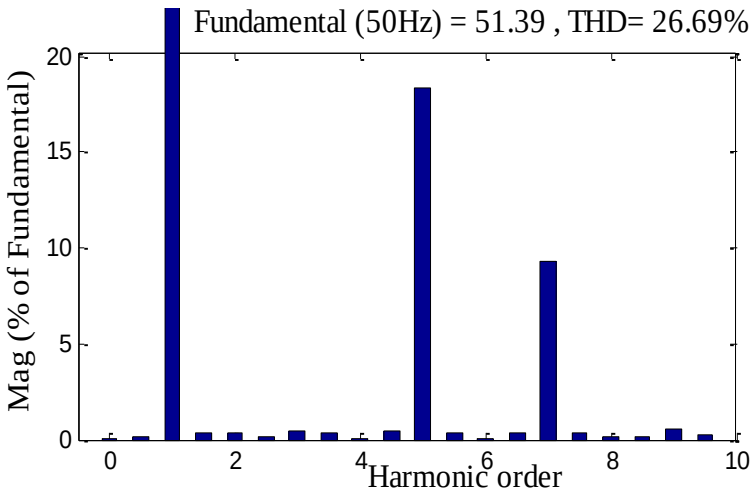

Fig. 5.7 e Load current THD with IC-DSTATCOM

Table.5.1 Performance parameter of DC-DSTATCOM and IC-DSTATCOM

Performance parameter	DSTATCOM at PCC	
	DC-DSTATCOM	IC-DSTATCOM
i_s(A), %THD	53.05, 4.00	52.27, 2.94
v_s (V), %THD	321.5, 2.24	321.3, 1.43
i_l (A), %THD	51.28, 26.32	51.39,26.69
Power Factor	0.94	0.99

Table.5.2 Simulation formation parameters

Symbol	Definition	Value
v_s	3- phase supply potential	230V/phase
f_s	Frequency	50Hz
R_s	Input resistance	0.5Ω
L_s	Input inductance	2mH
K_{pr}	AC 'P'controller	0.2
K_{ir}	'I' controller	1.1
v_{dc}	DC link potential	600V
C_{dc}	Capacitor	2000μF
K_{pa}	'P' controller of DC	0.01
K_{ia}	'I' controller of DC	0.05
R_c	VSC resistance	0.25Ω
L_c	VSC inductance	1.5mH

Table.5.3 Basic name plate rating parameters of the IFCT

	Grid side	Load side	Filtering side
Wiring scheme	**Wye**	**Wye**	**Wye**
Nominal power and frequency	**10kV, 50 Hz**	**10kV, 50 Hz**	**10kV, 50 Hz**
Voltage (ph-ph), R, and L	**230V, 0.002 (pu), 0.08 (pu)**	**230V, 0.002 (pu), 0.08 (pu)**	**230V, 0.002 (pu), 0.08 (pu)**
Magnetic resistance	**500Ω**	**500 Ω**	**500 Ω**
Magnetic inductance	**500 Ω**	**500 Ω**	**500 Ω**

Table.5.4 Measured active & reactive power of IFCT

Grid side	**Active power** **Reactive power**	**26 kW** **1.388 kVAR**
Load side	**Active power** **Reactive power**	**15 kW** **1.388 kVAR**
Filtering side	**Active power** **Reactive power**	**24 kW** **570 VAR**

5.6 Analysis and calculation of kVA rating, DF, HCR, DIN, FF, RF, HF and C-Message weights

5.6.1 Analysis of kVA rating

The Volt ampere (VA) rating=$\sqrt{3} * \frac{v_{dc}}{\sqrt{2}} * \frac{I_f}{\sqrt{2}}$

Where $v_{dc}$the DC potential of VSI & I_f is the inverter current

DC-DSTATCOM = $\sqrt{3} * \frac{541}{\sqrt{2}} * \frac{12.5}{\sqrt{2}} = 5.856\ kVA$

IC-DSTATCOM = $\sqrt{3} * \frac{541}{\sqrt{2}} * \frac{10.5}{\sqrt{2}} = 4.919$kVA

5.6.2 Calculation of Derating Factor (DF)

DF= 1-efficiency Efficiency = $\frac{\text{output power}}{\text{input power}} * 100$

The power efficiency of DC-DSTATCOM can be calculated by the following

kVA rating of CDC-DSTATCOM = 5.85 kVA, power factor cosϕ = 0.97

kW output of the CDC-DSTATCOM = kVA* cosϕ

=5.85*0.97

= 5.67 kW

Power losses of CDC-DSTATCOM = $3I_f^2 * R_c$

I_f is the inverter current= 12.5 A, R_c= 0.25 Ω

$3I_f^2 * R_c$ = 3*$12.5^2 * 0.25$ = 117.18 W

Power input = output power + losses

= 5670+117.18 = 5787.18 W = 5.787 kW

Efficiency of DC-DSTATCOM = $\frac{\mathbf{5.67}}{\mathbf{5.787}} * 100$ = 97.97%

DF of DC-DSTATCOM = 1- efficiency = 1- 0.97 = 0.03

The power efficiency of IC-DSTATCOM can be calculated by the following

kVA rating of IC-DSTATCOM = 4.919 kVA, power factor cosϕ = 0.99

kW output of the IC-DSTATCOM = kVA* cosϕ

=4.919*0.99

= 4.869 kW

I_f is the inverter current= 10.5 A, R_c= 0.25 Ω

$3I_f^2 * R_c$ = 3*$10.5^2 * 0.25$ = 82.68 W

Power input = output power + losses

= 4869 + 82.68 = 4951.68 W = 4.95 kW

Efficiency of IC-DSTATCOM = $\frac{4.86}{4.95} * 100$ = 98.18%

DF of IC-DSTATCOM = 1- efficiency = 1- 0.981 = 0.019

5.6.3 Harmonic compensation ratio (HCR)

The HCR of DC-DSTATCOM is calculated as follows

$$\text{HCR} = \frac{\text{THD\% after compensation}}{\text{THD\% before compensation}} = \frac{4.00}{26.32} = 0.151$$

Similarly, the HCR of IC-DSTATCOM is given as

$$\text{HCR} = \frac{THD\%\ after\ compensation}{\text{THD\% before compensation}} = \frac{2.94}{26.69} = 0.1101$$

5.6.4 Distortion index (DIN)

Taylor series expansion for small ranks of harmonics is below

$$\text{DIN} = \text{THD}\ (1 - \frac{1}{2}(\text{THD}))$$

DIN for DC-DSTATCOM = $4.00(1 - \frac{1}{2}\ 4.00) =$ -4

DIN for IC-DSTATCOM = $2.94\ (1 - \frac{1}{2}\ 2.94) =$ -1.38

5.6.5 Form factor (FF)

The form factor is defined as FF = $\frac{I_{rms}}{I_{avg}}$

FF for DC-DSTATCOM =

I_{rms}= 39.14 A $\qquad I_{rms} = \frac{\pi}{2\sqrt{2}} I_{avg}$

I_{avg}=35.23A $\qquad$ FF= $\frac{39.14}{35.23}$= 1.11

FF for IC-DSTATCOM =

I_{rms}= 37.65 A $\qquad I_{avg}$=33.89A

FF= $\frac{37.65}{33.89}$= 1.11

5.6.6 Ripple factor (RF)

RF= $\frac{I_{AC}}{I_{DC}}$

$$\text{RF} = \frac{\sqrt{(I_{rms})^2 - (I_{DC})^2}}{I_{DC}} = \sqrt{(FF^2) - 1}$$

RF for DC-DSTATCOM = $\sqrt{(FF^2) - 1} = \sqrt{(1.11^2) - 1}$ = 0.48

RF for IC-DSTATCOM = $\sqrt{(FF^2) - 1} = \sqrt{(1.11^2) - 1}$ = 0.48

5.6.7 Harmonic factor (HF)

$$HF = \frac{I_{rms}^{(h)}}{I_{rms}^{(1)}}$$

HF for DC-DSTATCOM = $\frac{39.14}{53.05} = 0.737$

HF for IC-DSTATCOM=$\frac{37.65}{52.27} = 0.72$

5.6.8 C-Message weights

C-Message weight

$$C = \frac{\sqrt{\sum_{i=1}^{\infty}(C_i I^{(i)})^2}}{\sqrt{\sum_{i=1}^{\infty}(I^{(i)})^2}} \qquad C = \frac{\sqrt{\sum_{i=1}^{\infty}(C_i I^{(i)})^2}}{I_{rms}}$$

C-Message weights for DC-DSTATCOM = $\frac{39.14^2}{53.05^2} = 0.54$

C-Message weights for IC-DSTATCOM = $\frac{37.65^2}{52.27^2} = 0.51$

Table.5.5 Comparative study on kVA rating, DF, HCR, DIN, FF, RF, HF and C-Message weight of DC-DSTATCOM and IC-DSTATCOM

Sl. No.	Types of configurations	Analysis of KVA rating	DF	HCR	DIN	FF	RF	HF	C-message weight
1	CDC-DSTATCOM	5.856	0.03	0.151	-4	1.11	0.48	0.737	0.54
2	CIC-DSTATCOM	4.919	0.019	0.1101	-1.38	1.11	0.48	0.72	0.51

C

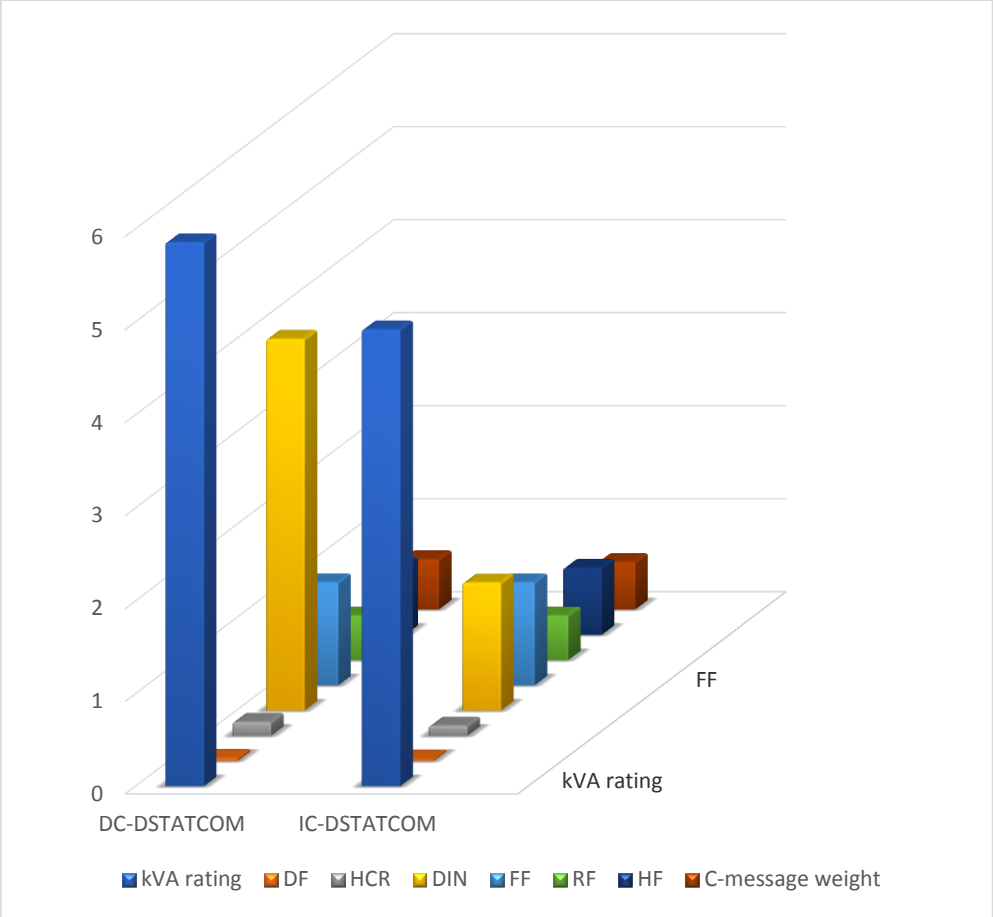

Fig. 5.8 Bar chart for the indexed parameters

It is observed that the proposed study reveals the applicability and suitability for the PQ improvement. Finally, the bar chart for the indexed parameters is presented in the Fig.5.8.

5.7 Chapter summary

This research work focuses on the analysis of two different types of IC-DSTATCOM and DC-DSTATCOM topologies. Firstly, this chapter analysed the motivation of DSTATCOM with direct coupling, secondly, analysed the efficiency of inductively coupled DSTATCOM. Finally, the proposed DBSCAN topology could realize more effective usage in terms of PQ.

The key features of the proposed topology is highlighted as follows:

(i) Inclusion of IFCT caused to improve the output AC voltage at inverter side as compared to other case studies.

(ii) The advantages like low voltage stress, less switching loss and higher efficiency are observed.

(iii) Apart from these above mentioned merits, load balancing, source current harmonics elimination, voltage regulation, pf improvement are obtained as per target value of IEEE and IEC grid code.

The simulation analysis is carried out for the selection of topology among two approaches under unavoidable circumstances of loading. With these benefits, a thorough real time analysis will be the key features for the future work.

CHAPTER-6

CHAPTER 6

Comparative analysis between DC-DSTATCOM and IC-DSTATCOM using Different control Algorithms

6.1 Comparative study between *ICOSϕ* and DBSCAN control algorithm

Here, we provide the results of our analysis contrasting the *ICOSϕ* control method with that of the DBSCAN control algorithm.

(i) The following table provides a comprehensive comparison of the harmonic spectrum. The following is an explanation for these findings: %THDs of input & load currents are observed by 3.57 & 27.90% correspondingly with *ICOSϕ* control algorithm with inductively coupled DSTATCOM, But coming to the proposed DBSCAN based inductively coupled DSTATCOM the %THDs of source & load currents are observed by 2.94 & 26.69% correspondingly. It is marked that DBSCAN based IC-DSTATCOM is keeping better harmonic distortion performance as per IEEE and IEC standards compared to *ICOSϕ* based IC-DSTATCOM.

(ii) The harmonic factor with *ICOSϕ* based IC-DSTATCOM is 0.127, for DBSCAN based IC-DSTATCOM it is 0.1101

Table.6.1 Comparative analysis between *ICOSϕ* control algorithm and *DBSCAN* control algorithm

Performance parameter	**DSTATCOM at PCC**	
	IC-DSTATCOM (*ICOSϕ* CONTROL ALGORITHM**)**	IC-DSTATCOM (*DBSCAN* CONTROL ALGORITHM)
%THD, i_s(A)	53.67, 3.57	52.27, 2.94
v_s (V), %THD	321, 1.42	321, 1.42
%THD ,i_l (A)	51.34 ,27.91	51.39,26.69
P.F	0.99	0.99

6.2 Comparative study between *ICOSϕ* and DBSCAN control algorithm

Here, we provide the results of our analysis contrasting the *ICOSϕ* control method with that of the DBSCAN control algorithm.

(i) The following table provides a comprehensive comparison of the harmonic spectrum. The following is an explanation for these findings: %THDs of input & load currents are observed by 3.14 & 27.90% correspondingly with *ICOSϕ* control algorithm with inductively coupled DSTATCOM, But coming to the proposed DBSCAN based inductively coupled DSTATCOM the %THDs of source & load currents are observed by 2.94 & 26.69% correspondingly. It is marked that DBSCAN based IC-DSTATCOM is keeping better harmonic distortion performance as per IEEE and IEC standards compared to *ICOSϕ* based IC-DSTATCOM.

(ii) The harmonic factor with *ICOSϕ* based DC-DSTATCOM is 0.1125, for DBSCAN based IC-DSTATCOM it is 0.1101

Table.6.2 Comparative analysis between *ICOSϕ* control algorithm and *DBSCAN* control algorithm for CIC-DSTATCOM.

Parameter	**CIC-DSTATCOM (***ICOSϕ* CONTROL ALGORITHM**)**	IC-DSTATCOM (*DBSCAN* CONTROL ALGORITHM)
%THD, i_s(A)	52.42, 3.14	52.27, 2.94
v_s (V), %THD	321, 1.42	321, 1.42
%THD, i_l (A)	51.24, 27.91	51.39,26.69
P.F	0.99	0.99

6.3 Comparative study between NBP based *ICOSϕ* and DBSCAN control algorithm

Here, we provide the results of our analysis contrasting the NBP based *ICOSϕ* control method with that of the DBSCAN control algorithm.

(i) The following table provides a comprehensive comparison of the harmonic spectrum. The following is an explanation for these findings: %THDs of input & load currents are observed by 3.52 & 21.75% correspondingly with NBP based *ICOSϕ* control algorithm with direct coupled DSTATCOM, where as %THDs of source & load currents are observed by 4.00 & 26.32% correspondingly with DBSCAN based control algorithm with direct coupled DSTATCOM. But coming to the proposed DBSCAN based inductively coupled DSTATCOM the %THDs of source & load currents are observed by 2.94 & 26.69% correspondingly. It is marked that DBSCAN based IC-DSTATCOM is keeping better harmonic distortion performance as per IEEE and IEC standards compared to NBP-based *ICOSϕ and* DBSCAN based DC-DSTATCOM.

(ii) The harmonic factor with NBP based DC-DSTATCOM is 0.161, for DBSCAN based DC-DSTATCOM 0.151 and for IC-DSTATCOM it is 0.1101.

Table.6.3 Comparative analysis between NBP Based *ICOSϕ* control algorithm and *DBSCAN* control algorithm.

Performance parameter	**DSTATCOM at PCC**		
	DC-DSTATCOM (NBP Based *ICOSϕ* CONTROL ALGORITHM)	DC-DSTATCOM (*DBSCAN* CONTROL ALGORITHM)	IC-DSTATCOM (*DBSCAN* CONTROL ALGORITHM)
i_s(A), %THD	54.54, 3.52	53.05, 4.00	52.27, 2.94
v_s (V), %THD	321, 1.42	321.4, 2.23	321, 1.42
i_l (A), %THD	53.5, 21.75	51.28, 26.32	51.39,26.69
Power Factor	0.98	0.94	0.99

6.4 Comparative study between CGBP based *ICOSϕ* and DBSCAN control algorithm

Here, we provide the results of our analysis contrasting the CGBP based *ICOSϕ* control method with that of the DBSCAN control algorithm.

(i) The following table provides a comprehensive comparison of the harmonic spectrum. The following is an explanation for these findings: %THDs of input & load currents are observed by 3.13 & 22.25% correspondingly with CGBP based *ICOSϕ* control algorithm with direct coupled DSTATCOM, where as %THDs of source & load currents are observed by 4.00 & 26.32% correspondingly with DBSCAN based control algorithm with direct coupled DSTATCOM. But coming to the proposed DBSCAN based inductively coupled DSTATCOM the %THDs of source & load currents are observed by 2.94 & 26.69% correspondingly. It is marked that DBSCAN based IC-DSTATCOM is keeping better harmonic distortion performance as per IEEE and IEC standards compared to CGBP-based *ICOSϕ and* DBSCAN based DC-DSTATCOM.

(ii) The harmonic factor with CGBP based DC-DSTATCOM is 0.14, for DBSCAN based DC-DSTATCOM 0.151 and for IC-DSTATCOM it is 0.1101

Table.6.4 Comparative analysis between CGBP Based *ICOSϕ* control algorithm and *DBSCAN* control algorithm.

Performance parameter	**DSTATCOM at PCC**		
	DC-DSTATCOM (CGBP Based *ICOSϕ* CONTROL ALGORITHM)	DC-DSTATCOM (*DBSCAN* CONTROL ALGORITHM)	IC-DSTATCOM (*DBSCAN* CONTROL ALGORITHM)
i_s(A), %THD	52.05, 3.13	53.05, 4.00	52.27, 2.94
v_s (V), %THD	321, 1.42	321.4, 2.23	321, 1.42
i_l (A), %THD	52.01, 22.25	51.28, 26.32	51.39,26.69
Power Factor	0.98	0.94	0.99

6.5 Comparative study between KHLMS based and DBSCAN control algorithm

Here, we provide the results of our analysis contrasting the KHLMS control method with that of the DBSCAN control algorithm.

(i) The following table provides a comprehensive comparison of the harmonic spectrum. The following is an explanation for these findings: %THDs of input & load currents are observed by 4.43 & 26.84% correspondingly with KHLMS based control algorithm with direct coupled DSTATCOM, where as %THDs of source & load currents are observed by 4.00 & 26.32% correspondingly with DBSCAN based control algorithm with direct coupled DSTATCOM. But coming to the proposed DBSCAN based inductively coupled DSTATCOM the %THDs of source & load currents are observed by 2.94 & 26.69% correspondingly. It is marked that DBSCAN based IC-DSTATCOM is keeping better harmonic distortion performance as per IEEE and IEC standards compared to KHLMS based *and* DBSCAN based DC-DSTATCOM.

(ii) The harmonic factor with KHLMS based DC-DSTATCOM is 0.165, for DBSCAN based DC-DSTATCOM 0.151 and for IC-DSTATCOM it is 0.1101

Table.6.5 Comparative analysis between KHLMS Based algorithm and *DBSCAN* control algorithm.

Performance parameter	**DSTATCOM at PCC**		
	DC-DSTATCOM (KHLMS Based ALGORITHM**)**	DC-DSTATCOM (*DBSCAN* CONTROL ALGORITHM)	IC-DSTATCOM (*DBSCAN* CONTROL ALGORITHM)
i_s**(A), %THD**	55.94, 4.43	53.05, 4.00	52.27, 2.94
v_s **(V), %THD**	321, 1.42	321.4, 2.23	321, 1.42
i_l **(A), %THD**	53.54, 26.84	51.28, 26.32	51.39,26.69
Power Factor	0.98	0.94	0.99

6.6 Comparative study between LMBP based *ICOSϕ* and DBSCAN control algorithm

Here, we provide the results of our analysis contrasting the LMBP based *ICOSϕ* control method with that of the DBSCAN control algorithm.

(i) The following table provides a comprehensive comparison of the harmonic spectrum. The following is an explanation for these findings: %THDs of input & load currents are observed by 3.17 & 21.23% correspondingly with LMBP based *ICOSϕ* control algorithm with direct coupled DSTATCOM, where as %THDs of source & load currents are observed by 4.00 & 26.32% correspondingly with DBSCAN based control algorithm with direct coupled DSTATCOM. But coming to the proposed DBSCAN based inductively coupled DSTATCOM the %THDs of source & load currents are observed by 2.94 & 26.69% correspondingly. It is marked that DBSCAN based IC-DSTATCOM is keeping better harmonic distortion performance as per IEEE and IEC standards compared to NBP-based *ICOSϕ and* DBSCAN based DC-DSTATCOM.

(ii) The harmonic factor with LMBP based DC-DSTATCOM is 0.149, for DBSCAN based DC-DSTATCOM 0.151 and for IC-DSTATCOM it is 0.1101

Table.6.6 Comparative analysis between LMBP Based *ICOSϕ* control algorithm and *DBSCAN* control algorithm.

Performance parameter	**DSTATCOM at PCC**		
	DC-DSTATCOM (LMBP Based *ICOSϕ* CONTROL ALGORITHM**)**	DC-DSTATCOM (*DBSCAN* CONTROL ALGORITHM)	IC-DSTATCOM (*DBSCAN* CONTROL ALGORITHM)
i_s(A), %THD	55.35, 3.17	53.05, 4.00	52.27, 2.94
v_s (V), %THD	321, 1.42	321.4, 2.23	321, 1.42
i_l (A), %THD	53.79, 21.23	51.28, 26.32	51.39,26.69
Power Factor	0.98	0.94	0.99

6.7 Comparative study between SLMS based and DBSCAN control algorithm

Here, we provide the results of our analysis contrasting the SLMS based control method with that of the DBSCAN control algorithm.

(i) The following table provides a comprehensive comparison of the harmonic spectrum. The following is an explanation for these findings: %THDs of input & load currents are observed by 3.32 & 18.91% correspondingly with SLMS based control algorithm with direct coupled DSTATCOM, where as %THDs of source & load currents are observed by 4.00 & 26.32% correspondingly with DBSCAN based control algorithm with direct coupled DSTATCOM. But coming to the proposed DBSCAN based inductively coupled DSTATCOM the %THDs of source & load currents are observed by 2.94 & 26.69% correspondingly. It is marked that DBSCAN based IC-DSTATCOM is keeping better harmonic distortion performance as per IEEE and IEC standards compared to SLMS-based *and* DBSCAN based DC-DSTATCOM.

(ii) The harmonic factor with SLMS based DC-DSTATCOM is 0.175, for DBSCAN based DC-DSTATCOM 0.151 and for IC-DSTATCOM it is 0.1101.

Table.6.7 Comparative analysis between SLMS Based and *DBSCAN* control algorithm.

Performance parameter	**DSTATCOM at PCC**		
	DC-DSTATCOM (SLMS Based *ICOSϕ* CONTROL ALGORITHM**)**	DC-DSTATCOM (*DBSCAN* CONTROL ALGORITHM)	IC-DSTATCOM (***DBSCAN* CONTROL** ALGORITHM)
i_s**(A), %THD**	45.31, 3.32	53.05, 4.00	52.27, 2.94
v_s **(V), %THD**	321, 1.42	321.4, 2.23	321, 1.42
i_l **(A), %THD**	42.96, 18.91	51.28, 26.32	51.39,26.69
Power Factor	0.98	0.94	0.99

6.8 Comparative study between HLMS based and DBSCAN control algorithm

Here, we provide the results of our analysis contrasting the HLMS based control method with that of the DBSCAN control algorithm.

(i) The following table provides a comprehensive comparison of the harmonic spectrum. The following is an explanation for these findings: %THDs of input & load currents are observed by 4.06 & 25.82% correspondingly with HLMS based control algorithm with direct coupled DSTATCOM, where as %THDs of source & load currents are observed by 4.00 & 26.32% correspondingly with DBSCAN based control algorithm with direct coupled DSTATCOM. But coming to the proposed DBSCAN based inductively coupled DSTATCOM the %THDs of source & load currents are observed by 2.94 & 26.69% correspondingly. It is marked that DBSCAN based IC-DSTATCOM is keeping better harmonic distortion performance as per IEEE and IEC standards compared to NBP-based *ICOSϕ and* DBSCAN based DC-DSTATCOM.

(ii) The harmonic factor with NBP based DC-DSTATCOM is 0.157, for DBSCAN based DC-DSTATCOM 0.151 and for IC-DSTATCOM it is 0.1101.

Table.6.8 Comparative analysis between HLMS and *DBSCAN* control algorithm

Performance parameter	**DSTATCOM at PCC**		
	DC-DSTATCOM (HLMS Based *ICOSϕ* CONTROL ALGORITHM**)**	DC-DSTATCOM (*DBSCAN* CONTROL ALGORITHM)	IC-DSTATCOM (***DBSCAN* CONTROL** ALGORITHM)
i_s**(A), %THD**	54.62, 4.06	53.05, 4.00	52.27, 2.94
v_s **(V), %THD**	321, 1.42	321.4, 2.23	321, 1.42
i_l **(A), %THD**	53.40, 25.82	51.28, 26.32	51.39,26.69
Power Factor	0.98	0.94	0.99

6.9 Comparative study between SRF based IC-DSTATCOM and DBSCAN based IC-DSTATCOM

Here, we provide the results of our analysis contrasting the SRF based IC-DSTATCOM with that of the DBSCAN control algorithm.

(i) The following table provides a comprehensive comparison of the harmonic spectrum. The following is an explanation for these findings: %THDs of input & load currents are observed by 3.99 & 27.45% correspondingly with SRF control algorithm with inductively coupled DSTATCOM, But coming to the proposed DBSCAN based inductively coupled DSTATCOM the %THDs of source & load currents are observed by 2.94 & 26.69% correspondingly. It is marked that DBSCAN based IC-DSTATCOM is keeping better harmonic distortion performance as per IEEE and IEC standards compared to *ICOSϕ* based IC-DSTATCOM

(ii) The harmonic factor with SRF based IC-DSTATCOM is 0.157, for DBSCAN based IC-DSTATCOM it is 0.1101.

Table.6.9 Comparative analysis between SRF Based IC-DSTATCOM and DBSCAN Based IC-DSTATCOM.

Parameter	**IC-DSTATCOM (SRF** ALGORITHM**)**	IC-DSTATCOM (*DBSCAN* CONTROL ALGORITHM)
i_s**(A), %THD**	4.142, 3.99	52.27, 2.94
v_s **(V), %THD**	321, 1.42	321, 1.42
i_l **(A), %THD**	8.478 ,27.45	51.39,26.69
Power Factor	0.99	0.99

CHAPTER 7

CONCLUSION & FUTURE SCOPE

7.1. Conclusion

The research findings of this thesis motivated to provide better shunt compensation followed by PQ improvement due to the existence of inductively coupled loads in 3P3W EPDS. Several types of conventional and adaptive control techniques are adopted for both DC-DSTATCOM and IC-DSTATCOM to select the appropriate solution which regarded as the sole contribution of this thesis. From these above studies, it is summarized that the DBSCAN controller performs better than the $icos\phi$ technique due to quick rate of convergence to achieve the global optimum. Also, further causes effective PQ improvement. Apart from these evaluation parameters, the other parameter indices are considered for the selection of the CPD to ensure the dynamic performance. A general illustration of the operational concept & design of the proposed configuration is presented below:

The following are the major contributions are investigated within this research study.

- Both DC-DSTATCOM and IC-DSTATCOM are implemented using $icos\phi$ control scheme for EPDS. The comparison analysis is showcased that DC-DSTATCOM performs poor under imbalanced loading conditions. But, IC-DSTATCOM performs better with THD 3.57%. Including this, the certain parameter indices are justified for the better comparative analysis which is presented in the chapter: 3.
- Similarly, both CDC-DSTATCOM and CIC-DSTATCOM are successfully implemented by using $icos\phi$ control scheme for EPDS. The analyzed comparative analysis yields that the better THD 3.14% is obtained from CIC-DSTATCOM as compared to CDC-DSTATCOM. Additionally, the certain parameter indices are justified for the better comparative analysis which is presented in the chapter: 4.
- In the same way, both DC-DSTATCOM and IC-DSTATCOM has been successfully implemented by using DBSCAN control scheme for EPDS. In both topologies the IC-DSTATCOM yields that the better THD 2.94% as compared

to DC-DSTATCOM. Including this, the certain parameter indices are justified for the better comparative analysis which is presented in the chapter: 5.

- Finally, the choice of DBSCAN based IC-DSTATCOM based technique indicates the reduced overall cost, quality solution & fit for low/high potential, various power applications. However, the THD is kept within acceptable ranges (less than 5%) as per IEEE-519-2017 & IEC- 41000-3 grid code.

7.2 **Future Scope**

The study conducted in this thesis aims to replace traditional controller with AI controller for various topologies. In view of this, different control approaches are implemented to enhance the performance of IC-DSTATCOM. The significant conclusions obtained from the above chapters, which are promoted to the interesting and useful aspects for further study of PQ improvement. The following aspects are listed below.

(i) The suggested DBSCAN controller can be implemented in CIC-DSTATCOM to achieve the better PQ performance.

(ii) It could be interesting to explore the possibility of carrying the investigation on the multilevel inverter fed IC-DSTATCOM and CIC-DSTATCOM to improve the PQ issues.

(iii) The proposed technique based IC-DSTATCOM and CIC-DSTATCOM with HCC can be extended to different modulation techniques.

(iv) The tuning of the PI controller parameters for both the topologies can be achieved using the optimization techniques for further enhancement of PQ issues.

(v) The proposed technique based IC-DSTATCOM, and CIC-DSTATCOM can be integrated with renewable energy sources for continuous compensation and better voltage restoration.

REFERENCES

[1] S. B. Karanki, N. Geddada, M. K. Mishra and B. K. Kumar, "A DSTATCOM Topology with Reduced DC-Link Voltage Rating for Load Compensation with Non-stiff Source," in *IEEE Transactions on Power Electronics*, vol. 27, no. 3, pp. 1201-1211, March, 2012. doi.org/10.1109/TPEL.2011.2163946

[2] Raveendra, N., Madhu, V. & Jaya L.A. 'Rflsa control scheme for power quality disturbances mitigation in DSTATCOM with n-level inverter connected power systems". *Energy Systems* vol. 11, pp. 753–778, 2020. Doi:10.1007/s12667-019-00330-6

[3] Kouadria M.A., Allaoui T. & Denai.M. 'A hybrid fuzzy sliding-mode control for a three-phase shunt active power filter". *Energy Systems*, vol. 8, pp. 297–308, 2017. doi:org/10.1007/s12667-016-0198-4.

[4] Bouafia, S., Benaissa, A., Barkat, S. *et al.* "Second order sliding mode control of three-level four-leg DSTATCOM based on instantaneous symmetrical components theory". *Energy Systems*, vol. 9, pp. 79–111, 2018. Doi:10.1007/s12667-016-0217-5

[5] B. Singh, P.J.prakash, D. P. Kothari, A. Chandra and K.A.Haddad, "Comprehensive Study of DSTATCOM Configurations," *IEEE Transactions on Industrial Informatics*, vol. 10, no. 2, pp. 854-870, May, 2014.doi: 10.1109/TII.2014.2308437.

[6] A. Michaelides and T. Nicolaou, "Constructing an Integrated Inductive-Capacitive Component to Filter Harmonic Modulations," in IEEE Transactions on Power Delivery, vol. 36, no. 4, pp. 2109-2117, 2021. doi: 10.1109/TPWRD.2020.3020703.

[7] M. V. M Kumar, M. K. Mishra and C. Kumar, "A Grid-Connected Dual Voltage Source Inverter with Power Quality Improvement Features," in *IEEE Transactions on Sustainable Energy*, vol. 6, no. 2, pp. 482-490, 2015. *doi: 10.1109/TSTE.2014.2386534.*

[8] A. Devanshu, K. Kumar and R. Kumar, "Implementation of SRF Theory to DSTATCOM for Power Quality Improvement," IEEE DELCON-2022, pp. 1-6. doi.org/10.1109/DELCON54057.2022.9753538.

[9] Q. Liu and Y. Li, "An Inductive Filtering-Based Parallel Operating Transformer with Shared Filter for Power Quality Improvement of Wind Farm," in IEEE Transactions on Power Electronics, vol. 35, no. 9, pp. 9281-9290, 2020. doi: 10.1109/TPEL.2020.2973702.

[10] Xu, K. Dai, X. Chen and Y. Kang, "Unbalanced PCC voltage regulation with positive- and negative-sequence compensation tactics for MMC-DSTATCOM," *IET Power Electronics*, vol. 9, no. 15, pp. 2846-2858, 2016. doi.org/10.1049/iet-pel.2015.1038

[11] T.M.T. Thentral, K.V. Kumar, R. Jegatheesan, "Performance comparison of hybrid active power filter for P-Q theory and SVPWM technique," International Journal of Electrical and Computer Engineering, Vol. 11, No. 1, Feb 2021, pp. 84~93, ISSN: 2088-8708.

[12] M. M. EI-sotouhy, A.A. Monsour, M.I. Marei, "Four-leg active power filter control with SUI-PI controller," International Journal of Electrical and Computer Engineering,Vol.11, No. 4, Aug 2021, pp 2768~2778, ISSN: 2088-8708.doi:10.11591/ijece.v11i4.pp2768-2778

[13] S. Pushpanjali, S.D Swain, P.K Ray and G.Panda. "Experimental verification of DSTATCOM for various non-linear load" International Journal of Emerging Electric Power Systems, vol., no., 2021. doi.org/10.1515/ijeeps-2021-0397.

[14] E. Lei, X. Yin, Z. Zhang and Y. Chen, "An Improved Transformer Winding Tap Injection DSTATCOM Topology for Medium-Voltage Reactive Power Compensation, "*IEEE Transactions on Power Electronics*, vol. 33, no. 3, pp. 2113-2126, 2018. doi: 10.1109/TPEL.2017.2698207.

[15] H. Myneni and G. S.Kumar, "Simple algorithm for current and voltage control of LCL DSTATCOM for power quality improvement," *IET Generation, Transmission & Distribution*, vol. 13, no. 3, pp. 423-434. 2019. doi:10.1049/iet-gtd.2018.6186.

[16] Y.A.G. Gomez, N.T. Garcia, F.E. Hoyos, "Unit vector template generator applied to a new control algorithm for an UPQC with instantaneous power tensor formulation, a simulation case study," International Journal of Electrical and Computer Engineering, Vol. 10, No. 4, 2020, pp 3889~3897, ISSN: 2088-8708. doi.org/10.11591/ijece.v10i4.pp3889-3897.

[17] B. N. Rao, Y. Suresh, A. K. Panda, B. S. Naik and V. Jammala, "Development of cascaded multilevel inverter based active power filter with reduced transformers, “Power Electronics and Applications, vol. 5, no. 2, pp. 147-157, doi.org/10.24295/CPSSTPEA.2020.00013.

[18] Y. Li, T. K. Saha, F. Yao, Y. Cao, W. Liu, F. Liu, S. Hu, L. Luo, Y. Chen, G. Zhou and C. Rehtanz, " An Inductively Filtered Multi-Winding Rectifier Transformer and Its Application in Industrial DC Power Supply System," in *IEEE Transactions on Industrial Electronics*, pp. 0278-0046, 2015. doi.org/10.1109/TIE.2016.2532282.

[19] J. Yu, Y. Lia, Y. Cao and Y. Xu, “An impedance-match design scheme for inductively active power filter in distribution networks,” International Journal of Electrical Power and Energy System, vol. 99, pp. 638-649, 2018, doi: 10.1016/j.ijepes.2017.12.008.

[20] Dwarakesh.k, ‘Capacitor clamped inverter-based d-statcom for voltage regulator in power quality improvement for distribution grids’ Malaya Journal of Matematik, Vol.5, No.2, 2602-2608, 2020, doi.org/10.26637/MJM0S20/0675.

[21] S. D. Swain, P. K. Ray and K. B. Mohanty, "Improvement of Power Quality Using a Robust Hybrid Series Active Power Filter," in *IEEE Transactions on Power Electronics*, vol. 32, no. 5, pp. 3490-3498,2017. doi: 10.1109/TPEL.2016.2586525.

[22] Y. Li, T. K. Saha, O. Krause, Y. Cao and C. Rehtanz, "An Inductively Active Filtering Method for Power-Quality Improvement of Distribution Networks with Nonlinear Loads," in *IEEE Transactions on Power Delivery*, vol. 28, no. 4, pp. 2465-2473, 2013.

[23] P. Salmeron and S. P. Litran, "Improvement of the Electric Power Quality Using Series Active and Shunt Passive Filters," in *IEEE Transactions on Power Delivery*, vol. 25, no. 2, pp. 0885-8977, 2010. doi: 10.1109/TPWRD.2009.2034902.

[24] M. Mangaraj, "Operation of Hebbian least mean square controlled distributed static compensator." IET Generation, Transmission & Distribution (2021). doi.org/10.1049/gtd2.12146.

[25] P. W. Sun, C. Liu, J. S. Lai, and C. L. Chen, “Cascade dual buck inverter with phase-shift control,” IEEE Trans. Power Electron., vol. 27, no. 4, Apr. 2012 ,doi: 10.1109/TPEL.2011.2169282.

[26] B. Singh, and S. Kumar, “Control of DSTATCOM using IcosΦ algorithm”, 2009 35th Annual Conference of IEEE Industrial Electronics, pp. 322-327. doi.org/10.1109/IECON.2009.5414942.

[27] A.Tiwari, M. Tomar, "An Extensive Literature Review on Power Quality Improvement using DSTATCOM," International journal of emerging Technology and advanced engineering, pp. 591-596, vol. 4, no. 5.

[28] F. A.Waishel, N. A. Ahmed and P. Enjeti, "Active output filter under nonlinear load condition for solar powered unmanned aircraft system," 2017 IEEE 6th (ICRERA), 2017, pp. 327-330, doi: 10.1109/ICRERA.2017.8191080.

[29] Yousfi.A, Tayeb.A, CH. Abdelkader, “power quality improvement based on five level shunt APF using sliding mode control scheme connected to photovoltaic,” International Journal of Smart Grid, Vol. 1, No. 1, 2017, pp. 09~15.

[30] M.Mangaraj and A. K. Panda, “NBP-based icosϕ control strategy for DSTATCOM,” *IET Power Electronics*, vol. 10, no. 12, pp. 1617 – 1625, 2017.

[31] M.Mangaraj and A. K. Panda, “DSTATCOM deploying CGBP based icos ϕ neural network technique for power conditioning,” *Ain Shams Engg. Journal*, vol. 9, no. 4, pp. 1535-1546, 2018.

[32] M.Mangaraj, A. K. Panda, T. Penthia and A. R. Dash, “An Adaptive LMBP Training Based Control Technique for DSTATCOM,” IET Generation, Transmission and Distribution, vol. 14, no. 3, pp. 516 – 524, 2020.

[33] G. S. Rao, B. S. Goud and C. R. Reddy, "Power Quality Improvement using ASO Technique," 2021 9th International Conference on Smart Grid (ic-SmartGrid), 2021, pp. 238-242, doi: 10.1109/icSmartGrid52357.2021.9551226.

[34] M. Mangaraj and A. K. Panda, "An efficient control algorithm based DSTATCOM for power conditioning," *2015 International Conference on Industrial Instrumentation and Control (ICIC)*, Pune, pp. 1069-1073. 2015.

[35] M. Mangaraj and A. K. Panda, "Performance analysis of DSTATCOM employing various control algorithms," *IET Generation, Transmission & Distribution*, vol. 11, no. 10, pp. 2643-2653, 2017.

[36] T. Ouyang, W. Pedrycz and N. J. Pizzi, "Rule-Based Modelling With DBSCAN-Based Information Granules," in *IEEE Transactions on Cybernetics*, vol. 51, no. 7, pp. 3653-3663, 2021.

[37] W.lai, M.zhou, F.hu, K.bian, and qi song, "A new DBSCAN parameters determination method based on improved MVO" *IEEE access*, vol. 7, pp. 104085-104095, 2019.

[38] A. K. Panda and M. Mangaraj, "DSTATCOM employing hybrid neural network control technique for power quality improvement," *IET Power Electronics*, vol. 10, no. 4, pp. 480-489, 2017.

[39] X. He, Y. Jiang, B. Wang, H. Ji and Z. Huang, "An Image Reconstruction Method of Capacitively Coupled Electrical Impedance Tomography Based on DBSCAN and Image Fusion," in *IEEE Transactions on Instrumentation and Measurement*, vol. 70, pp. 1-11, 2021.

[40] Y. Yang, M. Suliang, W. Jianwen, J. Bowen, L. Weixin and L. Xiaowu, "Fault Diagnosis in Gas Insulated Switchgear Based on Genetic Algorithm and Density- Based Spatial Clustering of Applications with Noise," in *IEEE Sensors Journal*, vol. 21, no. 2, pp. 965-973, 2021.

[41] M. Mangaraj and A.K Panda, "Modelling and simulation of KHLMS algorithm-based DSTATCOM," *IET Power Electronics*, vol. 12, no. 9, pp. 2304 – 2311, 2019.

[42] M.Mangaraj and J.Sabat, "MVSI and AVSI-supported DSTATCOM for PQ Analysis," IETE Journal of Research, 2021, DOI: 10.1080/03772063.2021.1920850.

[43] M. Srinivas, I. Hussain and B. Singh, "Combined LMS–LMF-Based Control Algorithm of DSTATCOM for Power Quality Enhancement in Distribution System," in IEEE Transactions on Industrial Electronics, vol. 63, no. 7, pp. 4160-4168, July 2016, doi: 10.1109/TIE.2016.2532278.

[44] S. R. Arya, R. Niwas, K. K.Bhalla, B. Singh, A. Chandra and K. Al-Haddad, "Power Quality Improvement in Isolated Distributed Power Generating System Using DSTATCOM," in IEEE Transactions on Industry Applications,

vol. 51, no. 6, pp. 4766-4774, Nov.-Dec. 2015, doi: 10.1109/TIA.2015.2451093.

[45] S. R. Arya and B. Singh, "Performance of DSTATCOM Using Leaky LMS Control Algorithm," in IEEE Journal of Emerging and Selected Topics in Power Electronics, vol. 1, no. 2, pp. 104-113, June 2013, doi: 10.1109/JESTPE.2013.2266372.

[46] Q. Liu et al., "Shipboard power quality management using the controllably inductive power filtering method," 2017 IEEE Transportation Electrification Conference and Expo, Chicago, IL, USA, 2017, pp. 257-262, doi: 10.1109/ITEC.2017.7993281.

[47] Mustakim, E. Rahmi, M. R. Mundzir, S. T. Rizaldi, Okfalisa and I. Maita, "Comparison of DBSCAN and PCA-DBSCAN Algorithm for Grouping Earthquake Area," 2021 ICOTEN, Taiz, Yemen, 2021, pp. 1-5, doi: 10.1109/ICOTEN52080.2021.9493497.

[48] C. Bhattacharjee, A. K. Roy and B. K. Roy, "Improvement of available load voltage for a constant speed WECS coupled with fuzzy-controlled DSTATCOM," 2012 IEEE 15th ICHQP, Hong Kong, China, 2012, pp. 637-641, doi: 10.1109/ICHQP.2012.6381304.

[49] K.Yang, X.Cheng, Y.Wang, L.Chen and G.Chen, "PCC voltage stabilization by D-STATCOM with direct grid voltage control strategy," 2012 IEEE International Symposium on Industrial Electronics, Hangzhou, 2012, pp. 442-446, doi: 10.1109/ISIE.2012.6237127.

[50] Sabat, J., Mangaraj, M. 'Experimental Study of T-I-VSI-Based DSTATCOM Using ALMS Technique for PQ Analysis'. J. Inst. Eng. India Ser. B 104, 165–174 (2023). doi.org/10.1007/s40031-022-00812-9.

[51] Mangaraj, M., Sabat.J. Ch. A.K. (2023). A Comparative Simulation Study between ZSI and BB-ZSI Based Distribution Static Compensator for Power Quality Improvement in Power Distribution Network. In Recent Advances in Power Electronics and Drives. Lecture Notes in Electrical Engineering, vol 973. Springer, Singapore. doi.org/10.1007/978-981-19-7728-2_12.

[52] M. Mangaraj, "Operation of Hebbian Least Mean Square controlled distributed Static Compensator," IET Generation, Transmission and Distribution, vol. 15, no. 13, pp. 1939 – 1948. Feb. 2021.

[53] N. M. Ismail and M. K. Mishra, "A multi-objective control scheme of a voltage source converter with battery–super capacitor energy storage system used for power quality improvement," 2023, International journal of electrical power and energy Systems, vol 142, doi.org/10.1016/j.ijepes.2022.108253.

[54] Manoj K.M.V., Mishra.M.K.: Three-leg inverter based distribution static compensator topology for compensating unbalanced and non-linear loads. IET Power Electron. 8(11), 2076–2084 (2015).

[55] Venkatraman, K., Selvan.M.P., Moorthi, S.: 'Predictive current control of distribution static compensator for load compensation in distribution system'. IET Generation. Transmission & Distribution. 10(10), 2410–2423 (2016).

[56] Barghi L.M., Teke.A. Yolda.Y. Mitigation of power quality problems using distribution static synchronous compensator: A comprehensive review. IET Power Electron. 8(7), 1312–1328 (2015).

[57] Badoni, M., Singh.A. Singh.B: Adaptive neuro-fuzzy inference system least-mean-square-based control algorithm for DSTATCOM. IEEE Trans. Ind. Inf. 12(2), 483–492 (2016).

[58] Juang, J.G., Chien, L.H., Lin, F.: Automatic landing control system design using adaptive neural network and its hardware realization. IEEE Syst. Journal. 5(2), 266–277 (2011).

[59] Saribulut.L, Teke.A, Tümay.M. 'Artificial neural network-based discrete fuzzy logic controlled active power filter. IET Power Electron. 7(6), 1536–1546 (2014).

[60] Mangaraj, M., et al. 'An adaptive LMBP training based control technique for DSTATCOM'. IET Generation. Transmission and Distribution. 14(3), 516–524 (2020) DOI: 10.1049/iet-gtd.2018.6295.

[61] Agarwal.R.K. Hussain.I., Singh.B. 'Application of LMS-based NN structure for power quality enhancement in a distribution network under abnormal conditions'. IEEE Trans. Neural Networks and Learning Systems. 29(5), 1598–1607 (2018).

[62] Srinivas.M., Hussain.I., Singh.B. 'Combined LMS–LMF based control algorithm of DSTATCOM for power quality enhancement in distribution system'. IEEE Trans. Ind. Electron. 63(7), 4160–4168 (2016).

[63] Mangaraj, M., Panda, A.K.: 'NBP-based icosϕ control strategy for DSTATCOM'. IET Power Electron. 10(12), 1617–1625 (2017).

[64] Kumar, P., Mahajan, 'Soft computing techniques for the control of an active power filter'. IEEE Trans. Power Delivery. 24(1), 452–461 (2009).

[65] Mangaraj, M., Panda A.K., Penthia.T. 'Investigating the performance of DSTATCOM using ADALINE based LMS algorithm'. 2016 IEEE 6th International Conference on Power Systems (ICPS), New Delhi, pp. 1–5 (2016).

[66] Widrow.B., Kim.Y., Park.D. 'The Hebbian-LMS learning algorithm'. IEEE Comput. Intell. Magazine. 10(4), 37–53 (2015).

[67] Siri, B., et al.: 'A mathematical analysis of the effects of Hebbian learning rules on the dynamics and structure of discrete-time random recurrent neural networks'. International Journal of Neural Comput. 20(12), 2937– 2966 (2008).

[68] Pehlevan, C., Hu, T., Chklovskii, D.B.: A Hebbian/anti-Hebbian neural network for linear subspace learning: A derivation from multidimensional scaling of streaming data. International Journal of Neural Comput. 27(7), 1461–1495 (2015).

[69] Luo, A., et al.: Distribution static compensator based on an improved direct power control strategy. IET Power Electron. 7(4), 957–964 (2014).

[70] Herman.L. Papic.I., Blazic.B.: A proportional-resonant current controller for selective harmonic compensation in a hybrid active power filter. IEEE Trans. Power Delivery. 29(5), 2055–2065 (2014).

[71] R. R. Behera, A. R. Dash and A. K. Panda, "Cascaded Transformer coupled Multi-level inverter based Shunt Active Power Filter," 2021 Asian Conference on Innovation in Technology (ASIANCON), PUNE, India, 2021, pp. 1-6, doi: 10.1109/ASIANCON51346.2021.9544884.

[72] B. Singh, K. Al-Haddad and A. Chandra, "A review of active filters for power quality improvement," in IEEE Transactions on Industrial Electronics, vol. 46, no. 5, pp. 960-971, Oct. 1999, doi: 10.1109/41.793345.

[73] S.ray, battacharya A, 'Improved tracking of shunt active power filter by sliding mode control', int J electr power energy syst 2016; 78; 916-25.

[74] Hoon, Y.; Radzi, M.A.M; Hassan, M.K.; Mailah, N.F. 'Control Algorithms of Shunt Active Power Filter for Harmonics Mitigation': A Review. *Energies* 2017, *10*, 2038. https://doi.org/10.3390/en10122038.

[75] G. W. Chang and T.Shee, "A novel reference compensation current strategy for shunt active power filter control," in IEEE Transactions on Power Delivery, vol. 19, no. 4, pp. 1751-1758, Oct. 2004, doi: 10.1109/TPWRD.2004.835430.

[76] S. Rahmani, N. Mendalek and K. Al-Haddad, "Experimental Design of a Nonlinear Control Technique for Three-Phase Shunt Active Power Filter," in IEEE Transactions on Industrial Electronics, vol. 57, no. 10, pp. 3364-3375, Oct. 2010, doi: 10.1109/TIE.2009.2038945.

[77] M. Qasim and V. Khadkikar, "Application of Artificial Neural Networks for Shunt Active Power Filter Control," in IEEE Transactions on Industrial Informatics, vol. 10, no. 3, pp. 1765-1774, Aug. 2014, doi: 10.1109/TII.2014.2322580.

[78] B. Singh, K. Al-Haddad and A. Chandra, "A review of active filters for power quality improvement," in IEEE Transactions on Industrial Electronics, vol. 46, no. 5, pp. 960-971, Oct. 1999, doi: 10.1109/41.793345.

[79] B. Singh and J. Solanki, "A Comparison of Control Algorithms for DSTATCOM," in IEEE Transactions on Industrial Electronics, vol. 56, no. 7, pp. 2738-2745, July 2009, doi: 10.1109/TIE.2009.2021596.

[80] A. Chandra, B. Singh, B. N. Singh and K. Al-Haddad, "An improved control algorithm of shunt active filter for voltage regulation, harmonic elimination, power-factor correction, and balancing of nonlinear loads," in IEEE Transactions on Power Electronics, vol. 15, no. 3, pp. 495-507, May 2000, doi: 10.1109/63.844510.

[81] M.Mehrasa, E. Pouresmaeil, M.F Akorede "Multilevel converter control approach of active power filter for harmonics elimination in electric grids." Elsevier on Energy, vol 84, 722–731.2015.

[82] Muraleedharan and M. K. Mishra, "A Multi-Objective Control Strategy for Power Quality Improvement with Enhanced LVRT Operation of a Grid-Interfaced Dual Voltage Source Inverter," 2023 IEEE International Conference on Recent Advances in Systems Science and Engineering, Kerala, India, 2023, pp. 1-8, doi: 10.1109/RASSE60029.2023.10363487.

[83] M. Mangaraj, V. D. Naidu, K. Priyanka and J. Sabat, "Comparative Analysis between Inductor Coupled T type split and self supported capacitor based DSTATCOM," 2020 IEEE International Symposium on Sustainable Energy,

Signal Processing and Cyber Security (iSSSC), 2020, pp. 1-5. Link: https://ieeexplore.ieee.org/document/9358812.

[84] Kannan, V. Kamatchi and N. Rengarajan. "Investigating the performance of photovoltaic based DSTATCOM using I cos Φ algorithm." *International Journal of Electrical Power & Energy Systems* 54 (2014): 376-386.

[85] M. G. Nair and G. Bhuvaneswari, "Design, Simulation and Analog Circuit Implementation of a Three-phase Shunt Active Filter using the Icos φ Algorithm," 2005 International Conference on Power Electronics and Drives Systems, Kuala Lumpur, Malaysia, 2005, pp. 553-556, doi: 10.1109/PEDS.2005.1619748.

[86] J. C. Vasquez, R. A. Mastromauro, J. M. Guerrero and M. Liserre, "Voltage Support Provided by a Droop-Controlled Multifunctional Inverter," in IEEE Transactions on Industrial Electronics, vol. 56, no. 11, pp. 4510-4519, Nov. 2009, doi: 10.1109/TIE.2009.2015357.

[87] C. Kumar and M. K. Mishra, "A Multifunctional DSTATCOM Operating Under Stiff Source," in IEEE Transactions on Industrial Electronics, vol. 61, no. 7, pp. 3131-3136, July 2014, doi: 10.1109/TIE.2013.2276778.

[88] S. B. Karanki, N. Geddada, M. K. Mishra and B. K. Kumar, "A DSTATCOM Topology With Reduced DC-Link Voltage Rating for Load Compensation With Nonstiff Source," in IEEE Transactions on Power Electronics, vol. 27, no. 3, pp. 1201-1211, March 2012, doi: 10.1109/TPEL.2011.2163946.

[89] J. Ye, H. B. Gooi, X. Zhang and H. H. C. Iu, "Simplified Four-Level Inverter-Based Single-Phase DSTATCOM Using Model Predictive Control," in IEEE Journal of Emerging and Selected Topics in Power Electronics, vol. 8, no. 4, pp. 3382-3395, Dec. 2020, doi: 10.1109/JESTPE.2020.2964005.

[90] C. Kumar and M. K. Mishra, "A Voltage-Controlled DSTATCOM for Power-Quality Improvement," in IEEE Transactions on Power Delivery, vol. 29, no. 3, pp. 1499-1507, June 2014, doi: 10.1109/TPWRD.2014.2310234.

[91] Luo, A., Xiao, H., Ma, F., Shuai, Z. and Wang, Y. (2014), Distribution static compensator based on an improved direct power control strategy. IET Power Electronics, 7: 957-964. https://doi.org/10.1049/iet-pel.2013.0265.

[92] U.M. Choi, F. Blaabjerg and K. -B. Lee, "Reliability Improvement of a T-Type Three-Level Inverter With Fault-Tolerant Control Strategy," in IEEE

Transactions on Power Electronics, vol. 30, no. 5, pp. 2660-2673, May 2015, doi: 10.1109/TPEL.2014.2325891.

[93] M. Mangaraj, A. K. Panda and T. Penthia, "Neural network control technique based sensorless DSTATCOM for the power conditioning," 2015 Annual IEEE India Conference (INDICON), New Delhi, India, 2015, pp. 1-6, doi: 10.1109/INDICON.2015.7443184.

[94] P. Kumar and A. Mahajan, "Soft Computing Techniques for the Control of an Active Power Filter," in IEEE Transactions on Power Delivery, vol. 24, no. 1, pp. 452-461, Jan. 2009, doi: 10.1109/TPWRD.2008.2005881.

[95] B. Widrow, Y. Kim and D. Park, "The Hebbian-LMS Learning Algorithm," in IEEE Computational Intelligence Magazine, vol. 10, no. 4, pp. 37-53, Nov. 2015, doi: 10.1109/MCI.2015.2471216.

[96] B. Singh, P. J.Prakash, D. P. Kothari, A. Chandra and K. A. Haddad, "Comprehensive Study of DSTATCOM Configurations," in IEEE Transactions on Industrial Informatics, vol. 10, no. 2, pp. 854-870, May 2014, doi: 10.1109/TII.2014.2308437.

[97] V. kumar, R.S.jyothi, "A Review of Different Configurations and Control Techniques for DSTATCOM in the Distribution system" article in E3S web of conferences 309(1): 1-5, 2021.

[98] B. Singh, P. J.Prakash, T.R. Somayajulu and D.P. Kothari, "Reduced Rating VSC With a Zig-Zag Transformer for Current Compensation in a Three-Phase Four-Wire Distribution System", *IEEE Transactions on Power Delivery*, vol. 24, no. 1, pp. 249-259, Jan. 2009.

[99] A. Fahmy, M.S. Hamad, A.K. Abdelsalam and A. Lotfy, "Power quality improvement in three-phase four-wire system using a shunt APF with predictive current control", *Proc. 38th IECON 2012)*, pp. 668-673, 25–28 Oct.

[100] U. Choi, F. Blaabjerg, K. Lee, Reliability improvement of a T-type three-level inverter with fault-tolerant control strategy. IEEE Trans on Power Electron. 30(5), 2660–2673 (2015)

LIST OF PUBLICATIONS

The publications listed below are the contributions made to this study. It consists of book chapters, presentations at conferences and peer-reviewed journals (Published/Under Review).

1. P. K. Y. Kundala, M. Mangaraj and S. K. Sudabattula, "Operation of Inductively Coupled DSTATCOM for Power Quality Enhancement," 2022 International Mobile and Embedded Technology Conference (MECON), Noida, India, 2022, pp. 210-214, doi: 10.1109/MECON53876.2022.9752372. **IEEE (SCOPUS) Published.**

2. P. K. Yadav Kundala, M. Mangaraj and S. K. Sudabattula, "An Inductively Coupled DSTATCOM using self and split capacitor supported Topology for Power Quality Enhancement," 2021 4th International Conference on Recent Developments in Control, Automation & Power Engineering (RDCAPE), Noida, India, 2021, pp. 52-56, doi: 10.1109/RDCAPE52977.2021.9633468. **IEEE (SCOPUS) Published.**

3. P. K. Yadav Kundala, M. Mangaraj and S. K. Sudabattula, "Inductively Coupled Distributed static compensator for Power Quality analysis of distribution networks," International journal of electrical and computer engineering, 2023, pp. 1387-1399, vol.13, ISS-2 doi: **10.11591/ijece.v13i2.pp1387-1399 (SCOPUS) Published.**

4. P. K. Yadav Kundala, M. Mangaraj and S. K. Sudabattula, "Cascaded Inductively Coupled DSTATCOM for Improved PQ Performance," International journal of renewable energy research, 2022, pp. 1787-1795, vol.12, no-4 doi: https://doi.org/10.20508/ijrer.v12i4.13420.g8604 **(SCOPUS) Published.**

5. P. K. Yadav Kundala, M. Mangaraj and S. K. Sudabattula, "DBSCAN Based inductively coupled DSTATCOM for PQ improvement," journal of Electrical systems, 2023, pp. 150-165, vol.19, no-1 **(SCOPUS) Published.**

6. P. K. Yadav Kundala, M. Mangaraj and S. K. Sudabattula, J.Sabat and R.Takur "DBSCAN Based cascaded inductively coupled DSTATCOM for PQ improvement," 4th Electric Power and Renewable Energy Conference (EPREC-2023) Published in the **Springer Conference.**